INDEPENDENT ASSESSMENT OF TRAC-PF1 (VERSION 7.0), RELAP5/MOD1 (CYCLE 14), AND TRAC-BD1 (VERSION 12.0) CODES USING SEPARATE-EFFECTS EXPERIMENTS

P. Saha, J.H. Jo, L. Neymotin, U.S. Rohatgi,
G.C. Slovik, and C. Yuelys-Miksis

Date Published — August 1985

LWR CODE ASSESSMENT AND APPLICATION GROUP
DEPARTMENT OF NUCLEAR ENERGY, BROOKHAVEN NATIONAL LABORATORY
UPTON, LONG ISLAND, NEW YORK 11973

bnl

INDEPENDENT ASSESSMENT OF TRAC-PF1 (VERSION 7.0), RELAP5/MOD1 (CYCLE 14), AND TRAC-BD1 (VERSION 12.0) CODES USING SEPARATE-EFFECTS EXPERIMENTS

P. Saha, J.H. Jo, L. Neymotin, U.S. Rohatgi,
G.C. Slovik, and C. Yuelys-Miksis

LWR CODE ASSESSMENT AND APPLICATION GROUP
DEPARTMENT OF NUCLEAR ENERGY
BROOKHAVEN NATIONAL LABORATORY
UPTON, LONG ISLAND, NEW YORK 11973

ABSTRACT

This report presents the results of independent code assessment conducted at BNL. The TRAC-PF1 (Version 7.0) and RELAP5/MOD1 (Cycle 14) codes were assessed using the critical flow tests, level swell test, countercurrent flow limitation (CCFL) tests, post-CHF test, steam generator thermal performance tests, and natural circulation tests. TRAC-BD1 (Version 12.0) was applied only to the CCFL and post-CHF tests.

The overall conclusions of the study are as follows:

1. The TRAC-PWR series of codes, i.e., TRAC-P1A, TRAC-PD2, and TRAC-PF1, have been gradually improved. However, TRAC-PF1 appears to need improvement in almost all categories of tests/phenomena attempted at BNL.

2. Of the two codes, TRAC-PF1 and RELAP5/MOD1, the latter needs more improvement particularly in the areas of:

   - CCFL

   - Level swell

   - CHF correlation and post-CHF heat transfer

   - Numerical stability.

3. For the CCFL and post-CHF tests, TRAC-BD1 provides the best overall results. However, the TRAC-BD1 interfacial shear package for the countercurrent annular flow regime needs further improvement for better prediction of CCFL phenomenon.

It is our understanding that both the TRAC-PF1 and RELAP5/MOD1 codes have been improved significantly so that the newer versions of these codes, i.e., TRAC-PF1/MOD1 and RELAP5/MOD2, should produce better results.

EXECUTIVE SUMMARY

Independent assessment of the TRAC-PF1 (Version 7.0), RELAP5/MOD1 (Cycle 14) and TRAC-BD1 (Version 12.0) codes has been performed using various separate-effect tests. The tests simulated can be grouped in the following six categories:

1. Critical flow tests (Moby-Dick nitrogen-water, BNL flashing flow, Marviken Test No. 24).

2. Level swell tests (GE large vessel test).

3. Countercurrent flow limiting (CCFL) tests (University of Houston, Dartmouth College single- and parallel-tube tests).

4. Post-CHF tests (Oak Ridge rod bundle test).

5. Steam generator tests (B&W 19-tube model S.G. tests, FLECHT-SEASET U-tube S.G. tests).

6. Natural circulation tests (FRIGG loop tests).

TRAC-PF1 and RELAP5/MOD1 were applied to all of the above categories; however, because of resource limitations, TRAC-BD1 was applied only to the CCFL and post-CHF tests.

Useful results were obtained for all TRAC-PF1 calculations except for the Dartmouth College parallel-tube CCFL tests. RELAP5/MOD1 did not produce any useful result for the Moby-Dick nitrogen-water tests and the code was not applied to the parallel-tube CCFL tests because of its poor prediction of the single-tube CCFL tests. TRAC-BD1 produced useful results for both CCFL and post-CHF tests.

Regarding the computer run time, both TRAC-PF1 and TRAC-BD1 took approximately 3 ms of CPU time (in the BNL CDC-7600) per cell per time step. In that respect, RELAP5/MOD1 was faster because it took approximately 1 ms per cell per time step. However, RELAP5/MOD1 usually took smaller time steps than TRAC-PF1, and thus, the CPU-to-real time ratio of these two codes was quite comparable. Sometimes, the RELAP5/MOD1 maximum time step had to be restricted to avoid numerical instabilities. In those cases, RELAP5/MOD1 was actually more expensive to run than TRAC-PF1.

From the results presented in Chapters 2 through 7, the following conclusions and recommendations are drawn for each code:

Conclusions and Recommendations for TRAC-PF1

1. For two-component two-phase critical flow without phase change, TRAC-PF1 can be expected to produce stable results for all void fractions, which is an improvement over the TRAC-P1A code. However,

the results are sensitive to the friction factor option selected for calculation. The homogeneous friction factor option overpredicts the mass flow rate by ~15 to 22%, whereas the annular friction factor option underpredicts the same by ~5 to 12%. It is recommended that the same single phase friction factor be used for both the homogeneous (NFF=1) and the annular (NFF=2) flow friction factor options.

2. For single-component (i.e., water) two-phase flow with phase change, TRAC-PF1 may significantly underpredict the subcooled critical flow rate by as much as 25%, as shown in the BNL flashing test simulations. An accurate flashing delay model seems to be a necessary (although not sufficient) condition for achieving better agreement with the subcooled critical flow data. Simulation of Marviken Test No. 24 also supports this conclusion.

3. The choking option of TRAC-PF1 seems to be reasonable for subcooled critical flow through short nozzles if "correct" upstream boundary conditions are provided.

4. TRAC-PF1 needs a more accurate flashing delay model for the bulk or pipe flow. The present delay model in the choked flow formulation cannot predict the early pressure undershoot observed in the experiment. This undershoot and the corresponding liquid superheat could be important in determining the vapor generation rate later in the transient.

5. TRAC-PF1 tends to overpredict the void fraction below the mixture level and the level swell during a rapid depressurization transient. A high interfacial shear in TRAC-PF1 is believed to be partially responsible for the higher void fraction and the higher level swell rate.

6. For situations where liquid is injected in the middle of a test channel, the CCFL phenomenon is greatly influenced by the liquid entrainment inception and rate. In such cases, TRAC-PF1 predicts an early liquid entrainment which results in lower liquid downflow rates. Therefore, the TRAC-PF1 entrainment model/correlation needs improvement.

7. For situations where liquid flows down from an upper plenum, the interfacial shear seems to be the dominant parameter for CCFL phenomenon. In such cases, TRAC-PF1 produced good agreement with data for small pipe diameters (~0.025 m I.D.). Thus, the Dukler correlation for interfacial shear seems reasonable for small-diameter pipes or channels. However, for large diameter pipes (~0.15 m I.D.), TRAC-PF1 produced anomalous behavior because of the discontinuities in the Dukler correlation. In this case, the Bharathan-Wallis correlation may be used.

8. A good prediction of single-tube CCFL data does not guarantee similar success for the parallel-tube CCFL data. For example, TRAC-PF1 produced good agreement with the Dartmouth College 0.0254 m I.D. single tube data. However, it could not even produce a stable result for the parallel-tube experiments conducted in three 0.0254 m I.D. tubes. Also, the interfacial shear package must include correlations valid for the entire countercurrent annular flow regime, i.e., wavy-transition-rough film regimes, to enable TRAC-PF1 to adequately predict the parallel-tube CCFL phenomenon.

9. TRAC-PF1 can not accurately predict the low flow CHF conditions as evidenced from the ORNL post-CHF and FRIGG loop tests. Correlations other than the Biasi CHF correlation, which was based on single tube data, should be investigated. However, TRAC-PF1 does calculate vapor superheating in the post-CHF regime.

10. TRAC-PF1 produces a more stable result for the integral economizer once-through steam generator (IEOTSG) heat transfer than its predecessor, TRAC-PD2, and yielded reasonable results for a load change transient.

11. For a loss-of-feedwater transient in a once-through steam generator (OTSG), TRAC-PF1 underpredicted the exit steam flow rate. This was caused by the lower initial water inventory due to a lower rate of condensation of the aspirated steam. An increase in the condensation rate improved the result, indicating that the direct-contact condensation rate in TRAC-PF1 is underestimated.

12. A noding study showed that approximately 10 nodes in each side of the steam generator are adequate for TRAC-PF1 for simulating transients such as loss-of-feedwater.

13. For large-break LOCA conditions, TRAC-PF1 tends to overpredict the secondary-to-primary heat transfer. The actual nonequilibrium effects are also somewhat underpredicted by TRAC-PF1. Thus, the code would tend to exaggerate the steam binding effects and would tend to predict slower core reflood.

14. TRAC-PF1 should have the capability of modeling the steam generator shell wall. Although not of utmost importance for a full-scale plant, this capability might be necessary for modeling tall-but-skinny model steam generators.

15. TRAC-PF1 with either the homogeneous or the annular two-phase friction factor option overpredicted the loop mass flow rate during natural circulation condition. However, the results obtained with the annular friction factor option have been closer to the data, both qualitatively and quantitatively.

Conclusions and Recommendations for RELAP5/MOD1

1. For single-component (i.e., water) two-phase flow with phase change, RELAP5/MOD1 may significantly underpredict the subcooled critical flow rate by as much as 25%, as shown in the BNL flashing test simulations. An accurate flashing delay model seems to be a necessary (although not sufficient) condition for achieving better agreement with the subcooled critical flow data. Simulation of Marviken Test No. 24 supports this conclusion.

2. For the RELAP5/MOD1 choking model, it seems that the short nozzles have to be treated as zero-volume area changes to obtain good agreement with data, even though this contradicts the reality. Also, the RELAP5/MOD1 choking model seems to be sensitive to nodalization.

3. RELAP5/MOD1 needs a more accurate flashing delay model for the bulk or pipe flow. The present delay model in the choked flow formulation cannot predict the early pressure undershoot observed in the experiment. This undershoot and the corresponding liquid superheat could be important in determining the vapor generation rate later in the transient.

4. RELAP5/MOD1 predictions for the average void fraction, level swell rate, and break flow rate during level swell due to rapid depressurization seem reasonable. However, the code underpredicts the vessel pressure and produces an irregular axial void fraction profile. It seems that the interfacial shear package of RELAP5/MOD1 needs re-examination and improvement.

5. There seems to be no need of representing a converging-diverging discharge nozzle with a zero-volume junction for RELAP5/MOD1 calculation, as suggested by the RELAP5 code developers.

6. The RELAP5/MOD1 flow regime map for high void fractions must be changed to include an annular-mist regime before the code can be expected to produce reasonable results for CCFL applications. At present, RELAP5/MOD1 cannot predict a CCFL situation even in a simple round pipe.

7. RELAP5/MOD1 cannot accurately predict the low flow CHF conditions as evidenced from the ORNL post-CHF and FRIGG loop tests. Other CHF correlations should be investigated.

8. RELAP5/MOD1 tends to overpredict the vapor generation rate at the post-CHF region. This results in almost no vapor superheating until all the liquid droplets are evaporated in the RELAP5/MOD1 calculation. However, this does not represent the reality. Thus, the RELAP5/MOD1 model for vapor generation in the post-CHF regime should be improved.

9. For the steam generator (IEOTSG) tests, the RELAP5/MOD1 (Cycle 14) results are slightly improved over those of Cycle 1. However, the new results still suffer from numerical instability. Therefore, restrictions on the maximum time steps is necessary for the RELAP5/MOD1 calculation. This is valid for both once-through and U-tube steam generator simulations.

10. For RELAP5/MOD1, use of more nodes does not necessarily lead to better agreement with the experimental data of steam generator (IEOTSG) thermal performance.

11. Although RELAP5/MOD1 produced reasonable results for the OTSG loss-of-feedwater transient, it fails to predict the initial superheated steam condition at the exit of the secondary side. Consequently, the total primary-to-secondary heat transfer at steady state is underpredicted by as much as 10%.

12. For large-break LOCA conditions, RELAP5/MOD1 tends to overpredict the secondary-to-primary heat transfer. The actual nonequilibrium effects are also underpredicted by RELAP5/MOD1 as in the post-CHF tests. Thus, the code would tend to exaggerate the steam binding effects and would tend to predict slower core reflood.

13. RELAP5/MOD1 tends to overpredict the vapor-to-droplet heat transfer in the dispersed droplet regime. Improvement in this area is needed.

14. RELAP5/MOD1 also produced an anomalous void profile in the secondary side of the FLECHT-SEASET U-tube steam generator which indicated some errors in the code (either FORTRAN or in interfacial shear).

15. The bundle mass flux during natural circulation has been overpredicted by RELAP5/MOD1 for all three sets of FRIGG loop runs. The overprediction is believed to be due to underestimation of the two-phase wall friction losses.

16. Further efforts should be directed toward improving the numerical stability of RELAP5/MOD1.

Conclusions and Recommendations for TRAC-BD1

1. For situations where liquid is injected in the middle of a test channel, the CCFL phenomenon is greatly influenced by the liquid entrainment inception and rate. In such cases, TRAC-BD1 tends to predict good agreement with data. Thus, the TRAC-BD1 entrainment inception and rate correlations seem to be reasonable.

2. For situations where liquid flows down from an upper plenum, the interfacial shear seems to be the dominant parameter for the CCFL phenomenon. In such cases, TRAC-BD1 tends to overpredict the liquid downflow rate, indicating a lower interfacial shear.

3. The interfacial shear coefficient used in the TRAC-BD1 code overpredicts the liquid downflow rate. Use of the Kutateladze CCFL correlations tends to improve the prediction. However, the Kutateladze constant in the CCFL correlation has to be adjusted to achieve a good prediction. It seems that a combination of the Dukler correlation (for small-diameter pipe) and the Bharathan-Wallis correlation (for large-diameter pipe) should produce a better interfacial shear correlation for the counter-current annular flow regime.

4. For parallel-tube CCFL tests, the TRAC-BD1 results were, at best, in some qualitative agreement with the data. It seems that the interfacial shear package must include correlations valid for the entire countercurrent annular flow regime, i.e., wavy-transition-rough film regimes, to enable TRAC-BD1 to adequately predict the parallel-tube CCFL phenomenon.

5. The CHF correlation used in the TRAC-BD1 code, i.e., the Biasi critical quality boiling length correlation, seems to be adequate. Vapor superheating calculated in the post-CHF regime also looks reasonable. However, further assessment with more post-CHF experiments is needed to make a definitive statement about the TRAC-BD1 post-CHF model accuracy.

As a final note, the code assessment conducted at BNL was directed at evaluating the adequacy of the thermal-hydraulic models and recommending areas of further improvement. Thus, only the separate-effects experiments were simulated. Conclusions regarding the overall code accuracy for full-scale reactor application can only be made by assimilating all code assessment results obtained at BNL, INEL, LANL, and SNL. This last task is beyond the scope of the present effort.

TABLE OF CONTENTS

CONTENTS (cont)

CONTENTS (cont)

CONTENTS (cont)

TABLES

FIGURES

FIGURES (cont)

FIGURES (cont)

ACKNOWLEDGEMENTS

1. INTRODUCTION

1.1 Background

TRAC and RELAP5 are two of the best-estimate, advanced systems codes which have been developed under the sponsorship of the U. S. Nuclear Regulatory Commission (USNRC) for analysis of various accidents and transients in Light Water Reactor (LWR) systems. Several versions of TRAC, i.e., TRAC-P1A (Liles et al., 1979), TRAC-PD2 (Liles et al., 1981), TRAC-PF1 (Liles et al., 1984), and TRAC-PF1/MOD1 (Liles et al., 1983), for Pressurized Water Reactor (PWR) analysis have been developed at the Los Alamos National Laboratory (LANL). Starting from a preliminary version of TRAC-PF1, Idaho National Engineering Laboratory (INEL) has developed TRAC-BD1 (Spore et al., 1981), and TRAC-BD1/MOD1 (Taylor et al., 1984) for Boiling Water Reactor (BWR) analysis. INEL has also developed the RELAP5 series of codes, i.e., RELAP5/MOD1 (Ransom et al., 1982), and RELAP5/MOD2 (Ransom et al., 1984) for analysis of both PWR and BWR.

USNRC had decided that after a major code version was released, the code would go through an independent assessment process by groups that had not taken part in its development or developmental assessment. Such an assessment effort began at three national laboratories, namely, Brookhaven National Laboratory (BNL), INEL, and LANL with the TRAC-P1A code released by LANL in March 1979. As more codes were released, the independent assessment activity grew, and Sandia National Laboratory (SNL) became the fourth laboratory to join the NRC code assessment program.

The ultimate objective of the code assessment program is to arrive at a qualified judgement on the code accuracy for predicting various accidents and transients in full-scale LWRs. Since there is a scarcity of challenging plant transient/accident data, the code assessment has to rely heavily on simulation of the experiments conducted in subscale test facilities such as LOFT, Semiscale, TLTA, etc. It is also important to determine whether the thermal-hydraulic phenomena that are expected to control the accident or transient in a full-scale reactor can be adequately modeled. This is accomplished by simulating various separate-effects tests, some of which have been conducted in full scale. Further discussion on code assessment strategies is given by Fabic and Andersen (1981), and Saha (1982a).

At BNL, emphasis was placed on assessing the thermal-hydraulic models used in the TRAC and RELAP5 codes. Therefore, several basic and separate-effects experiments were simulated with various versions of TRAC and RELAP5. Results of the TRAC-PD2, and RELAP5/MOD1 (Cycle 1) assessment at BNL have been reported by Saha et al., (1982b), whereas analysis of BCL ECC bypass tests using TRAC-PD2/MOD1 is presented by Slovik and Saha (1985). In addition, detailed reviews of constitutive packages used in TRAC-P1A, TRAC-PD2, TRAC-PF1, and RELAP5/MOD1 (Cycle 14) codes are presented in several BNL reports (Rohatgi and Saha 1980; Rohatgi et al., 1982; Rohatgi et al., 1985). The purpose of this report is to present the results of the TRAC-PF1 (Version 7.0), RELAP5/MOD1 (Cycle 14), and TRAC-BD1 (Version 12.0) assessments using various basic and separate-effects experiments. Comments will be made on the adequacy of the thermal-hydraulic models used in these codes, and the areas of further improvement, if needed, will be recommended.

1.2 Objective and Experiments Simulated

As discussed by Saha (1982a), different types of accidents or transients in full-scale reactors are expected to be controlled by different types of physical or thermal-hydraulic phenomena. With this in mind, the TRAC-PF1, RELAP5/MOD1 (Cycle 14), and TRAC-BD1 codes have been assessed using various types of separate-effects experiments. Table 1.2.1 shows the experiments simulated, the codes used, and the thermal-hydraulic effects assessed. The assessment matrix was, of course, limited by the time and budgetary constraints.

Experiments selected for independent code assessment at BNL do cover a wide range of thermal-hydraulic phenomena. The critical flow experiments will help assess the codes' capability in predicting the break flow rate which is an important parameter for loss-of-coolant accident (LOCA) analysis. The countercurrent flow limitation (CCFL) or "flooding" is another important phenomenon which determines the rate of emergency core cooling (ECC) water penetration into the reactor in the event of a LOCA. CHF and post-CHF heat transfer usually play a significant role in determining the peak clad temperature during all accidents and transients in LWRs. However, level swell and steam generator thermal performance are usually important during small-break LOCAs, steam line breaks, and operational transients in a PWR. Level swell is also important during BWR accidents and transients. Heat transfer in the natural circulation mode is also important during small-break LOCAs and other transients after the reactor coolant pumps are turned off. As shown in Table 1.2.1, the TRAC-PF1 and RELAP5/MOD1 codes were applied to all of the six categories of experiments. However, because of resource limitations, TRAC-BD1 was applied only to the CCFL and post-CHF experiments, although the code should be applicable to the critical flow, the level swell, and the natural circulation tests as well.

The main objective of this report is to present the results of the code predictions with the experimental data and to determine the adequacy of the code's thermal-hydraulic models and constitutive packages. In case of poor agreement between the code predictions and experimental data, attempts will be made to determine the reasons and suggest appropriate remedies. Attempts will also be made to provide user guidelines for application of these codes to full-scale LWR accidents and transients. However, judgement regarding the overall code accuracy for reactor application can only be made after assimilation of all the code assessment results obtained at BNL, INEL, LANL and SNL. This last task is outside the scope of the present work.

1.3 Brief Description of Codes

Detailed descriptions of the TRAC-PF1, RELAP5/MOD1, and TRAC-BD1 codes can be found in the respective code documentations (Liles et al., 1984; Ransom et al., 1982; Spore et al., 1981). However, a few words on these codes should help a reader better understand the assessment calculations that follow this introduction.

TABLE 1.2.1 BNL INDEPENDENT ASSESSMENT MATRIX FOR TRAC-PF1 (VERSION 7.0),
RELAP5/MOD1 (CYCLE 14), AND TRAC-BD1 (VERSION 12.0) CODES

| | CODE USED | | | |
EXPERIMENTS	TRAC-PF1	RELAP5/MOD1	TRAC-BD1	PHENOMENA STUDIED
1. Critical Flow				
a) Moby-Dick Nitrogen-Water Tests (Run Nos. 3087 and 3141).	X	X		Steady-state critical flow with no phase change.
b) BNL Flashing Tests (Run Nos. 291-295, 309-311, 318-321, and 339-342)	X	X		Steady-state critical flow with phase change.
c) Marviken Critical Flow Test (Run No. 24).	X	X		Large-scale transient critical flow test with small length-to-diameter ratio.
2. Level Swell				
a) GE Large-Vessel Test (Run No. 5801-15)	X	X		Two-phase mixture level swell during rapid depressurization.

TABLE 1.2.1 (cont)

EXPERIMENTS	CODE USED			PHENOMENA STUDIED
	TRAC-PF1	RELAP5/MOD1	TRAC-BD1	
3. Counter-current Flow Limitation (CCFL)				
a) University of Houston Tests (two different water feed rates).	X	X	X	CCFL in single round tube with no phase change. Assess the interfacial shear and entrainment models.
b) Dartmouth College Single Tube Tests(two different tube inside diameters).	X	X	X	Same as above.
c) Dartmouth College Parallel-Tube Tests (one series with three 0.0254m I.D. tubes).	X		X	CCFL in multiple channels with no phase change.
4. Post-CHF Heat Transfer				
a) ORNL Rod Bundle Tests (Run No. 3.07.9H).	X	X	X	CHF and Post-CHF heat transfer in a typical rod bundle under low flow condition.

1
4
1

TABLE 1.2.1 (cont)

EXPERIMENTS	CODE USED			PHENOMENA STUDIED
	TRAC-PF1	RELAP5/MOD1	TRAC-BD1	
5. Steam Generator Thermal Performance				
a) B&W Once-Through Steam Generator Tests (Series 68-69-70 & 28-29).	X	X	Not Applicable	B&W IEOTSG and OTSG performance during operational transients.
b) FLECHT-SEASET U-Tube Steam Generator Tests (Run Nos. 21806 & 22010)	X	X	Not Applicable	U-tube steam generator performance under large-break LOCA conditions.
6. Natural Circulation				
a) FRIGG-Loop Tests (three series with different entrance loss coefficients).	X	X		Natural circulation flow rates at different bundle powers. (Balance between the gravity head and friction including form losses.)

1.3.1 TRAC-PF1

TRAC-PF1 (Liles et al., 1984) was developed at LANL to improve the capability of TRAC-PD2 (Liles et al., 1981) for analysis of small-break LOCA and other operational transients in PWRs. TRAC-PF1, therefore, has all the major improvements of TRAC-PD2; however, it uses a full two-fluid model in the reactor vessel as well as in the loop components. In addition, it uses a two-step numerics in the one-dimensional components to improve the computer run time.

Following the earlier versions of TRAC-PWR series of codes, TRAC-PF1 consists of several modules, namely, VESSEL, PIPE, TEE, PRESSURIZER, ACCUMULATOR, PUMP, STEAM GENERATOR, VALVE, etc., to represent various components of a PWR system. By suitable connection of these modules, one may model a reactor system or a wide spectrum of test facilities ranging from LOFT to a simple round tube test section. Two special components, namely, BREAK and FILL, are used to provide the boundary conditions. A CORE component may also be used if a one-dimensional axial representation is considered sufficient to model the reactor. The code uses a point-reactor kinetics model and includes models for structural heat transfer.

The VESSEL module represents the reactor vessel of a PWR. By suitable partitioning and nodalization, one can model the upper and lower plena, the downcomer and the core within this module. The module uses a three-dimensional three-field seven-equation two-fluid formulation of two-phase flow. The three fields are: (a) liquid, (b) vapor including noncondensable gas or combined vapor, and (c) noncondensable gas in vapor. All other modules, i.e., the loop components, use a one-dimensional three-field seven-equation two-fluid model for two-phase flow. The same field equations are used in all components: (a) three conservation-of-mass equations (one for the liquid, one for the combined vapor, and one for the noncondensable gas in vapor), (b) two equations of motion (one for the liquid and the other for the combined vapor), (c) two energy equations (one for the mixture and the other for the combined vapor). However, for the VESSEL module, the equations of motion are resolved into three coordinates, namely, axial, radial, and azimuthal, to obtain the phasic velocities in three directions. Many constitutive relations for the interfacial and wall-to-fluid momentum and heat transfer are used in both the VESSEL and the loop components to close the formulation. These constitutive relations play a major role in the code predictions, and the assessment activity at BNL is directed at verifying their adequacy or reliability in various situations pertinent to the PWR safety.

As mentioned earlier, there is a one-dimensional CORE component in TRAC-PF1 which may be used instead of the three-dimensional VESSEL module if multi-dimensional thermal-hydraulics is not important for a particular accident or transient. This is usually true for transients with symmetric loop conditions.

A two-step numerics which can violate the material Courant condition has been used for the one-dimensional components. Thus, large time steps can be taken for slow transients resulting in a significant saving in the computer running time. However, the three-dimensional VESSEL component still uses the

semi-implicit numerics as in TRAC-PD2, and the time step there is restricted
by the material Courant condition.

1.3.2 RELAP5/MOD1

This code (Ransom et al., 1982) was developed at INEL with the objective
of producing an economic and user-convenient computer code for best-estimate
analyses of the light water reactor accidents and transients. The code in-
cludes component models for pipes, branches, abrupt flow area changes, pumps,
valves, control systems, etc., to represent a reactor system (both PWP and
BWR) or a test facility. Special components such as time-dependent volumes
and time-dependent junctions are used to provide boundary conditions. Heat
structures are available to model heat transfer to or from the fluid. The
code also includes a point-reactor kinetics model with reactivity feedback.

The basic hydrodynamic model is based on a one-dimensional five-equation
two-fluid formulation of two-phase flow. It consists of two phasic conserva-
tion of mass equations, two phasic conservation of momentum equations, and one
mixture energy equation. The code also accounts for the noncondensable gases
in the vapor phase. However, since only one energy equation is used, an addi-
tional specification regarding one-phase (liquid or vapor) being at the local
saturation temperature has to be made. Furthermore, constitutive relations
for the nonequilibrium phase change rate, interfacial momentum transfer, and
the correlations for wall friction and wall heat transfer are needed to close
the formulation. As such, RELAP5 is based on a nonhomogeneous and nonequili-
brium (at least, partial) description of two-phase flow. However, it does not
have a three-dimensional capability for reactor vessel as available in TRAC.

The code uses a semi-implicit numerical technique, and the time step is
limited by the material Courant condition and other parameters such as mass or
density error.

1.3.3 TRAC-BD1

This code (Spore et al., 1981) was also developed at INEL as a best-esti-
mate tool for BWR LOCA analysis. The code development started from an interim
version of the TRAC-PF1 code described in Section 1.3.1. Therefore, TRAC-BD1
consists of a three-dimensional two-fluid VESSEL module, and several one-
dimensional two-fluid non-VESSEL components such as PIPE, PUMP, VALVE, etc.
The code also uses a point-reactor kinetics. However, many modifications to
the interim version of TRAC-PF1 were made to produce the TRAC-BD1 code.

The major change in the TRAC-BD1 code was the use of the CHAN component
to represent the channel boxes containing the fuel bundles in a BWR core. The
CHAN component is a one-dimensional flow component developed from the TRAC-PF1
PIPE component by adding the fuel rod heat convection and radiation models. A
number of parallel CHAN components connecting the lower and upper plena of the
VESSEL module can be used to model a BWR core. The remainder of the VESSEL
module is basically the same as in TRAC-PF1. However, typical BWR components
such as jet pumps and separators were placed inside the VESSEL module.

Several changes were also made in the constitutive relations package. First, the Kutateladze-type CCFL correlations are added to limit liquid down-flow at the upper tie plate and side entry orifices. These can be activated by user options. Secondly, an integral or critical quality-boiling length type CHF correlation is used rather than the local-type correlation used in TRAC-PF1. Also, the Version 12.0 assessed at BNL contained the Ishii-Andersen shear package (Mohr, 1981) and an improved subcooled boiling model (Phillips, 1981a).

The numerical scheme is basically the same as in the TRAC-PD2 code (Liles et al., 1981). The time step is, therefore, restricted by the material Courant limit.

1.4 Report Outline

Chapters 2 through 7 present the bulk of the TRAC-PF1, RELAP5/MOD1 and TRAC-BD1 assessment work performed at BNL. Each chapter deals with a single type or category of experiments such as critical flow, level swell, etc. The order of discussion is the same as shown in Table 1.2.1. Within each chapter, the assessment results for each test including user experience are presented, and summary and conclusions for each type of experiment are reported. This format allows a more convenient intercode comparison for the same experiment or phenomenon.

Finally, the overall summary, conclusions, and recommendations, including user guidelines for each code, are presented in Chapter 8.

2. SIMULATION OF CRITICAL FLOW EXPERIMENTS

Experiments conducted in three different critical flow test facilities were simulated with TRAC-PF1 and RELAP5/MOD1. The Moby-Dick nitrogen-water experiments (Jeandey and Barriere, 1979) provide small-scale steady-state two-component two-phase critical flow data with no phase change. The BNL flashing experiments (Abuaf et al., 1981) conducted in a small-scale converging-diverging nozzle produced data for steady-state steam-water critical flow with phase change. Area-averaged axial void fractions were also measured in the BNL experiments. Finally, the Marviken critical flow tests (Marviken, 1982) provided large-scale transient steam-water critical flow data. Advanced best-estimate codes such as TRAC-PF1 and RELAP5/MOD1 should adequately predict the data obtained in all of these test facilities.

2.1 Moby-Dick Nitrogen-Water Experiments

2.1.1 Test Description

Several steady-state nitrogen-water two-component two-phase flow tests were conducted in the Moby-Dick test facility at Grenoble (Jeandey and Barriere, 1979). The test section had three parts. The first part was a vertical straight pipe section of 14 mm inside diameter and approximately 2.67 m length. This was followed by a 7° diverging nozzle 0.254 m long. The final section was another straight pipe of 45 mm inside diameter and 0.42 m length. Water entered through the bottom of the test section and independently metered nitrogen was injected into the test section approximately 1.68 m from the bottom.

Experimental measurements included the pressure (for all tests) and diametral void fraction (for only a few tests) along the length of the test section. In addition, the pressure and temperature at the test section inlet and exit, the nitrogen temperatures (near room temperature), the water and nitrogen flow quality, and the water mass flow rate were also measured.

Two tests have been simulated with TRAC-PF1: Run Nos. 3087 and 3141, which correspond to the flow qualities of 5.91×10^{-4} and 51.3×10^{-4}, respectively. Simulation of the same two tests was also attempted with the RELAP5/MOD1 code. In spite of many attempts, the RELAP5 code produced severe oscillations for both tests, and no useful results were obtained. The input decks were sent to the code developers at INEL and no further calculations were attempted at BNL. Thus, only the TRAC-PF1 results for the Moby-Dick nitrogen-water tests will be discussed here.

2.1.2 Input Models

For TRAC-PF1 calculations, the test section was simulated by a series combination of a TEE and a PIPE component as shown in Figure 2.1.1. Forty-two cells or volumes were used to represent the entire test section. Cells with different lengths were used, with greater resolution in the throat area. Two BREAK components, one at the entrance and the other at the exit of the test section, were used to impose the pressure boundary conditions. The nitrogen mass flow rate was needed to effect closure and was specified with a FILL component attached to the free end of the secondary side of the TEE component.

BREAK

PIPE

IO CELLS EACH
0.042 m

2 CELLS EACH
OF 0.027m

IO CELLS EACH OF
0.020 m

TEE

IO CELLS EACH
OF 0.020 m

0.06 m

4 CELLS EACH OF 0.10m

0.15

FILL
N_2

0.35 m

3 CELLS EACH
OF 0.01 m

0.50m

0.50m

0.50m
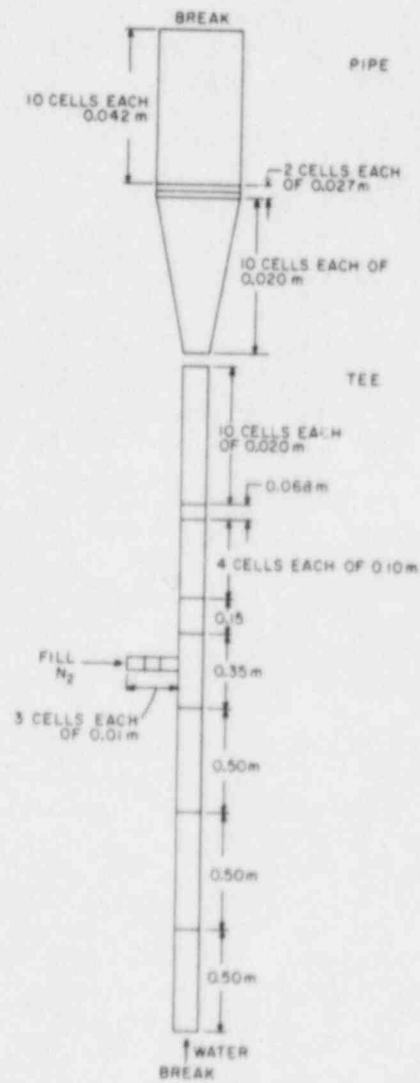
WATER
BREAK

Figure 2.1.1 TRAC-PF1 Noding for Moby-Dick Nitrogen-Water Tests.

TRAC-PF1 was run with fixed boundary conditions to reach a steady state for each of the tests considered. The air-water option of the code was selected and the air partial pressure was set to zero as recommended by the LANL staff (Woodruff, 1982). Both the homogeneous (NFF=1) and the annular (NFF=2) wall friction factor options were used to study the sensitivity of the predicted mass flow rate to the friction factor options. No additive loss coefficients were used in any calculations.

2.1.3 Code Predictions and Comparison with Data

The TRAC-PF1 predictions of the water mass flow rate are shown in Table 2.1.1. The results obtained using the homogeneous friction factor option (NFF=1) are compared to those obtained using the annular friction factor option (NFF=2). As can be seen, the two options as available in TRAC-PF1 produced significantly different water mass flow rates. Note that the experimental values of the water mass flow rate fall between the two TRAC predictions.

Table 2.1.1 Summary of Moby-Dick Nitrogen-Water Test Results

Run Number	Flow Quality	Water Mass Flow Rate (kg/s)				
		Experiment	TRAC-PF1 Calculation		TRAC-PF1 Calculation	
			Annular Friction Factor Option	Error (%)	Homogeneous Friction Factor Option	Error (%)
3087	5.91×10^{-4}	1.915	1.786	-6.7	2.205	+15.1
3141	51.3×10^{-4}	1.222	1.074	-12.1	1.4978	+22.5

The code (TRAC-PF1) produced stable solutions for all cases. This is a significant improvement over the TRAC-P1A code which could not reach a steady state for the high void fraction test, i.e., Test No. 3141 (Saha, 1980). However, it can be seen from Table 2.1.1 that for Run No. 3087, i.e., a low quality test, the predictions are closer to the experimental values than those for the high quality test, i.e., Run No. 3141. It can also be seen that the water flow rate is underpredicted by the annular friction factor option, whereas it is overpredicted by the homogeneous friction factor. However, the results using the annular friction factor option are closer to the experimental mass flow rates. This is in agreement with the results obtained with the TRAC-P1A code (Saha, 1980), and is caused primarily by the large difference in the single-phase friction factors used in these options. (The homogeneous friction factor option uses a smooth wall, Blasius-type single-phase friction factor correlation, whereas the annular friction factor option uses a rough-wall, Colebrook-type single-phase friction factor with roughness heights equal to 5×10^{-6} m.)

Comparisons between the predicted and the measured axial pressure distributions for both runs are shown in Figures 2.1.2 and 2.1.3. Good agreement between the data and the pressure predictions was achieved. However, the homogeneous friction factor option slightly underpredicted the pressure at the throat for Run No. 3087. The pressure returned to the correct pressure in all the predictions because pressure boundary conditions were imposed at the entrance and exit of the test section.

2.1.4 Discussion

The key parameter, i.e., water mass flow rate, calculated by TRAC-PF1 is very sensitive to the friction factor option chosen for the calculation. The code underpredicted the water mass flow rate when the annular friction factor was used and overpredicted the same when the homogeneous friction factor option was chosen. Although the differences between the two axial pressure predictions, i.e., with the annular friction factor and the homogeneous friction factor, are small, the differences in the predicted water mass flow rate are quite large. The primary reason for this is the large difference in the single-phase friction factors used in these options. However, TRAC-PF1 is an improvement over the TRAC-P1A code, as stable steady-state results were obtained for both tests simulated with TRAC-PF1.

2.1.5 User Experience

No difficulty was encountered in running the TRAC-PF1 code for the Moby-Dick nitrogen-water tests. Relatively fine nodalization was used to ensure that the results are independent of node size. Similar nodalization was previously used for TRAC-P1A assessment. The computer run time statistics are shown in Table 2.1.2.

For RELAP5/MOD1, no useful calculation could be performed at BNL despite many attempts. The input deck was sent to the code developers at INEL; however, no response was received.

2.2 BNL Flashing Tests

2.2.1 Test Description

The BNL flashing tests (Abuaf et al., 1981) were simulated with the TRAC-PF1 (Version 7.0) and RELAP5/MOD1 (Cycle 14) codes to determine the capability of the codes in predicting the steady-state steam-water critical flow rate through a pipe or nozzle. Steady-state steam-water flashing tests at low pressures (p < 7 bar) were conducted in a vertical converging-diverging nozzle. The test section was made of stainless steel and it was symmetric about the throat. The throat inside diameter was 0.0254 m and the inside diameter at the inlet and outlet of the test section was 0.0508 m. The length of the converging-diverging portion of the test section was approximately 0.57 m. The total angle of convergence and divergence was approximately 5°. Subcooled water entered at the bottom of the test section and flowed upwards. As the pressure dropped, flashing began at or near the throat, and a two-phase mixture flowed through the diverging part of the test section. The vapor was condensed in the exit tank by spraying cold water, and the water from the exit tank was pumped back to the test section entrance.
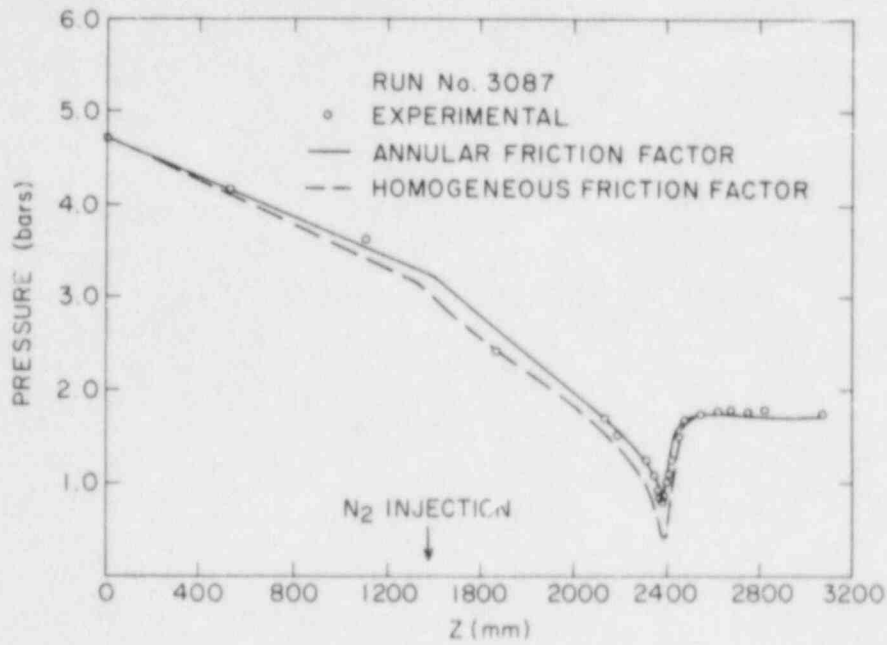
Figure 2.1.2 Comparison Between TRAC-PF1 Prediction and Experimental Data for Pressure (Run No. 3087).
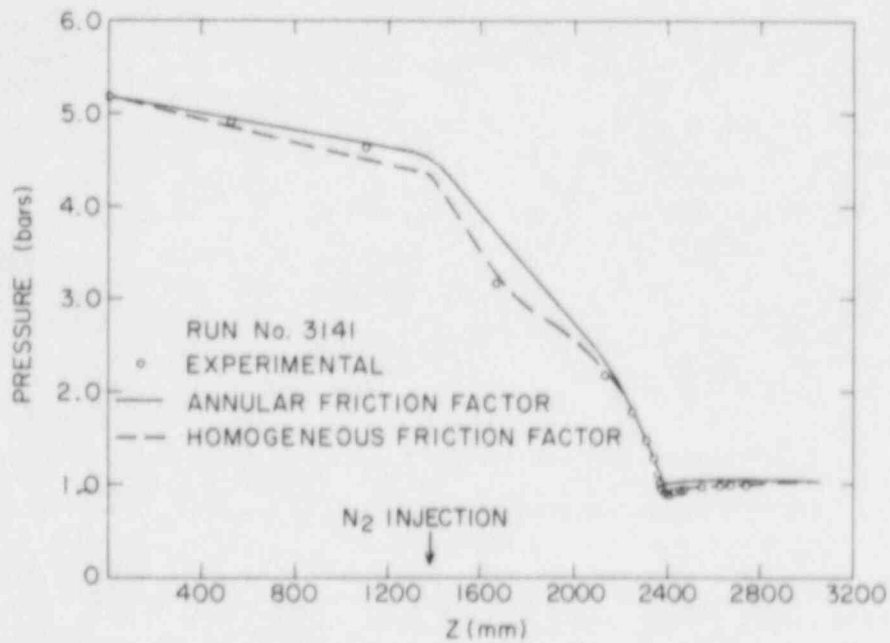
Figure 2.1.3 Comparison Between TRAC-PF1 Prediction and Experimental Data for Pressure (Run No. 3141).

Table 2.1.2 Computer Run Time for Moby-.ick Nitrogen-Water
Test Simulations

Computer: BNL CDC-7600
Code: TRAC-PF1 (Version 7.0)

Calculation Item	Test No. 3087		Test No. 3141	
	Annular Friction Factor	Homogenous Friction Factor	Annular Friction Factor	Homogeneous Friction Factor
No. of Cells	42	42	42	42
Problem Time (s)	3.92	10.3	2.004	1.137
No. of Time Steps	331	352	377	309
CPU Time (s)	49	54	64	42.8
CPU-to-Problem Time	12.5	5.2	31.9	37.6
CPU (s)/Cel` `Time Step	3.5×10^{-3}	3.6×10^{-3}	4.0×10^{-3}	3.3×10^{-3}

Experimental measurements included the axial pressure and area-averaged void fraction distribution along the test section. In addition, the pressure, temperature and the water flow rate at the test section inlet, and the pressure and temperature at the exit tank were measured. The measurement accuracies were:

Temperature:	$\pm$	0.1°C
Pressure:	$\pm$	1% of reading
Flow rate:	$\pm$	0.5% of reading
Void fraction:	$\pm$	0.05

Four tests have been simulated with TRAC-PF1 and RELAP5/MOD1. These are Run Nos. 291-295, 309-311, 318-321, and 339-342. Earlier, the same tests were simulated with TRAC-P1A and TRAC-PD2 (Saha et al., 1982b).

2.2.2   Input Models

The converging-diverging test section was represented in TRAC-PF1 with two PIPE components of forty-seven (47) cells each in series. All cell lengths were 0.00635 m, and the cell centers coincided with the pressure tap locations. The pressure boundary conditions at the inlet and exit of the test section and the water temperature at the inlet were specified, and the code

predicted the water mass flow rate through the test section. No choking model was used, allowing the code to calculate natural or self-choking condition. This allowed direct comparison between the TRAC-PF1 and TRAC-PD2 results. The homogeneous friction factor option (NFF=1) was used for all runs.

For RELAP5/MOD1, the converging-diverging test section was modeled with one PIPE component with forty eight (48) volumes. All cells were 0.0127 m long, except for the two on either side of the throat which had lengths of 0.00635 m each. The pressure boundary conditions at the inlet and exit of the test section and the water temperature at the inlet were specified, and the code predicted the water mass flow rate through the test section.

The RELAP5/MOD1 choking option had to be used for Run No. 291-295; otherwise the code would not produce a stable solution. For all other runs, the code was allowed to calculate a natural or self-choking condition like the TRAC calculations. Thus, the combined effects of the interfacial shear and the interfacial mass transfer were being assessed through these flashing tests.

2.2.3 Code Prediction and Comparison with Data

Both TRAC-PF1 and RELAP5/MOD1 flow predictions were much lower than the experimental values. These results were comparable to the TRAC-PD2 predictions as shown in Table 2.2.1. It can be seen that all codes significantly underpredicted the water mass flow rate data.

In general, the annular flow friction factor option of TRAC results in a lower prediction of the mass flow rate. However, the predictions were not expected to be very sensitive to this option since the frictional pressure drop component is a small fraction of the total pressure drop in a converging-diverging test section. This was confirmed by recalculating Runs 339-342 with TRAC-PF1, using the annular flow friction factor option. The predicted mass flow rate was 7.58 kg/s, which is less than 1% lower than the value (7.63 kg/s) predicted with the homogeneous friction factor option.

Figures 2.2.1 through 2.2.4 depict the pressure and area-averaged void fraction distributions along the length of the test section as predicted by the TRAC-PF1 and RELAP5/MOD1 codes, and the comparisons with the experimental data. In general, the predictions are significantly different from the data, as can be expected from the predicted lower mass flow rates shown in Table 2.2.1. Except for Run Nos. 291-295 where the RELAP5 choking option was used, the RELAP5/MOD1 and TRAC-PF1 results are close to each other. However, both codes significantly overpredicted the throat pressure for all tests, which is consistent with the predicted lower mass flow rates. This has also resulted in an overprediction of void fraction in the diverging part for most runs.

As shown in Figure 2.2.1, the choking option in RELAP5/MOD1 caused pressure oscillations just downstream of the throat for Run Nos. 291-295. As a result, the void fraction showed oscillations and the velocity decreased significantly. For all other runs, RELAP5/MOD1 predicted slightly higher void

fraction than TRAC-PF1, with some delay in void inception. These two effects, however, tend to compensate each other resulting in a very small difference in the predicted mass flow rates as shown in Table 2.2.1.

2.2.4 Discussion

Simulation of the BNL flashing tests with RELAP5/MOD1 and TRAC-PF1 showed similar results. In both cases, the code underpredicted the mass flow rate significantly. As expected, the TRAC-PF1 predictions were not very sensitive to the friction factor option since the frictional pressure drop component was a small fraction of the total pressure drop in the converging-diverging test section. Also, the mass flow rates predicted by TRAC-PF1 and RELAP5/MOD1 are quite close to those predicted by TRAC-PD2.

It should be noted that the TRAC-PF1 and RELAP5/MOD1 pressures in the converging section are very close to each other. However, they both overpredicted the experimental pressures in the converging section including the throat. In the experiment, no significant vapor generation or flashing occurred until the liquid reached the throat. As a result, there was a large pressure undershoot and liquid superheat (on the order of $5 - 10^\circ K$ for the experiments considered here) at the throat. Neither TRAC-PF1 nor RELAP5/MOD1 was able to predict this. Both codes predicted that flashing would occur upstream of the throat as soon as the liquid became slightly superheated (0.1 to $0.2^\circ K$ for TRAC-PF1 and $0.5 - 1^\circ K$ for RELAP5/MOD1). This resulted in a higher pressure prediction at the throat and, consequently, a lower mass flow rate. Therefore, inclusion of an accurate flashing delay model seems to be a necessary condition for achieving better agreement with the BNL flashing data.

Improved modeling is also necessary to achieve better agreement with the pressure and void fraction data in the diverging part of the test section. However, this seems to be of little or secondary importance in predicting the "correct" mass flow rate. Figures 2.2.1 and 2.2.4 show the TRAC-PF1 and RELAP5/MOD1 predictions for the pressure and void fractions in the diverging section to be quite different; yet, the mass flow rate predictions for these test were quite close (see Table 2.2.1). Therefore, the pressure calculations in the converging section, which were indeed quite close for the TRAC and RELAP5 calculation, dominate the mass flow rate prediction for subcooled critical flow. It should also be noted that TRAC-PF1 uses a two-fluid model in contrast to the drift-flux model previously used by TRAC-PD2. This brought about some changes in the pressure and void fraction predictions in the diverging section, but no significant change in the mass flow rate. Thus, a better agreement in the converging section is much more important for achieving a better agreement in the mass flow rate.

2.2.5 User Experience

No difficulty was encountered in running TRAC-PF1 for any of the BNL flashing tests. However, for one test, namely, Run Nos. 291-295, RELAP5/MOD1 produced severe oscillations when the choking option was not used. The test was then simulated with RELAP5/MOD1 using the choking option.

Table 2.2.1 Summary of BNL Flashing Flow Test Results

Run Nos.	Inlet Pressure (kPa)	Inlet Temperature (°C)	Exit Pressure (kPa)	Experiment Mass Flow Rate (kg/s)	TRAC-PF1		TRAC-PD2		RELAP5/MOD1	
					Mass Flow Rate (kg/s)	% Error	Mass Flow Rate (kg/s)	% Error	Mass Flow Rate (kg/s)	% Error
291-295	502	148.9	471	6.43	4.74	-26.2	5.08	-21.0	4.92*	-23.5
309-311	556	149.1	397	8.79	7.10	-19.2	7.28	-17.2	7.12	-19.0
318-321	322	121.1	167	8.98	7.74	-13.8	7.79	-13.2	7.85	-12.6
339-342	320	121.3	252	8.97	7.63	-14.9	7.69	-14.3	7.62	-15.1

*Prediction using the RELAP5 choking option; the calculation without the choking option failed.

COMPARISON OF PRESSURE DATA
BNL TESTS 291-295
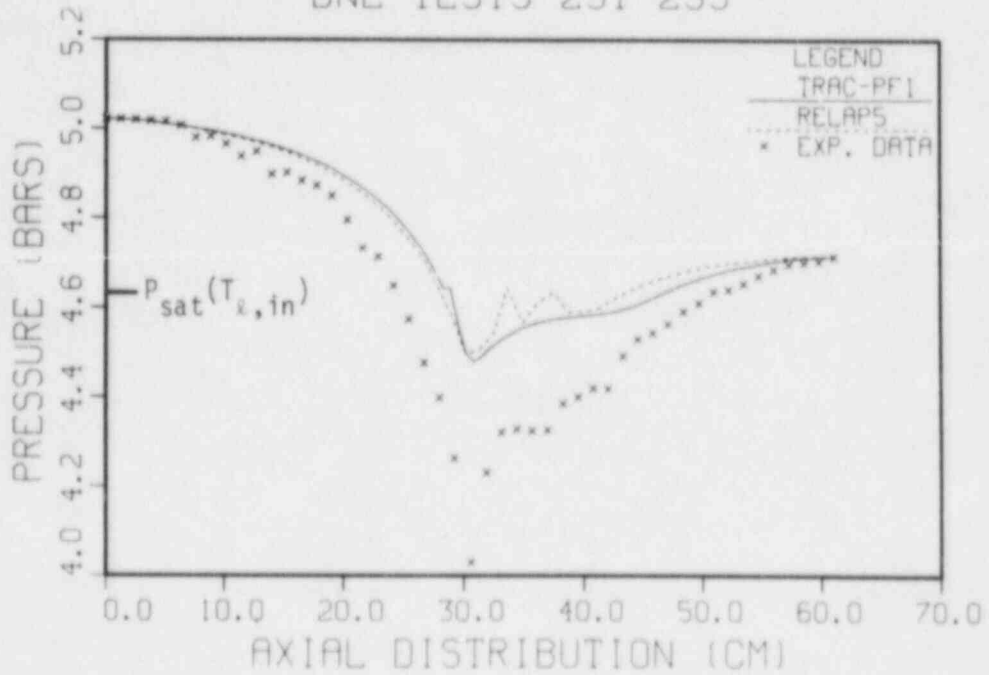
COMPARISON OF VOID FRACTION DATA
BNL TESTS 291-295
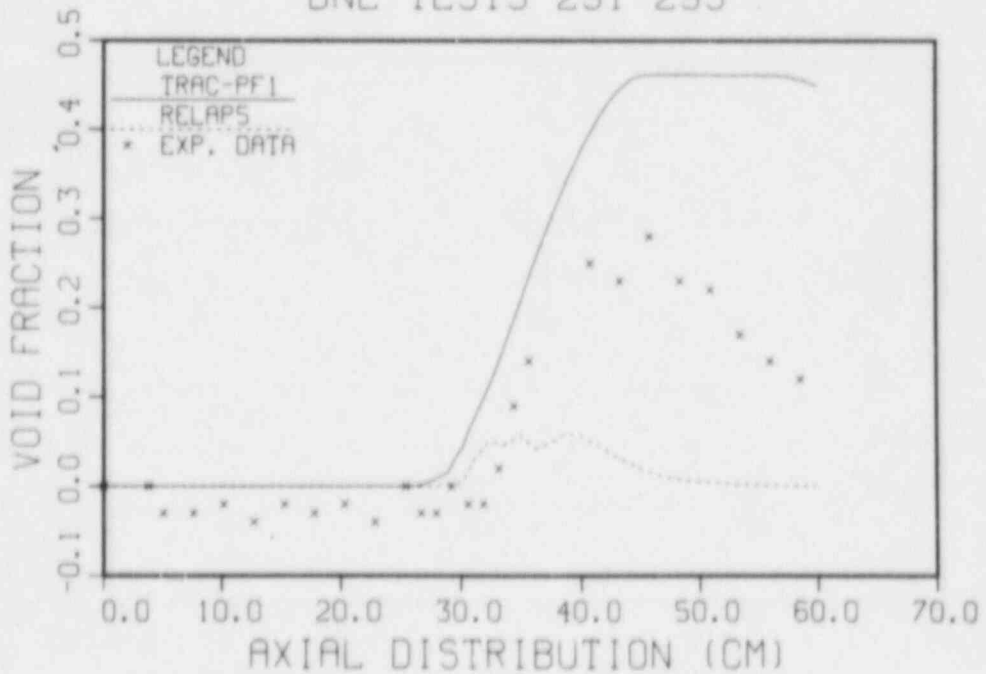
Figure 2.2.1 Comparison of TRAC-PF1 and RELAP5/MOD1 Predictions
for Pressure and Area-Averaged Void Fraction With
Experimental Data (Run Nos. 291-295).

COMPARISON OF PRESSURE DATA
BNL TESTS 309-311
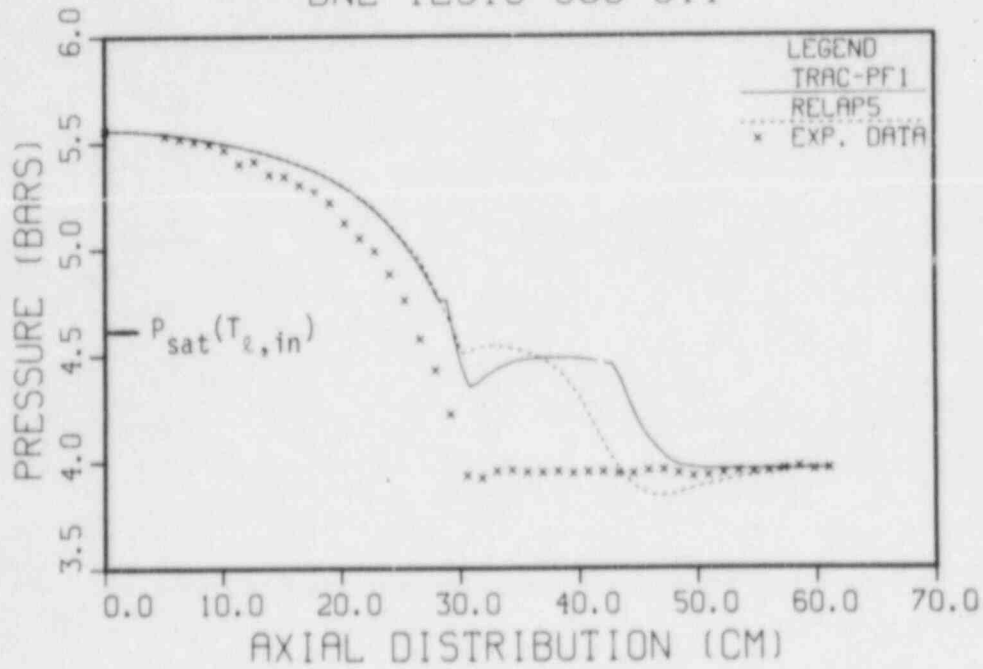
COMPARISON OF VOID FRACTION DATA
BNL TESTS 309-311
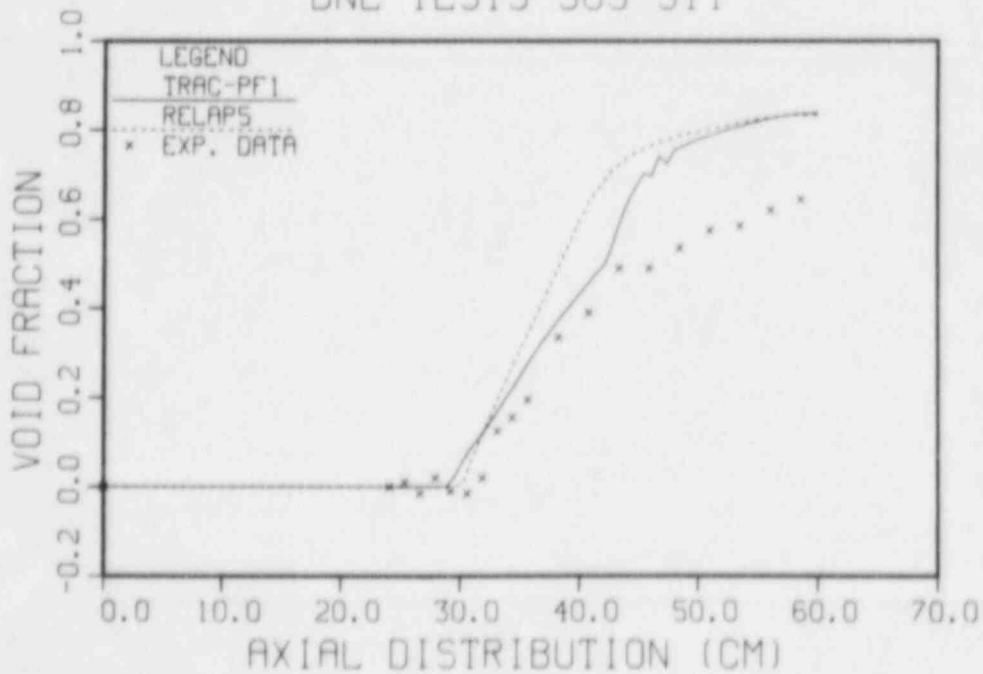
Figure 2.2.2 Comparison of TRAC-PF1 and RELAP5/MOD1 Predictions
for Pressure and Area-Averaged Void Friction With
Experimental Data (Run Nos. 309-311).

- 19 -

COMPARISON OF PRESSURE DATA
BNL TESTS 318-321

LEGEND
TRAC-PF1
RELAP5
× EXP. DATA

$P_{sat}(T_{\ell,in})$

PRESSURE (BARS)

AXIAL DISTRIBUTION (CM)

COMPARISON OF VOID FRACTION DATA
BNL TESTS 318-321

LEGEND
TRAC-PF1
RELAP5
× EXP. DATA

VOID FRACTION

AXIAL DISTRIBUTION (CM)
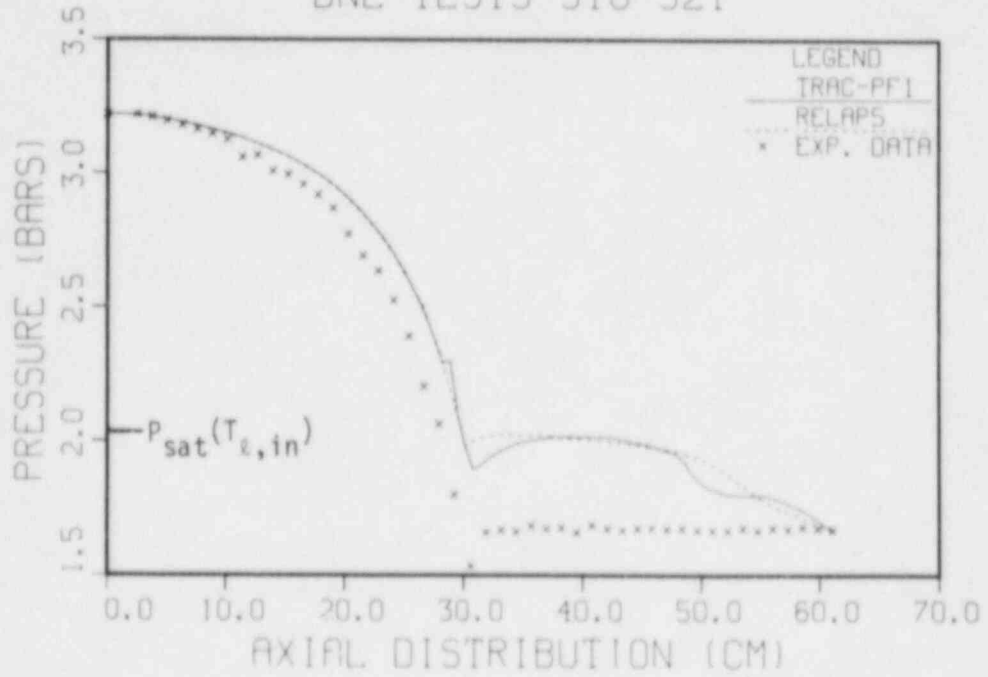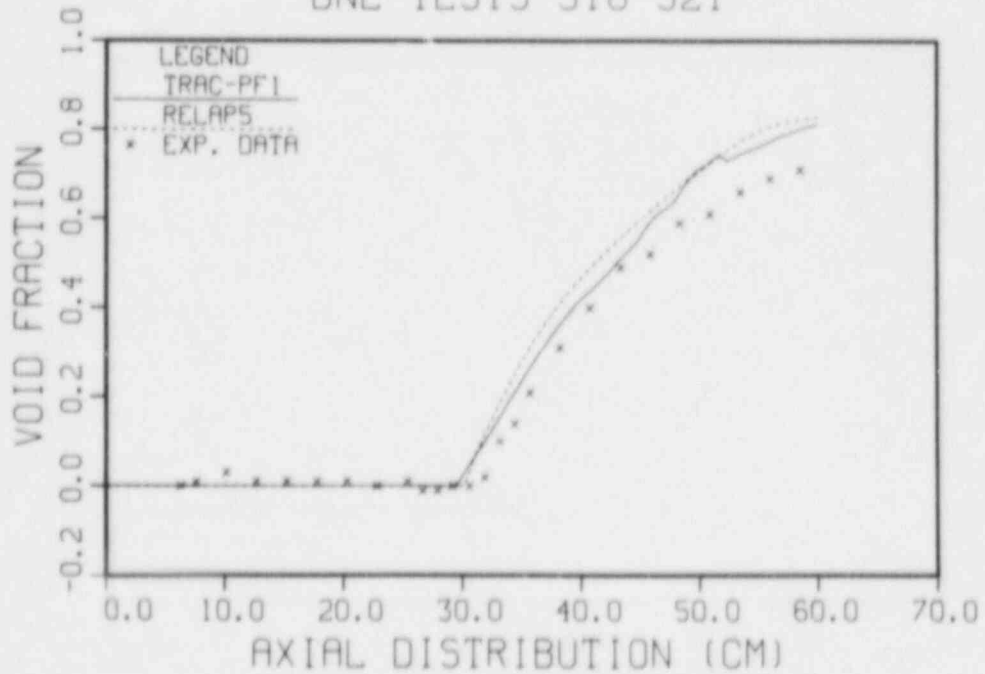
Figure 2.2.3 Comparison of TRAC-PF1 and RELAP5/MOD1 Predictions
for Pressure and Area-Averaged Void Fraction With
Experimental Data (Run Nos. 318-321).

COMPARISON OF PRESSURE DATA
BNL TESTS 339-342
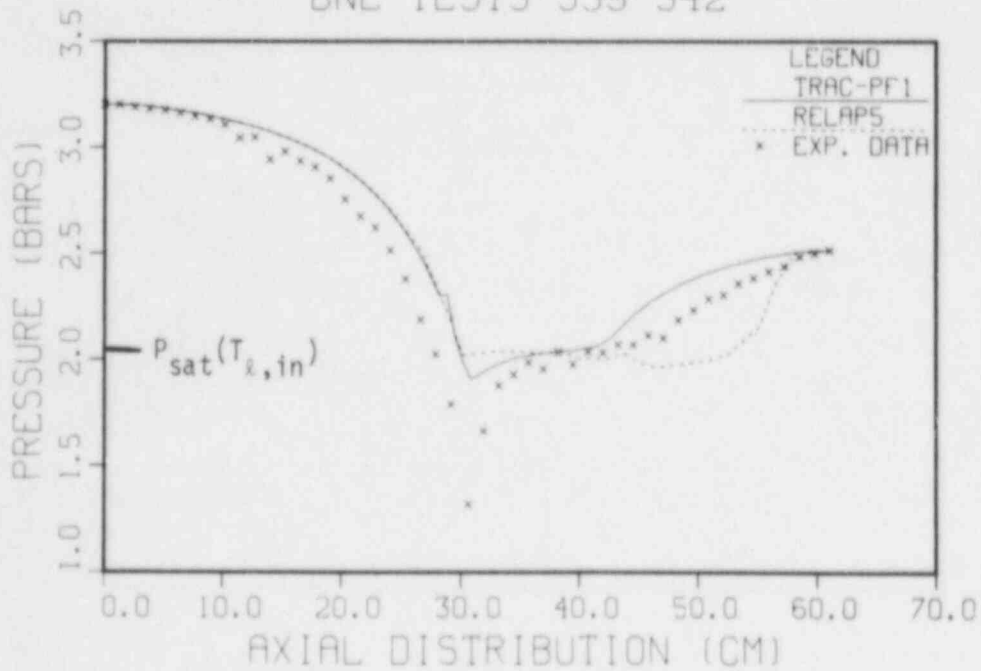
COMPARISON OF VOID FRACTION DATA
BNL TESTS 339-342
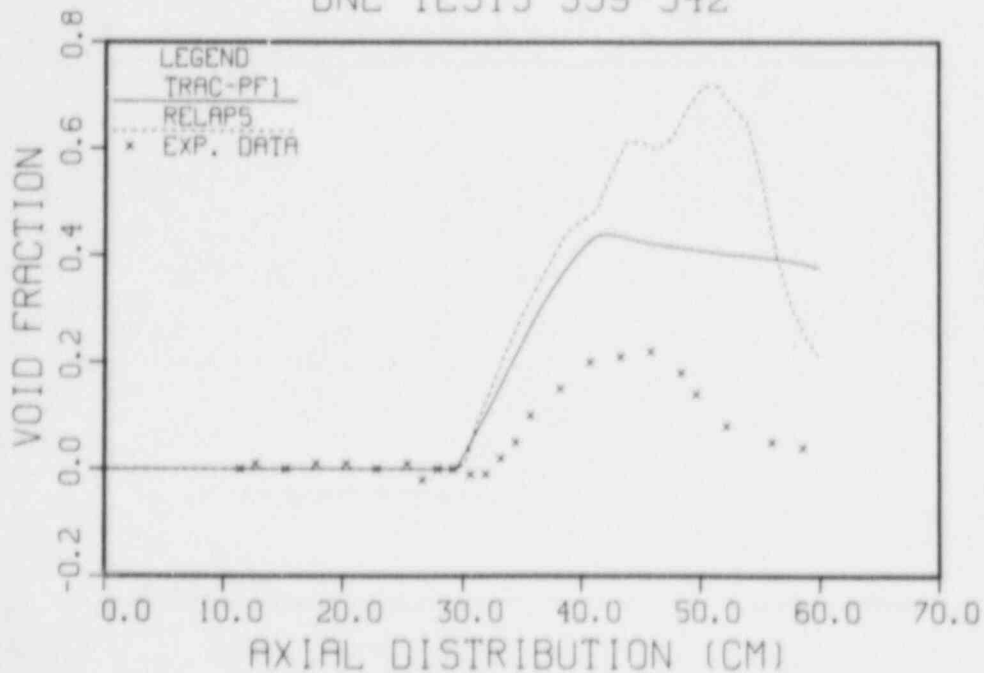
Figure 2.2.4   Comparison of TRAC-PF1 and RELAP5/MOD1 Predictions
for Pressure and Area-Averaged Void Fraction With
Experimental Data (Run Nos. 339-342).

Fine nodalization was used for both the TRAC-PF1 and RELAP5/MOD1 calculations in order to avoid any node size sensitivity in the results. Similar noding was also used in the previous TRAC-PD2 and TRAC-P1A simulations of the BNL flashing tests. The computer run time statistics for the present calculations are shown in Table 2.2.2.

2.3 Marviken Critical Flow Test

2.3.1 Test Description

The Marviken critical flow tests (Marviken, 1982) were conducted to study the blowdown of initially subcooled water from a full-scale reactor vessel through large-diameter pipes. The test apparatus consisted of a vessel with an inside diameter of 5.22 m and a height of 23.14 m. A vertical discharge pipe 6.3 m long with an inside diameter of 0.76 m was attached to the vessel bottom. The same vessel and discharge pipe were used for all tests. However, various-size vertical nozzles were attached to the bottom of the discharge pipe to study the effect of break diameters and nozzle lengths. A rupture disc assembly was installed at the downstream end of the test nozzle and it was burst to initiate the blowdown. Initially, the apparatus was partially filled with water at medium pressure (~50 bar) with a vapor region at the top of the vessel. The liquid level in the vessel, the amount of water sub-cooling, and the initial water temperature profile were varied from one test to another.

For the current assessment effort, Test No. 24 (Ericson, 1979) was se-lected. This test used a short nozzle with 0.5 m inside diameter. The nozzle had a rounded entrance section followed by a constant diameter (0.5 m) section 0.166 m in length. Thus, the length-to-diameter ratio of the nozzle was only 0.33. The initial average liquid subcooling in the vessel was 33°C. This test provides a formidable challenge to the code to predict the transient cri-tical flow rate accurately through full-scale short pipes. The test was pre-viously simulated with the TRAC-PD2 and TRAC-P1A codes (Section 2.4 of Saha et al., 1982b).

The experimental measurements included pressures, differential pressures, and fluid temperatures at many locations in the test apparatus. A three-beam gamma densitometer was employed to measure the fluid density in the discharge pipe, approximately 3.18 m above the nozzle entrance. The mass flow rate out of the nozzle was evaluated mainly by two methods: 1) by calculating the ves-sel mass inventory from the differential pressure measurements; 2) by using the pitot-static and fluid density measurements in the discharge pipe. The two methods produced reasonably close values of the mass flow rates. The errors in the measurements were as follows (Ericson, 1979):

Pressure:	$\pm$ 9 to $\pm$ 90 kPa
Temperature:	$\pm$ 0.6 to $\pm$ 2°C
Fluid density:	$\pm$ 50 kg/m^3 or more

Table 2.2.2 Computer Run Time Statistics for BNL Flashing Test Simulations

Computer: BNL CDC-7600

Calculation / Item	TRAC-PF1				RELAP5/MOD1			
	Run Nos. 291-295	Run Nos. 309-311	Run Nos. 318-321	Run Nos. 339-342	Run Nos. 291-295	Run Nos. 309-311	Run Nos. 318-321	Run Nos. 339-342
No. of Cells	94	94	94	94	48	48	48	48
Problem Time (s)	10.1	10.1	10.1	10.1	9.0	4.0	4.0	9.0
No. of Time Steps	277	371	977	282	15388	25920	25261	28258
CPU Time (s)	64	115	309	64	676	889	851	998
CPU-to-Problem Time	6.34	11.4	30.6	6.34	75.1	222.2	212.8	110.9
CPU (s)/Cell/Time-step	2.5×10^{-3}	3.3×10^{-3}	3.4×10^{-3}	2.4×10^{-3}	0.9×10^{-3}	0.7×10^{-3}	0.7×10^{-3}	0.7×10^{-3}

Mass flow rate:

a) Vessel inventory method: $\pm$ 5 to $\pm$ 12%

b) Pitot-static method: $\pm$ 3 to $\pm$ 10% in subcooled water region,

$\pm$ 8 to $\pm$ 15% in two-phase region.

2.3.2 Input Model Description

The test was simulated by both TRAC-PF1 (Version 7.0), and RELAP5/MOD1 (Cycle 14). One-dimensional components with the two-fluid formulation such as PIPE, BREAK and FILL of TRAC-PF1 were used. The vessel and the discharge pipe together were modeled by a PIPE component with 40 cells. The test nozzle was initially modeled by a PIPE component with 40 cells. The nodalization for the vessel and discharge pipe is shown in Figure 2.3.1. The cell lengths in the vessel and the discharge pipe varied from 0.02 m to 1.0 m. The cell lengths in the nozzle were smaller. Sixteen cells near the break were each 0.002875 m long, while 15 cells in the middle were each 0.008 m, and 9 cells near the discharge pipe were each 0.025 m long. Finer nodalizations were used around the vapor-liquid interface in the vessel, the area changes, and the nozzle exit where steep gradients in flow parameters could be expected.

A zero-flow boundary condition at the top of the vessel was provided by a FILL component, and a pressure boundary condition of 1.0 bar at the exit of the nozzle was provided by a BREAK component. Initially, there was no flow in the test apparatus and the pressure and the temperature conditions were provided from the data. The initial condition for fluid temperature is given in Figure 2.3.2. It was found that the wall friction factor options did not affect the large diameter system. Therefore, the annular friction factor option was used. No additive friction factor was used in any cell.

The simulation was performed in two ways. In the first calculation, the nozzle was modeled with the 40-volume PIPE described above, and the code was allowed to compute natural choking. The calculation took 417 CPU seconds for 55 seconds of transient time in the BNL CDC-7600 computer. In the second calculation, the nozzle was modeled with a 2 equal volume PIPE, and the TRAC-PF1 choking option at the BREAK was used. This calculation was faster and took only 128 CPU seconds for 55 seconds of transient in the same computer.

This test was also simulated with the RELAP5/MOD1/(Cycle 14) code. The nodalization for the vessel and the discharge pipe was exactly the same as in the TRAC-PF1 calculation, and it included a PIPE, a SINGLE VOLUME, and a TIME DEPENDENT VOLUME. The nozzle was modeled with a single volume, and the RELAP5 choking model was applied. The calculation took 189 CPU seconds for 60 seconds of transient on the BNL CDC-7600 computer.

- 24 -

MARVIKEN CRITICAL FLOW TEST
NODALIZATION
VESSEL AND DISCHARGE PIPE
PIPE COMPONENT, 40 CELLS

28.71 m ────

0.0 m ────

TO SCALE

Figure 2.3.1 Nodalization for Marviken Vessel and Discharge Pipe.
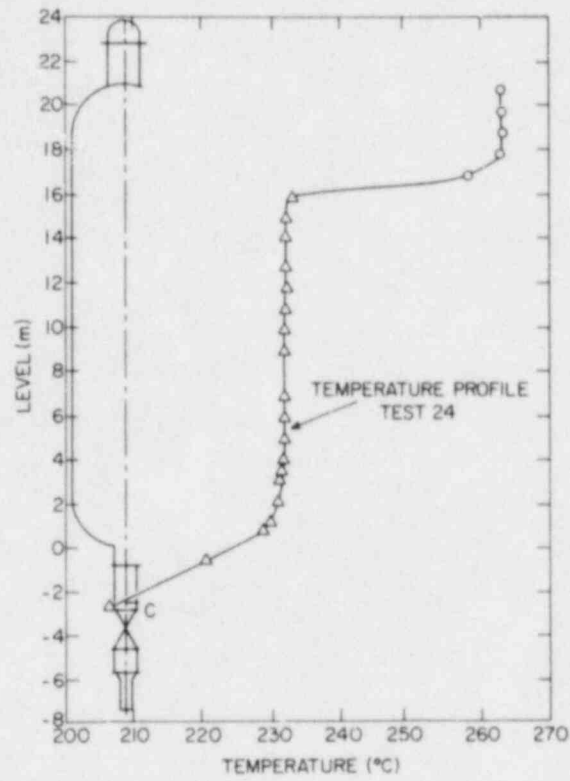
Figure 2.3.2   Initial Fluid Temperature Distribution for Marviken
Test No. 24.

2.3.3 Code Prediction and Comparison with Data

Figure 2.3.3 shows the comparison of the computed break mass flow rates with the data. TRAC-PF1 underpredicted the break mass flow rate for both cases. However, the first case with the 40-cell nozzle was slightly better than the second case with the two-cell nozzle. Figure 2.3.4 shows a comparison of computed vessel top pressure with the data. Here again, TRAC-PF1 underpredicted the pressure during the subcooled blowdown stage, and overpredicted the same during the saturated blowdown stage. However, both calculations are self-consistent, i.e., the case with the lower mass flow rate prediction computed the higher pressure. On the other hand, there is an anomaly between the computed break mass flow rate and the vessel top pressure; both are underpredicted during the subcooled blowdown period. Furthermore, both calculations failed to predict the initial pressure undershoot observed in the experiment. This indicates that TRAC-PF1 needs a flashing delay model as pointed out in Section 2.2.4.

TRAC-PF1 uses a two-fluid formulation for the PIPE component, as opposed to the drift-flux formulation used in TRAC-PD2. There have also been changes in the constitutive relationships. However, the TRAC-PF1 prediction for this test did not improve over the previous predictions with TRAC-PD2 (Section 2.4 of Saha et al., 1982b). TRAC-PF1 underpredicted the break flow rate by as much as 29% during the subcooled blowdown period (t < 20 seconds), whereas TRAC-PD2 underpredicted the same by no more than 25%. The error in the measured (or evaluated) mass flow rate was not more than 12%.

Figures 2.3.3 and 2.3.4 also show the comparison of RELAP5/MOD1 predictions with the data, and the TRAC-PF1 calculation. RELAP5/MOD1 also underpredicted the mass flow rate, but its prediction was closer to the data than that of TRAC-PF1. The largest discrepancy between the RELAP5/MOD1 break flow rate and the data was no more than 17%. RELAP5/MOD1 calculation also showed the same anomalous behavior between the vessel pressure and the mass flow rate, both being underpredicted in the subcooled blowdown region. However, it should be noted that RELAP5/MOD1 predicted a lower vessel top pressure than TRAC-PF1. This is consistent with the RELAP5/MOD1 break flow rate being larger than that of TRAC-PF1 in the subcooled blowdown period.

2.3.4 Further Analysis and Discussion

It is evident from Figures 2.3.3 and 2.3.4 that the TRAC-PF1 code predicted different mass flow rates and vessel top pressures depending on the type of modeling used for the nozzle. As these results were based on a complete modeling of the test apparatus, the break flow rates were affected by conditions inside the vessel. In order to study only the critical flow model in the subcooled blowdown period, the test nozzle and a small part of the discharge pipe, where temperature and pressure were measured, were simulated. The new set-up was modeled with two BREAK and one PIPE components for TRAC-PF1. The pressure and temperature boundary conditions at the inlet were specified from the data. The atmospheric pressure was provided as the boundary condition at the exit BREAK. The test section was modeled in two ways. In
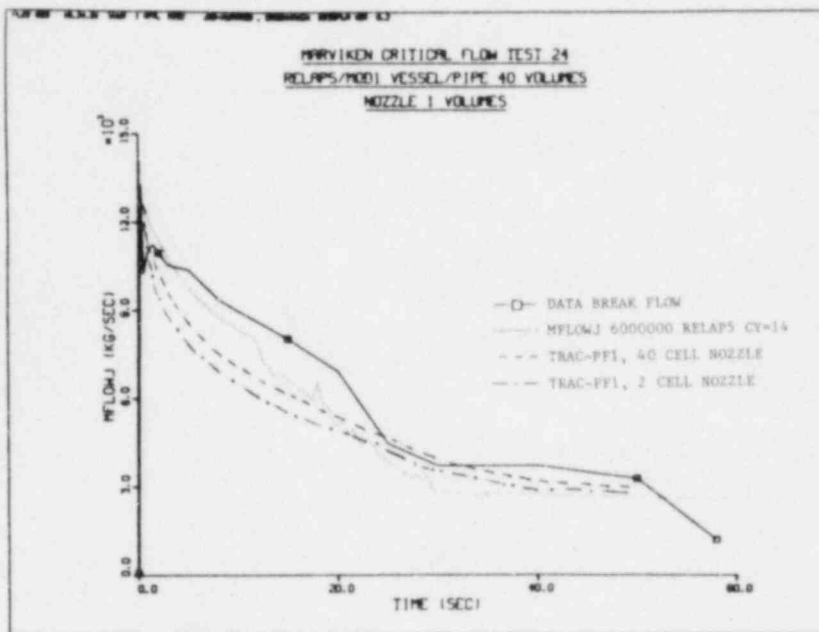
Figure 2.3.3 Comparison Between the Predicted (TRAC-PF1 and
RELAP5/MOD1) and the Measured Break Flow Rate for
Marviken Test No. 24.
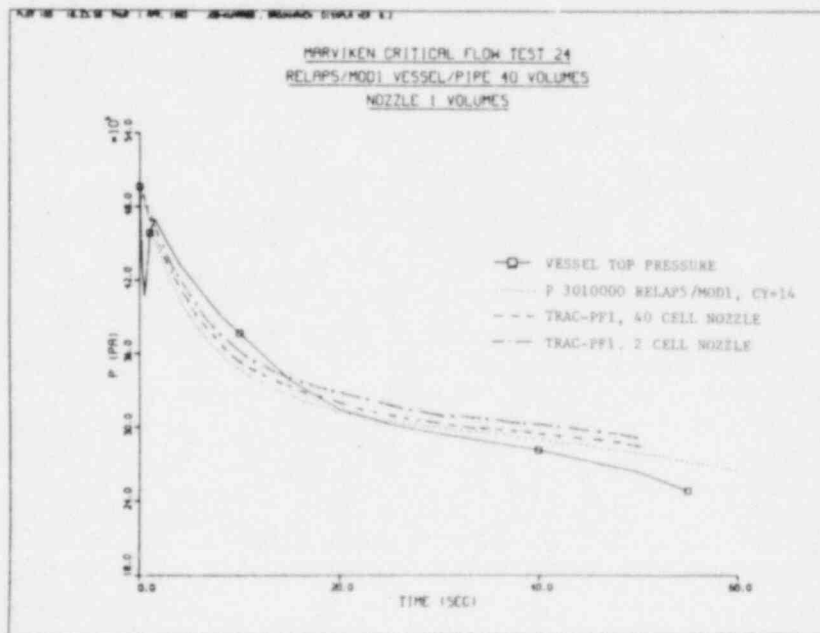
Figure 2.3.4 Comparison Between the Predicted (TRAC-PF1 and
RELAP5/MOD1) and the Measured Vessel Top Pressure
for Marviken Test No. 24.

the first approach, the PIPE component had 49 cells and the lower 40 cells represented the nozzle. No choking model was used for this approach; instead, the code was allowed to compute a natural or self-choking condition. In the second approach, the PIPE component had four cells and the lower two cells represented the nozzle. The choking model of TRAC-PF1 was used. This same setup was modeled in RELAP5/MOD1 with two TIME DEPENDENT VOLUMES, two JUNCTIONS, and a PIPE component. The PIPE component was modeled with various combinations of volumes to study the effect of nodalization on the critical flow model, and also to have the same nodalization as TRAC-PF1 simulation for intercode comparison.

Figure 2.3.5 shows a comparison of experimental and predicted break flow rates for TRAC-PF1 and RELAP5/MOD1 with the same nodalization. The first TRAC-PF1 calculation with the 40-cell nozzle and the self-choking option, underpredicted the mass flow rate which is consistent with the earlier full test simulation shown in Figure 2.3.3. However, the second approach with the 2-cell nozzle and the TRAC-PF1 choking option, yielded better agreement with the data than both the first approach (49 cell) of the TRAC-PF1 and RELAP5/MOD1 calculation. In fact, RELAP5/MOD1 results are quite close to the self choking case of TRAC-PF1. Figure 2.3.6 shows a comparison between the data and the predicted pressure at 76 mm above the nozzle exit. For all three calculations, the predicted pressures were higher than the data in the subcooled part of the transient. TRAC-PF1 and RELAP5/MOD1 have similar choked flow models. Both of them account for a flashing delay in computing pressure near the choked point. RELAP5 uses the Alamagir-Lienhard-Jones (Jones, 1980) model and TRAC-PF1 uses a modified Burnell model (Burnell, 1947; Zaloudek, 1963). This explains the difference in the predicted pressure near the choke point. Figure 2.3.7 shows a comparison of predicted void fractions near the exit. As the nodalizations for two TRAC calculations are different, the exit void fractions are not exactly at the same location but are in the last cell. RELAP5/MOD1 predicted a void fraction lower by an order of magnitude than both TRAC-PF1 calculations. The discrepancy can be attributed to the differences between the flashing delay and vapor generation models in the codes. There is also a difference between the two TRAC-PF1 calculations. The predicted void fraction is larger for the 49-cell self choking case, and so the fluid is probably closer to the equilibrium in this case. The above study also indicates that the vapor generation model in TRAC-PF1 is dependent on nodalization. It should be noted that the RELAP5/MOD1 calculation had better agreement with the data than other TRAC-PF1 calculations for full test simulations, and had worst agreement with the data for nozzle simulations. The reason for this discrepancy was probably due to the differences in the interfacial mass and momentum transfer models in these two codes. This phenomenon was more effective when large volumes with two phase regions were simulated for the full Marviken test.

The RELAP5/MOD1 code was also applied to the same nozzle/discharge pipe with three different nodalizations, and the results for break flow rate are shown in Figure 2.3.8. The best agreement with the data was obtained for the case where the discharge pipe was modeled with a three-volume pipe, and the nozzle was modeled as an area change junction. However, when the number of

- 29 -
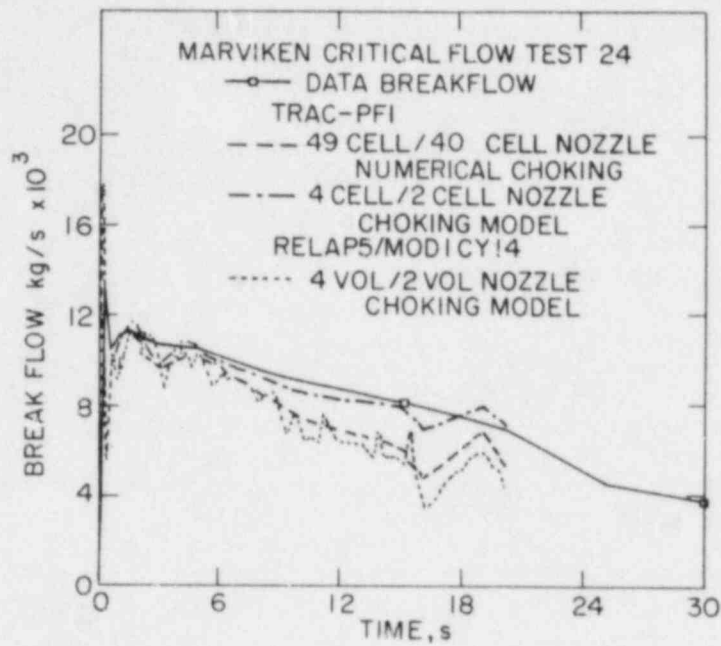
Figure 2.3.5   Comparison Between the Predicted and Measured Break
Flow Rates With Nozzle and Discharge Flow
Simulation Only.
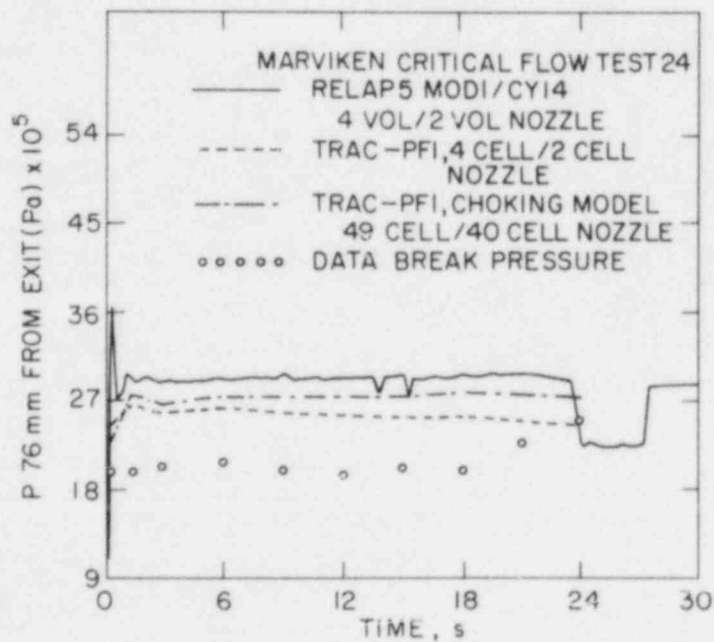
Figure 2.3.6   Comparison Between the Predicted and Measured Nozzle
Pressure With Nozzle and Discharge Pipe Simulation Only.
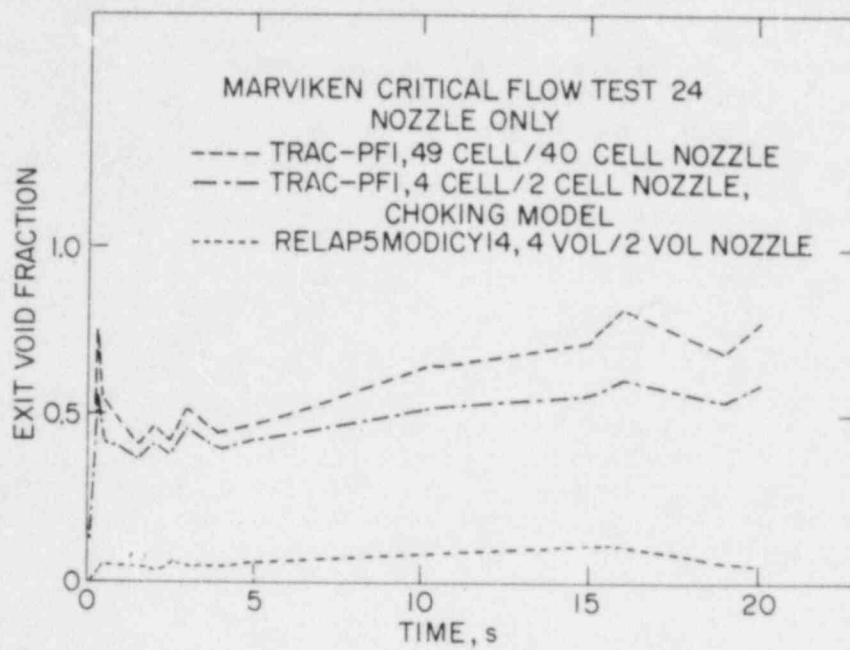
Figure 2.3.7   Various Predictions for Exit Void Fractions With
Nozzle and Discharge Pipe Simulation Only.
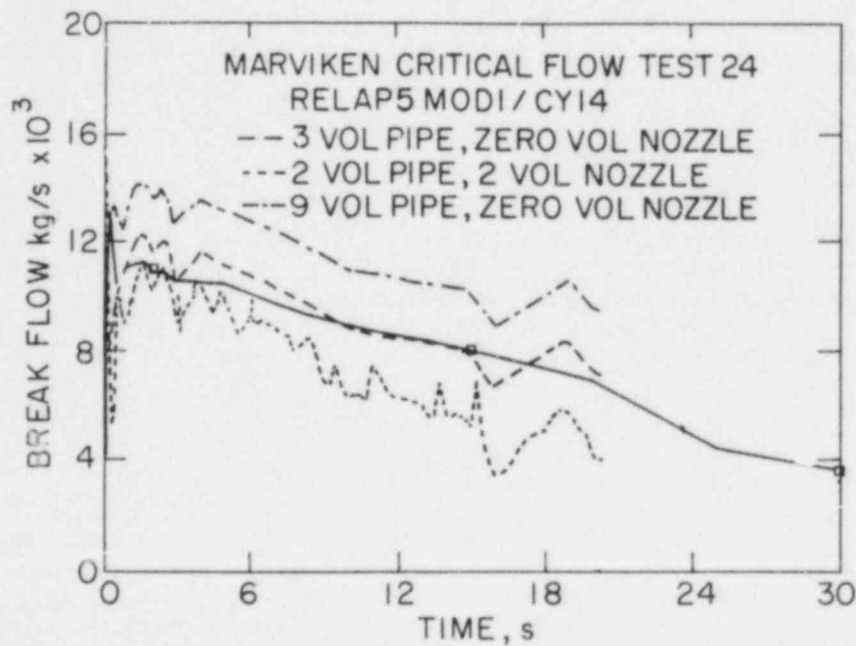
Figure 2.3.8   Various RELAP5/MOD1 Predictions and Comparison
With Break Flow Rate Data With Nozzle and Discharge
Pipe Simulation Only.

volumes in the discharge pipe was increased to nine, the code overpredicted the break flow rate. For the case with two volumes each in the discharge pipe and the nozzle, the code underpredicted the break flow rate. It should also be noted that in their original calculation for this test INEL modeled the nozzle as a zero volume area change and this is also their recommendation. The RELAP5/MOD1 results are clearly very sensitive to the nodalization which should be resolved by the code developers.

The following observations are made from the TRAC-PF1 and RELAP5/MOD1 predictions of the Marviken Test 24:

a) Neither TRAC-PF1 nor RELAP5/MOD1 predicted the pressure and mass flow rate undershoot due to lack of proper flashing delay correlations in their vapor generation models. However, this improvement alone may not be sufficient to achieve better agreement with the data for the entire transient. The codes do have different flashing delay models for computing the critical flow rate, but that does not affect the bulk vapor generation rate.

b) Two approaches to modeling the critical flow rate with TRAC-PF1 were tested. Both produced reasonable predictions, but the natural choking option (with a 40-cell nozzle) produced slightly better results for the mass flow rate for the full test prediction. The largest error here was comparable to the largest error in the earlier TRAC-PD2 calculation of this test (~25% in the subcooled blowdown stage).

c) The choking model in TRAC-PF1 produced better agreement with the mass flow rate and pressure data than the natural choking or RELAP5 calculation when only the nozzle part of the test was simulated. This is a better test of the code's ability to predict the critical flow, and the TRAC-PF1 choking model appears to be superior to that of the RELAP5/MOD1 code.

d) In the RELAP5/MOD1 simulation of the nozzle, the calculation had a strong dependence on nodalization. This should be resolved by the code developers through user guidelines. Since the nozzle section has a finite volume, we believe that it should be explicitly modeled. This is contrary to the code developer's recommendation of treating the nozzle as a zero-volume area change.

2.3.5 User Experience

No difficulty was encountered in running either the TRAC-PF1 or RELAP5/ MOD1 code for Marviken Test No. 24. Use of coarse noding at the nozzle with the choking option did reduce the computer running time. The run time statistics for the base calculations presented in Section 2.3.3 are shown in Table 2.3.1.

Table 2.3.1 Computer Time Statistics for Marviken Test No. 24 Simulation
Computer: BNL CDC-7600

Calculation / Item	TRAC-PF1		RELAP5/MOD1
	Without Choking Option	With Choking Option	With Choking Option
No. of Cells	80	42	41
Problem Time (s)	55	55	60
No. of Time Steps	2114	1202	6034
CPU Time (s)	419	128	189
CPU-to-Problem Time	7.62	2.33	3.15
CPU (s)/Cell/Time Step	2.5×10^{-3}	2.5×10^{-3}	0.76×10^{-3}

2.4 Summary and Conclusions

Both TRAC-PF1 (Version 7.0) and RELAP5/MOD1 (Cycle 14) were applied to several critical flow tests conducted in Moby-Dick nitrogen-water, BNL flashing, and Marviken critical flow test facilities. With the exception of RELAP5/MOD1 simulation of Moby-Dick nitrogen-water tests, all calculations provided useful results as presented in Sections 2.1 through 2.3. From these results the following conclusions can be drawn:

1. For the two-component, two-phase critical flow without phase change, TRAC-PF1 can be expected to produce stable results for all void fractions, which is an improvement over the TRAC-P1A code. However, the results are sensitive to the friction factor option selected for calculation. The homogeneous friction factor option overpredicts the mass flow rate by ~15 to 22%, whereas the annular friction factor option underpredicts the same by ~5 to 12%. It is recommended that the same single-phase friction factor be used for both the homogeneous (NFF=1) and the annular (NFF=2) flow friction factor options.

2. For the single-component (i.e., water) two-phase flow with phase change, both TRAC-PF1 and RELAP5/MOD1 may significantly underpredict the subcooled critical flow rate by as much as 25%, as shown in the BNL flashing test simulations. An accurate flashing delay model seems to be a necessary (although not sufficient) condition for achieving better agreement with the subcooled critical flow data. Simulation of Marviken Test No. 24 also supports this conclusion.

3. The choking option of TRAC-PF1 seems to be reasonable for subcooled critical flow through short nozzles if "correct" upstream boundary conditions are provided. For the RELAP5/MOD1 choking model, it seems that the short nozzles have to be treated as zero-volume area changes to obtain good agreement with data, even though this contradicts the reality. Also, the RELAP5/MOD1 choking model seems to be sensitive to nodalization. (Such a nodalization study was not performed for the TRAC-PF1 choking model.)

3. SIMULATION OF LEVEL SWELL EXPERIMENT

The GE large-vessel blowdown Test No. 5801-15 (Findlay, 1981) was simulated with both the TRAC-PF1 (Version 7.0) and the RELAP5/MOD1 (Cycle 14) codes. The purpose of this experiment was to study blowdown from the top of a large vessel partially filled with saturated water and the level swell caused by the rapid depressurization due to blowdown. These phenomena, i.e., top blowdown and level swell, are important for LOCA and steam line break analysis. Also, the water level in a BWR and in the steam generator secondary side of a PWR affects the function of the plant control system, and thus governs the course of many operational transients.

3.1 GE Large Vessel Test

3.1.1 Test Description

As shown in Figure 3.1.1, the test facility consisted of a carbon steel pressure vessel of 4.5 m³ (160 ft³) volume, 1.19 m (47 in.) inside diameter and 4.3 m (14 ft) height. The vessel was fitted with a blowdown line and a dip tube of 0.254 m (10 in.) diameter for top blowdown tests. The entrance to the dip tube was at 3.2 m (10.5 ft) elevation from the bottom of the pressure vessel. The blowdown flow rate and depressurization rate were varied by mounting different sized flow limiting venturi nozzles in the horizontal portion of the blowdown line. The tests were initiated by rupturing the disc assembly at the end of the venturi nozzle.

The experiment simulated at BNL, i.e., Test No. 5801-15, was a top blowdown test. The throat inside diameter of the venturi nozzle for this test was 0.0635 m (2.5 in.), and the vessel was initially filled with saturated water up to 1.68 m (5.5 ft) elevation at a pressure of 73.1 bar (1060 psia). The vessel pressure and axial void fraction distribution were measured during the transient.

3.1.2 Input Models

The base nodalizations used for TRAC-PF1 and RELAP5/MOD1 calculations are shown in Figure 3.1.2 along with a schematic of the test apparatus. For TRAC-PF1, the pressure vessel and the vertical dip tube leading to the venturi nozzle were modeled by a TEE component. The 7-volume primary pipe of the TEE represented the vessel, whereas the secondary pipe with four volumes modeled the dip tube. The vessel cross-sectional area was appropriately reduced to take into account the presence of the dip tube inside the vessel. A 3-volume PIPE component represented the converging straight and diverging sections of the venturi nozzle. Two zero-velocity FILL components and one BREAK component where the atmospheric pressure was specified, completed the TRAC model. Choking option was applied at the venturi nozzle.

The RELAP5/MOD1 model was practically the same as the TRAC-PF1 model. The pressure vessel was represented with a 5-volume PIPE, a BRANCH and a one-volume PIPE in series. The dip tube was modeled with a four-volume pipe connecting the BRANCH and the venturi nozzle represented by a three-volume PIPE.
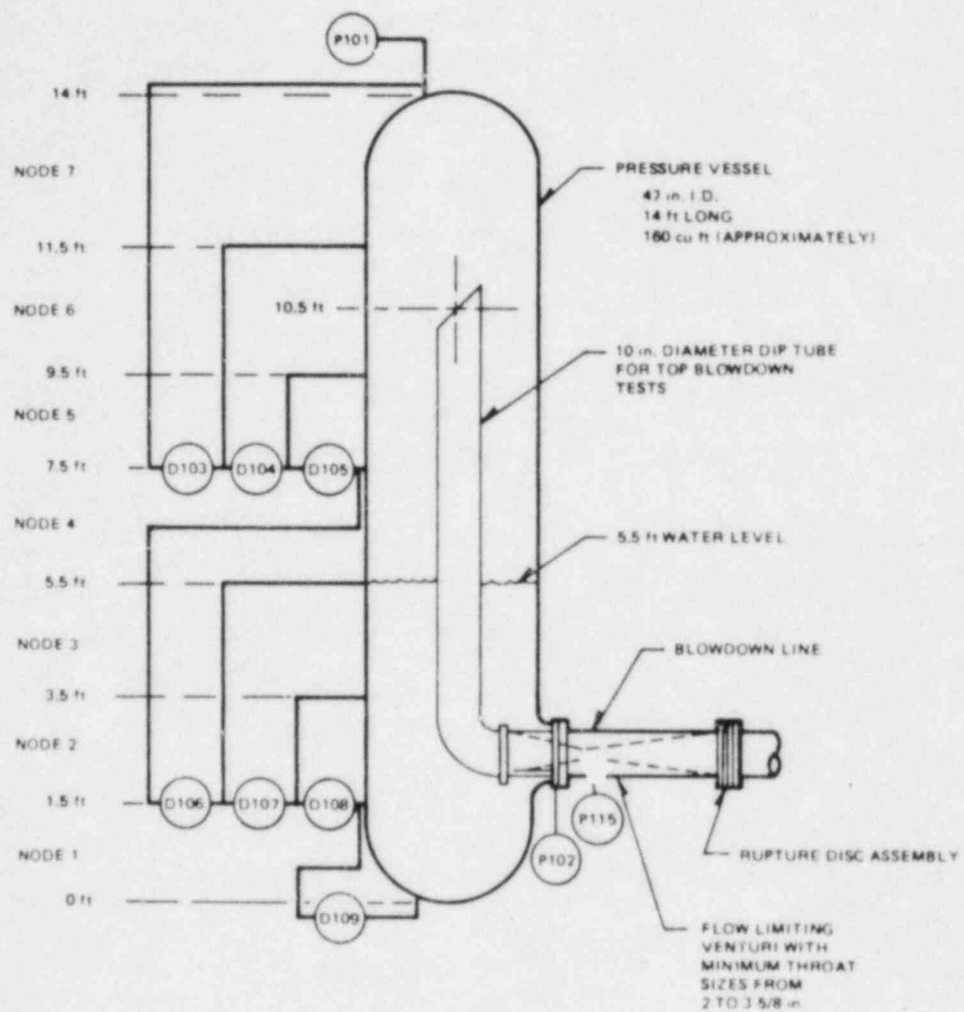
Figure 3.1.1 GE Large Vessel Test Facility.

A time-dependent volume (TMDPVOL) with atmospheric pressure completed the model. The RELAP5/MOD1 choking option was applied at the nozzle.

To study the effect of nodalization, both the TRAC and RELAP5 calculations were repeated with different nodalizations (e.g., 21-volume vessel with 2-volume nozzle, 7-volume vessel with 2-volume nozzle, 7-volume vessel with 6-volume nozzle, etc.). In addition, a RELAP5/MOD1 calculation was run where the nozzle was represented with a junction only as recommended by the code developers. The junction had the nozzle throat area.

3.1.3 Code Predictions and Comparison with Data

Only the base case results with seven volumes in the vessel and three volumes in the nozzle are discussed in this section. As shown in Figure 3.1.3, the vessel pressure calculated by the TRAC-PF1 code agreed closely with the data except for the initial two seconds, while the agreement between the computed and the measured vessel pressure was not as good for RELAP5/MOD1. Neither calculation showed a slight dip in pressure before a steady decline occurred because neither code includes a flashing delay model for bulk flow.

Figure 3.1.4 shows the predicted axial void fraction distributions along with the data at various times during the transient. The void fractions calculated by TRAC-PF1 were generally higher, and the calculated level swell rate was faster than the data. On the other hand, the void fractions calculated by RELAP5/MOD1, although relatively close to the data, showed an irregular axial distribution.

The higher void fractions and the faster level swell rate calculated by TRAC-PF1 were believed to be caused by a high interfacial shear. High interfacial shear reduces the bubble rise velocity and retains the bubbles longer in the water, thus swelling the water level at a faster rate. Likewise, an improper interfacial shear package is probably responsible for the irregular axial void fraction profiles predicted by the RELAP5/MOD1 code.

Figure 3.1.5 shows the total break flow integrated over time plotted with respect to time. The data for the break flow rate were not directly available, but were estimated from the data on void fraction distribution. TRAC-PF1, while adequately predicting the vessel pressure, overpredicted the data for the integrated break flow rate. This appears to indicate that the flashing or vapor generation rate during depressurization is too high in TRAC-PF1. This seems consistent with the higher TRAC-PF1 void fraction prediction which creates more interfacial area for larger vapor generation rate. In contrast, RELAP5/MOD1 shows the opposite trend. It underpredicts the pressure while showing good agreement with the data for the integrated break flow rate, indicating a lower flashing rate. Note that the RELAP5/MOD1 void fractions below the mixture level are indeed lower than those for TRAC-PF1. Thus, there seems to be a consistency between the void fraction and the vapor generation rate for both codes.

NODALIZATION DIAGRAM

TEST   TRAC-PFI   RELAP5
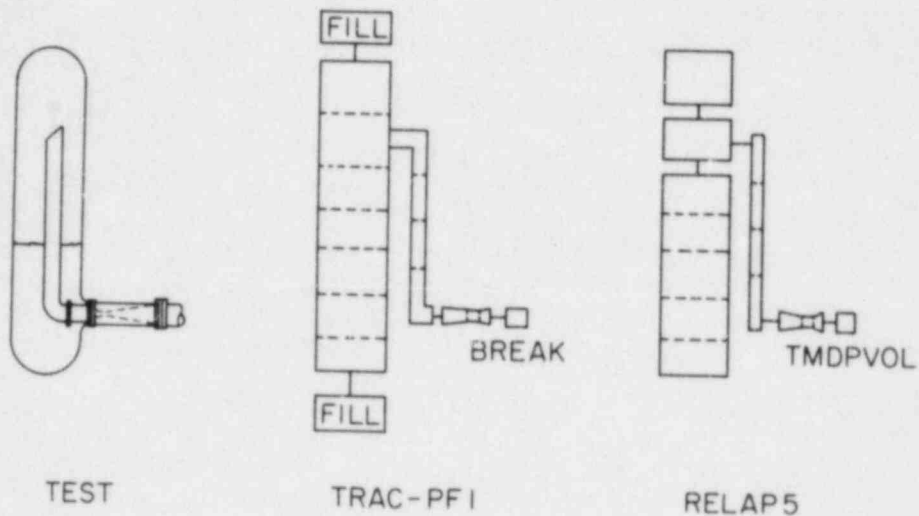
Figure 3.1.2   Noding Diagrams of TRAC-PF1 and RELAP5/MOD1
               Input Models for GE Level Swell Test.
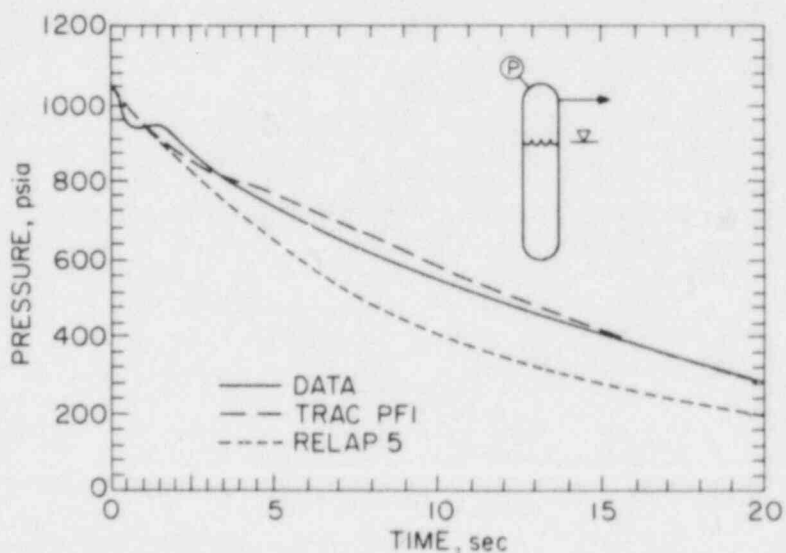
Figure 3.1.3   Comparison Between the Predicted (TRAC-PF1 and
               RELAP5/MOD1) and Measured Pressure in the Vessel.

G. E. LARGE VESSEL BLOWDOWN TEST

AXIAL VOID DISTRIBUTION
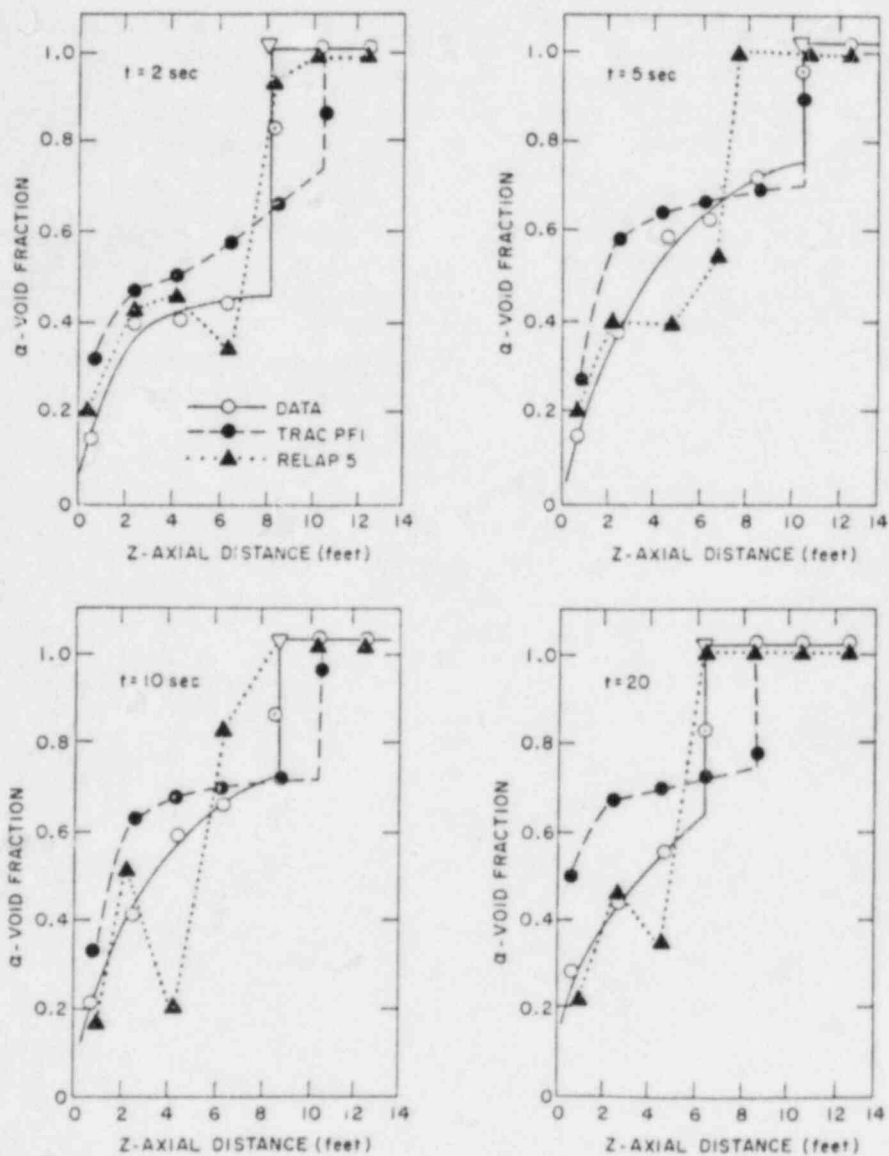
Figure 3.1.4 Comparison Between the Predicted (TRAC-PF1 and RELAP5/MOD1)
and Measured Axial Void Fractions at Various Times.

3.1.4 Further Analysis and Discussion

As mentioned in Section 3.1.2, calculations were performed with different nodalizations. For both TRAC-PF1 and RELAP5/MOD1, the new results were very close to the base results shown in Figures 3.1.3 through 3.1.5. Only the RELAP5/MOD1 calculations with a zero volume nozzle showed some difference. This is shown in Figures 3.1.6 and 3.1.7. However, note that all RELAP5/MOD1 calculations including the one with the zero volume nozzle showed an irregular axial void fraction profile and significantly underpredicted the vessel pressure. Therefore, it can be concluded that the RELAP5/MOD1 interfacial shear (or drag) package needs improvement. It is our understanding that the shear package has been significantly revised for the newer version of RELAP5, i.e., RELAP5/MOD2.

TRAC-PF1 also needs improvement in the interfacial shear package since it tends to overpredict the void fraction and the level swell rate. Also, the TRAC-PF1 results obtained for the GE large vessel test were very similar to those obtained for the Battelle-Frankfurt top blowdown test with TRAC-PD2 (Section 2.5 of Saha et al., 1982b). Therefore, it can be concluded that changes made to the TRAC-PD2 code did not significantly improve the predictions of the level swell tests.

3.1.5 User Experience

There was no difficulty in running either the TRAC-PF1 or the RELAP5/MOD1 code for the GE large-vessel top blowdown test. The base nodalization with a 7-volume vessel and a 3-volume nozzle was found to be adequate for both TRAC-PF1 and RELAP5/MOD1 calculations. From the accuracy viewpoint, it was not necessary to treat the nozzle as a zero-volume junction as suggested by the RELAP5 code developers, although, this does improve the computer running time. The run time statistics for both TRAC-PF1 and RELAP5/MOD1 calculations for this test are given in Table 3.1.1.

3.2 Summary and Conclusions

Both the TRAC-PF1 (Version 7.0) and the RELAP5/MOD1 (Cycle 14) code were assessed using the GE large vessel Test No. 5801-15. Neither code experienced any particular difficulty in calculating the test. From the results presented in Sections 3.1.3 and 3.1.4, the following conclusions can be drawn:

1. Both the TRAC-PF1 and the RELAP5/MOD1 code need a more accurate flashing delay model for the bulk or pipe flow. The present delay models in the choked flow formulation cannot predict the early pressure undershoot observed in the experiment. This undershoot and the corresponding liquid superheat could be important in determining the vapor generation rate later in the transient.

2. TRAC-PF1 tends to overpredict the void fraction below the mixture level and the level swell. It also overpredicts the break flow rate (by as much as 20%), although the pressure prediction agrees quite well with the data. A high interfacial shear in the TRAC-PF1 code is believed to be partially responsible for higher void fraction and higher level swell rate.

GE LARGE VESSEL BLOWDOWN TEST
TOTAL BREAKFLOW
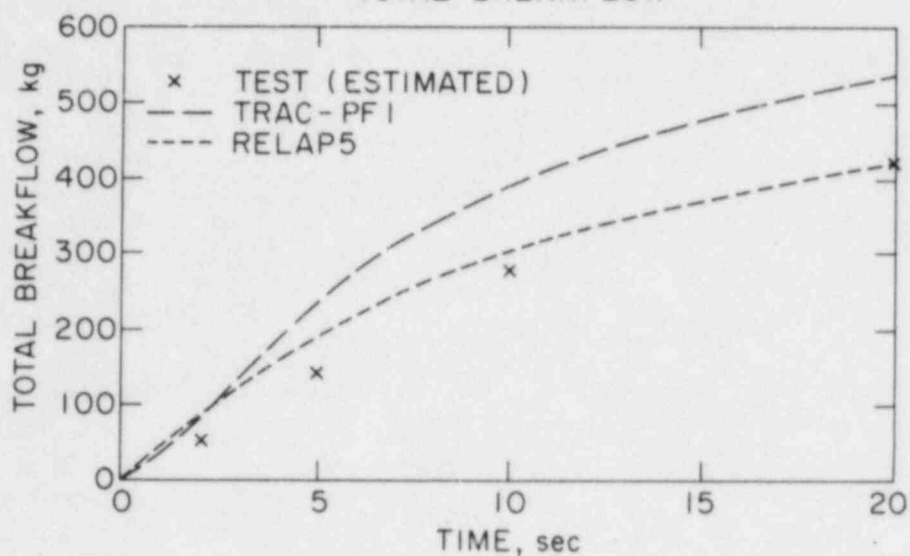
Figure 3.1.5 Comparison Between the Predicted (TRAC-PF1 and RELAP5/MOD1) and Estimated Total Break Flow.
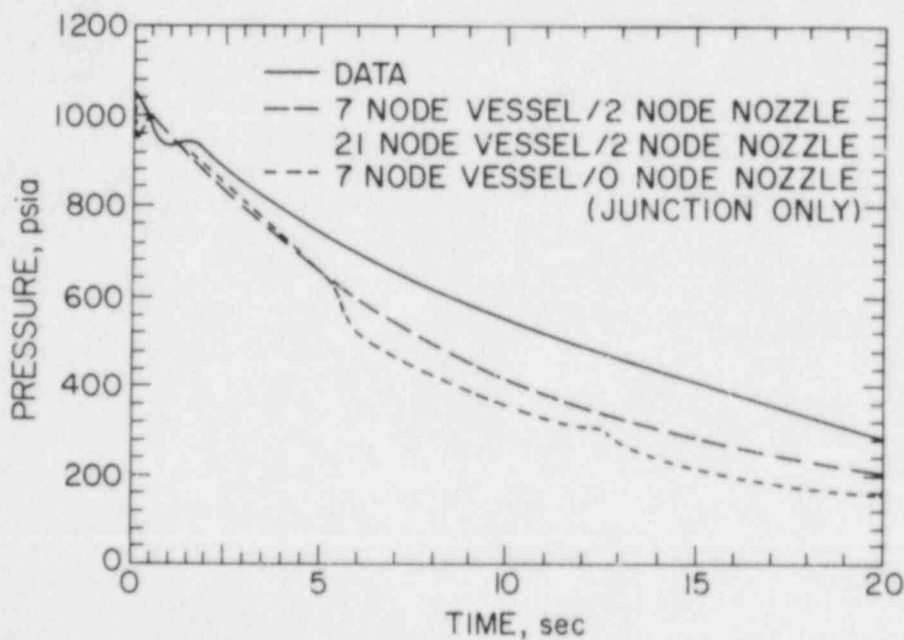
Figure 3.1.6 Comparison of Various RELAP5/MOD1 Predictions of Vessel Pressure With the Measured Data.
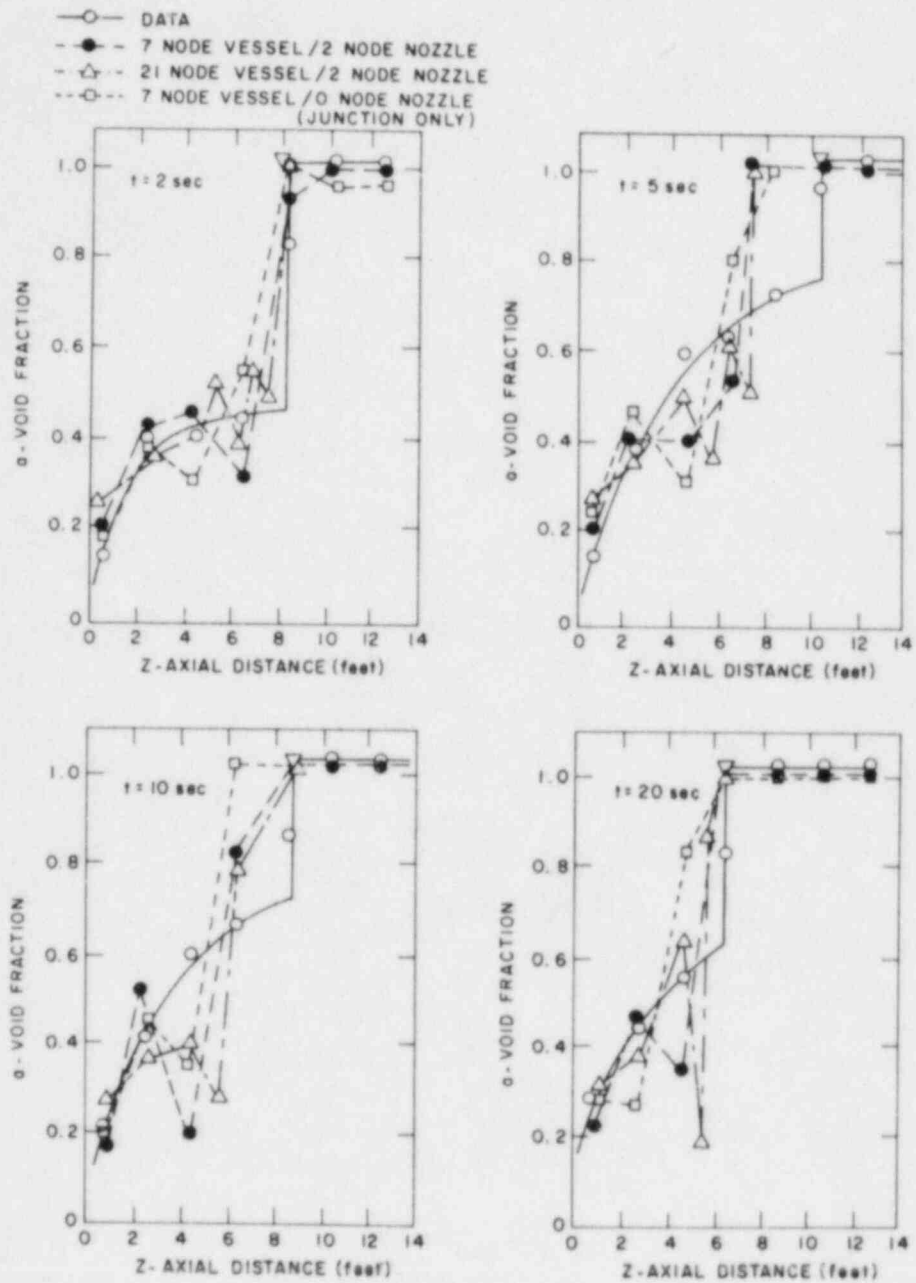
Figure 3.1.7   Comparison of Various RELAP5/MOD1 Predictions of Axial
Void Distribution With Experimental Data at
Different Times.

3.   RELAP5/MOD1 predictions for average void fraction, level swell rate, and break flow rate seem reasonable. However, the code underpredicts the vessel pressure and produces an irregular axial void fraction profile. It seems that the interfacial shear package of RELAP5/MOD1 needs reexamination and improvement.

4.   The base nodalization as shown in Figure 3.1.2 seems to be adequate for calculation of the level-swell-type phenomenon. Also, there seems to be no need of representing the discharge nozzle with a zero volume junction for the RELAP5/MOD1 calculation, as suggested by the RELAP5 code developers.

Table 3.1.1   Computer Run Time Statistics for GE Large Vessel
Test No. 5801-15

Computer: BNL CDC-7600

Calculation / Item	TRAC-PF1 3-Volume Nozzle	RELAP5/MOD1 3-Volume Nozzle	RELAP5/MOD1 Zero-Volume Nozzle
No. of Cells	14	14	11
Problem Time (s)	20	20	20
No. of Time Steps	236	28814	7798
CPU Time (s)	21	400	115
CPU-to-Problem Time	1.05	20	5.75
CPU (s)/Cell/Time Step	6.3×10^{-3}	0.99×10^{-3}	1.34×10^{-3}

4. SIMULATION OF COUNTERCURRENT FLOW LIMITATION (CCFL) EXPERIMENTS

Countercurrent flow limitation (CCFL) or "flooding" is an important phenomenon for both PWR and BWR LOCAs. Because of steam upflow in a PWR downcomer and a BWR core during the ECC (Emergency Core Cooling) water injection, there will be some delay before the ECC water can reach the core. This delay is expected to be important in determining the peak clad temperature (PCT) during a LOCA. CCFL is also important in a Once-Through Steam Generator (OTSG) operation since the auxiliary feedwater is injected at the top of the steam generator.

The amount of liquid downflow for a given upflow of gas or vapor depends primarily on the interfacial shear and liquid entrainment. Therefore, air-water tests can be used as a first step for assessing the CCFL prediction capability of the advanced codes. At BNL, all three codes, namely, TRAC-PF1 (Version 7.0), RELAP5/MOD1 (Cycle 14), and TRAC-BD1 (Version 12.0), were applied to the air-water flooding tests conducted at the University of Houston and Dartmouth College. First, the tests conducted in single round tubes will be discussed. Later, the TRAC-PF1 and TRAC-BD1 results for parallel-tube CCFL tests conducted at Dartmouth College will be presented. (Based on the RELAP5/MOD1 predictions of the single-tube tests, the code was not applied to the parallel-tube tests.)

4.1 University of Houston Tests

4.1.1 Test Description

The test section was a 4.11 m long, 0.05 m I.D. vertical tube. Water at ambient pressure and temperature was injected into the middle of the test section through a 0.225 m long porous section surrounded by a jacket. Air at ambient pressure and temperature was supplied at the bottom through a collecting chamber, which was also used to collect and measure the water downflow rate. The top of the test section was connected to another chamber in which the liquid film was separated from the air-droplet mixture and the upward film flow rate was measured. The air-droplet mixture was passed through a separator and the entrained liquid flow rate was measured. There were four stations on the test section for film thickness measurements and four more stations for pressure measurements. A schematic of the test facility is shown in Figure 4.1.1. Further details of the test section and instrumentation can be found in the data report (Dukler and Smith, 1979).

Four different water feed rates were used: 100 lb/hr (0.0126 kg/s), 250 lb/hr (0.0315 kg/s), 500 lb/hr (0.063 kg/s), and 1000 lb/hr (0.126 kg/s). In each series of tests, the air flow rate was gradually increased from 120 lb/hr (0.01512 kg/s) to 300 lb/hr (0.0378 kg/s). The air flow rate at the flooding point or the onset of liquid upflow increased as the water feed flow rate was decreased.

For the current assessment, the test series with water feed rates of 100 lb/hr and 1000 lb/hr were chosen. These two water feed rates produced two distinctly different flooding situations.

4.1.2 Input Models

In principle, the test could be simulated either with the one-dimensional TEE components or with the VESSEL module of TRAC-PF1 with one cell per axial level. However, both components use the same two-fluid formulation with only minor differences in the constitutive package. Also, one-dimensional components take much less computer time per cell than the VESSEL module. Therefore, it was decided to use the TEE components for most of the calculations.

For both the TRAC-PF1 and TRAC-BD1 calculations, the test set-up was modeled with two TEE components as shown in Figure 4.1.2. The bottom TEE had 8 cells in the primary pipe and the side pipe for air injection was connected to the 6th cell. A zero-flow FILL component was attached to the bottom of this TEE to simulate the closed end. The top TEE which represented most of the test section had 23 cells in the primary pipe and the water was injected through the side pipe connected at the 12th cell. The top of this TEE was connected to a BREAK component where the system or atmospheric pressure was imposed as a boundary condition.

The RELAP5/MOD1 model for the test apparatus was also similar to that shown in Figure 4.1.2. Two BRANCH and three PIPE components were used. The branches were connected to two TIME DEPENDENT JUNCTIONS for simulating the air and water injections. The top PIPE was connected to a TIME DEPENDENT VOLUME where the system pressure was imposed. The middle PIPE represented the section between the water and air injection points, whereas the bottom PIPE with a closed end represented the lower part of the test section. Thus, the same nodalization and node sizes were used for all three codes.

The codes were run for a given water and air injection rate until a "stable" situation was achieved. The calculated liquid downflow rate was time averaged and compared with the data. Each calculation represented a point on the CCFL or flooding curve. Thus, several calculations were needed to generate the CCFL curve for a given water injector rate (e.g., 100 lb/hr or 1000 lb/hr). Each calculation took anywhere from 50 to 140 CPU seconds in the BNL CDC-7600 computer. The CPU-to-real time ratio for TRAC-PF1 and RELAP5/MOD1 was 2 to 4, whereas that for TRAC-BD1 was 15 to 20.

4.1.3 Code Predictions and Comparison with Data

A test case with water feed rate of 100 lb/hr and air flow rate of 200 lb/hr was simulated with TRAC-PF1, first using the VESSEL module and then using the TEE component. Figure 4.1.3 shows a comparison of liquid velocities and void fraction distributions at the upper part of the test section as predicted by TRAC-PF1 with two different approaches. It seems that using the VESSEL module, TRAC-PF1 predicted a higher liquid velocity and a higher void fraction than that using the TEE component. Higher liquid velocity implies a thinner film or a smaller area fraction for the liquid phase, and so the void fraction will be higher. Thus, both calculations are self-consistent. However, it was surprising that although both the VESSEL and the TEE components use the same two-fluid formulation, slightly different results were obtained. Slightly different interfacial momentum transfer or shear packages were used

- 45 -
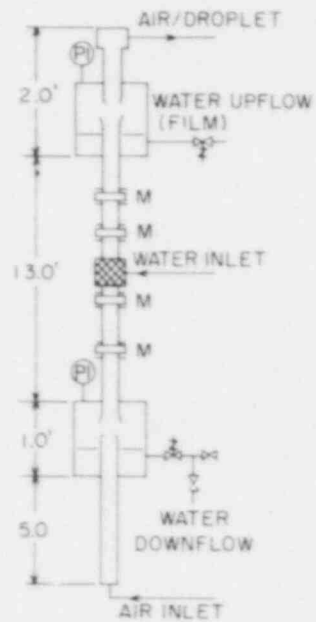
Figure 4.1.1   Schematic of the University of
Houston Flooding Test Facility.
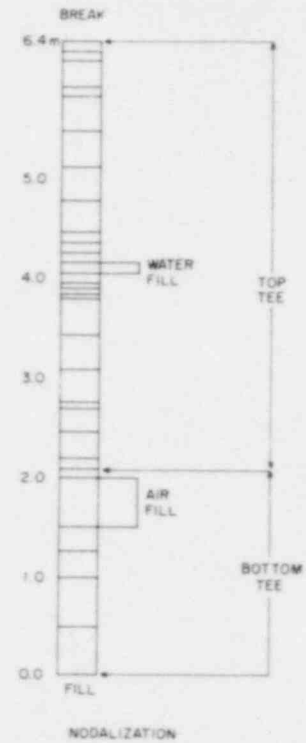
Figure 4.1.2   TRAC-PF1 and TRAC-BD1 Noding Diagram
for the University of Houston
Flooding Tests.
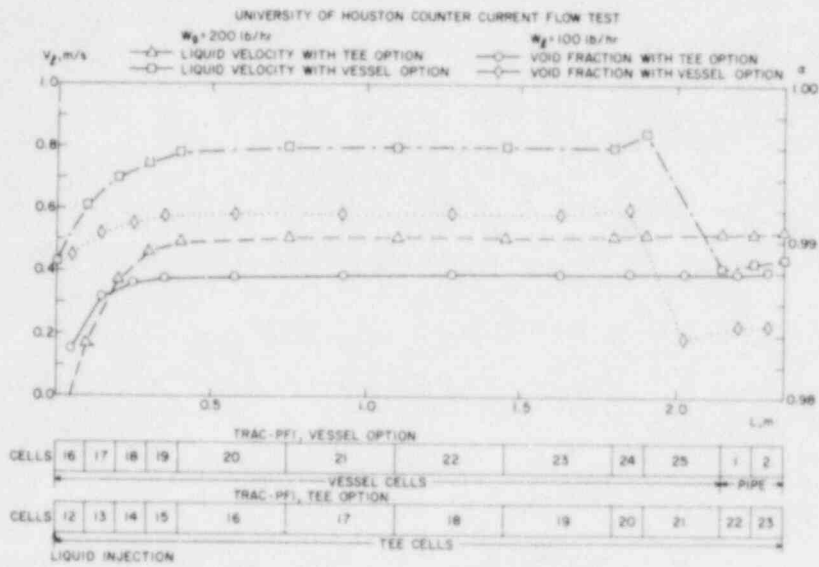
Figure 4.1.3 Comparison of TRAC-BD1 Results Using Two Different Modeling Approaches (VESSEL vs. TEE).

in these modules yielding different liquid velocities. This was confirmed when the FORTRAN coding of these components were reviewed at BNL; there were indeed some differences. Finally, it was decided to use the TEE components for TRAC calculations, as less computer time was required. Also, as shown in Figure 4.1.3, there were some irregularities in the TRAC-PF1 VESSEL results at the exit of the test pipe.

4.1.3.1 Water Feed Rate of 100 lb/hr

In the first series of tests, the water injection rate was 100 lb/hr and the air flow rate varied from zero to 300 lb/hr. This test was simulated with TRAC-PF1, RELAP5/MOD1, and TRAC-BD1, and the comparison of predicted liquid downflow rate for specified air flow rate with the data is shown in Figure 4.1.4. For comparison purposes, the TRAC-PD2 result reported earlier (Section 2.6 of Saha et al., 1982b) is also shown in the figure. It can be seen that TRAC-PF1 underpredicted the liquid downflow rates and showed some oscillations in the filling rate. This indicates that either the interfacial shear or the entrainment rate or both were overpredicted.

The RELAP5/MOD1 results were in poor agreement with the data. At only 50 lb/hr air flow rate, the code predicted a total upflow of all the injected water. The reason for this poor prediction is that RELAP5/MOD1 assumes a droplet flow regime for void fraction greater than 0.95 and does not allow for a liquid film on the wall. However, in the University of Houston tests, liquid flowed down as a film on the wall even when the void fraction was greater than 0.95. RELAP5/MOD1 was unable to recognize this film or annular flow regime and, therefore, predicted a total upflow of liquid in the droplet form.

Of the three codes, TRAC-BD1 yielded the best agreement with the data. Two TRAC-BD1 predictions are shown in Figure 4.1.4. One was obtained using the CCFL option available in TRAC-BD1, and the other without it. The TRAC-BD1 result without the CCFL option slightly overpredicted the liquid downflow rate, indicating that either the interfacial shear or the entrainment rate or both were slightly underpredicted. However, when the CCFL option was used, the liquid downflow rate was restricted to what was allowed by the Kutateladze flooding correlation for a specified air flow rate. This set of calculations slightly underpredicted the liquid downflow rate. Note that the experimental data lie between these two sets of TRAC-BD1 calculations.

4.1.3.2 Water Feed Rate of 1000 lb/hr

The second series of tests which were simulated with all three codes used a water injection rate of 1000 lb/hr. In this case also, the comparison between the code predictions and the data was the same as the previous series with a water feed rate of 100 lb/hr. As shown in Figure 4.1.5, the TRAC-BD1 predictions are in best agreement with the data. Also, most of the experimental data points do lie between the two TRAC-BD1 predictions, one with and the other without the CCFL correlation.

TRAC-PF1 again underpredicted the liquid downflow rate, as did RELAP5/MOD1. As a matter of fact, RELAP5/MOD1 predicted a total upflow of injected water at only 50 lb/hr air flow rate.

4.1.4 Discussion

The countercurrent flow in these University of Houston tests was governed by the interfacial shear at the liquid film and the liquid entrainment rate. In case of no air flow rate, all the liquid flowed down. As the air flow rate was gradually increased, the liquid film interface became rough and led to inception of liquid entrainment. Some of the entrained droplets were deposited on the wall above the water injection point and formed a film. Figures 4.1.4 and 4.1.5 show the air flow rates at which the liquid downflow rate started to decrease from the total liquid injection rate. These points (e.g., air flow rate of 250 lb/hr for the water feed rate of 100 lb/hr, and the air flow rate of 135 lb/hr for the water feed rate of 1000 lb/hr) represent the inception of liquid entrainment. It should be noted that TRAC-PF1 underpredicted these entrainment inceptions for both water feed rates, whereas TRAC-BD1 which uses the Ishii-Mishima model (Ishii, 1981) produced mixed results. RELAP5/MOD1, on the other hand, did not have an entrainment model and assumed a pure mist or droplet flow for void fractions greater than 0.95.

Figures 4.1.4 and 4.1.5 also show the air flow rates at which the liquid downflows approached zero owing to sufficiently high air flow rates. Good prediction of this part of the test will depend upon correct interfacial shear and entrainment rates. TRAC-BD1 uses an interfacial shear model based on the Ishii (1977) drift velocity and the void distribution parameter, C_0. TRAC-PF1 uses a model of interfacial shear based on Dukler's correlation (1980). RELAP5/MOD1 computes the interfacial shear at the annular film from the Wallis correlation (1970). These models have been compared in Figure 4.1.6. In general, the Wallis correlation (1970) yields a lower interfacial shear coefficient than the Dukler correlation (1980). Thus, a code using the Wallis correlation would predict a higher liquid downflow rate than a code using the Dukler correlation.

In general, the University of Houston tests are more useful for assessing the entrainment model than the interfacial shear model. However, if the entrainment rate from the test could be substituted in a code, then the interfacial shear model can be explicitly assessed. A study (Popov, 1983) was undertaken at BNL to assess the various models for entrainment rate and interfacial shear which have been used in the advanced code or are currently available in the literature. The study concluded that the modified Ishii entrainment model and the Bharathan-Wallis model (1979) for interfacial shear are probably the best for countercurrent flow applications.

4.1.5 User Experience

No particular difficulty was experienced in running the TRAC-PF1, RELAP5/MOD1, and TRAC-BD1 codes for the University of Houston tests. However, the calculations never reached a "steady state"; therefore, the calculated liquid downflow rates had to be averaged over certain time periods for comparison with the data.
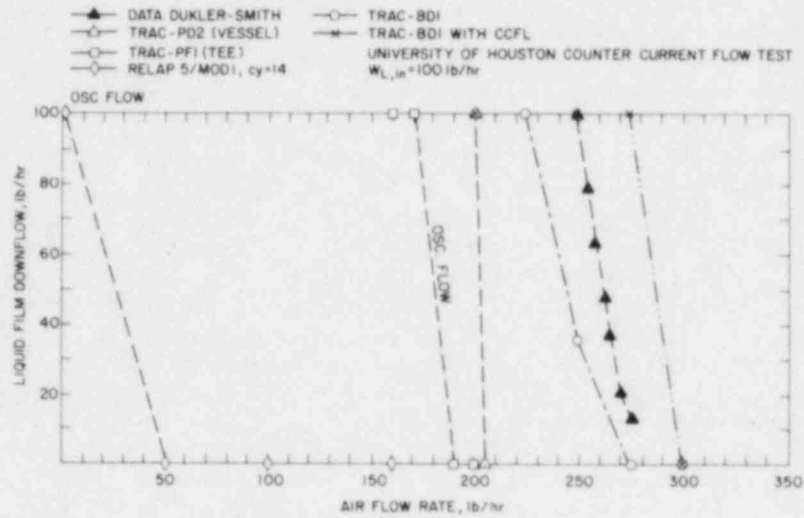
Figure 4.1.4   Comparison Between the Predicted (TRAC-PF1, RELAP5/MOD1, TRAC-BD1) and Measured Data Liquid Downflow for Water Feedrate of 100 lb/hr.
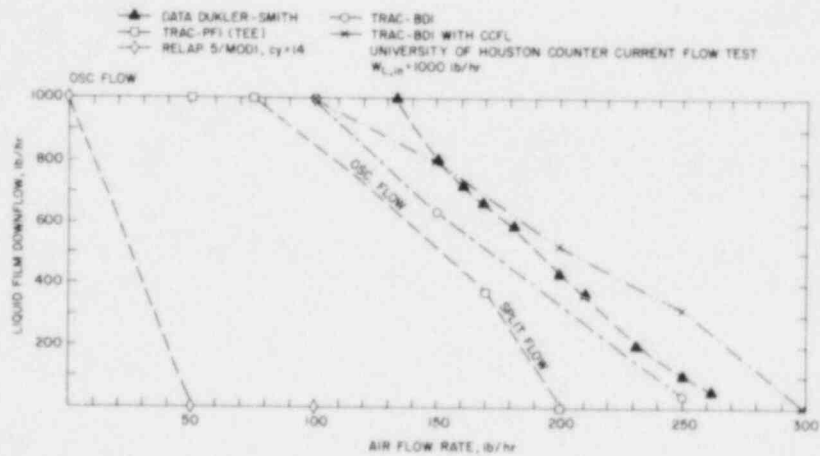
Figure 4.1.5   Comparison Between the Predicted (TRAC-PF1, RELAP5/MOD1, TRAC-BD1) and Measured Data on Liquid Downflow for Water Feedrate of 1000 lb/hr.
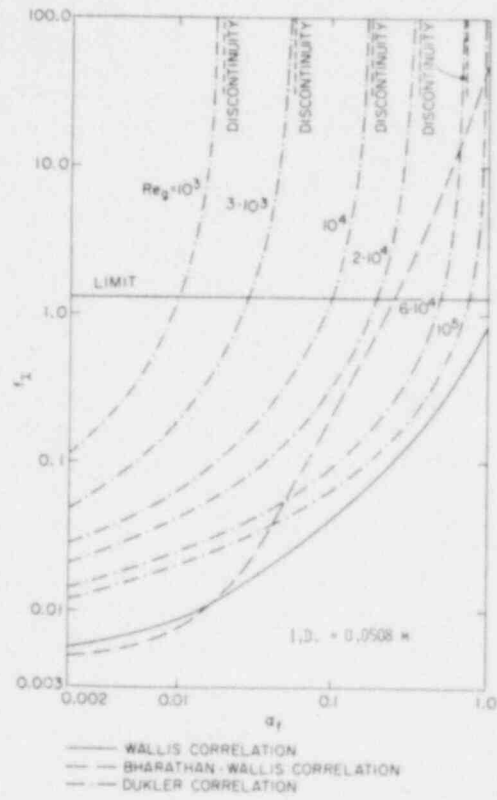
Figure 4.1.6 Comparison of Various Interfacial Shear Correlations for Annular Flow for 0.0508 m Pipe I.D.

4.2 Dartmouth College Single Tube Tests

4.2.1 Test Description

The test set-up, shown in Figure 4.2.1, consisted of a vertical test section (pipe) connected to an upper and a lower plenum. Water at room temperature was injected in the upper plenum, where a liquid level was maintained by controlling the height of a drain pipe and the water flow rate. Air was injected in the lower plenum. The water downflow rate was determined from the water collected in the lower plenum over a fixed time. The tests were conducted for various pipe and plena sizes and test section to plena junction geometry. The details of the test results can be found in Bharathan (1979).

For the purpose of code assessment, the test sections of the inside diameter of 0.0254 m and 0.152 m with square-edge entrance were selected. The tests with a pipe inside diameter of less than 0.0254 m were not selected because a pattern of periodic water filling and blowing was observed for these cases (Clark et al., 1978). Two separate test apparatus were used for these tests. The smaller tube (0.0254 m I.D.) was connected to two plena each of 0.33 m I.D. The test section was 1.51 m long. The air flow rate varied from 0.0064 to 0.0215 kg/s. The larger test section (0.152 m I.D.) was connected to two 55 gallon drums with an internal diameter of 0.554 m. The length of the test section in this case was 3.66 m. The air flow rate varied from 0.103 to 0.274 kg/s. The test report (Bharathan, 1979) did not provide any information about the water level in the upper plenum, but it was approximately 4 to 5 times the I.D. of the test section (Bharathan, 1982).

Unlike the University of Houston tests discussed in Section 4.1, the Dartmouth College tests had almost no liquid entrainment. Therefore, the countercurrent flow behavior in these tests should mostly depend on the interfacial shear stress, including form losses, and the data are more appropriate for assessing the interfacial momentum transfer models used in the advanced codes.

4.2.2 Input Models

The tests were modeled with all three codes, namely, TRAC-PF1 (Version 7.0), RELAP5/MOD1 (Cycle 14), and TRAC-BD1 (Version 12.0). The input configuration used for the TRAC-PF1 and TRAC-BD1 codes was the same, and is shown in Figure 4.2.2. The test set-ups (small pipe of 0.0254 m I.D. and large pipe of 0.152 m I.D.) were modeled with three TEE components. Part of the upper plenum and drain pipe were modeled with the upper TEE, part of the upper plenum with water injection, the test section and part of the lower plenum were modeled with the middle TEE, and the bottom TEE represented part of the lower plenum and the air injection pipe. The water and air injection pipes and the close end at the bottom were modeled with FILL components while the upper open end and the end of drain pipes were modeled with BREAK components. The nodalizations for the two test sections are shown in Figure 4.2.3. There were 18 cells for the 0.0254 m I.D. pipe and 25 cells for the 0.152 m I.D. pipe. The cell lengths varied from 0.074m to 0.01 m in the test section for the smaller diameter tube and from 0.02m to 0.18 m in the larger pipe.
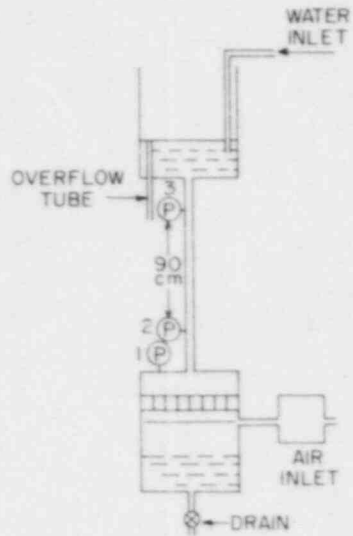
Figure 4.2.1   Schematic of the Dartmouth College
               Single-Tube CCFL Test Facility.
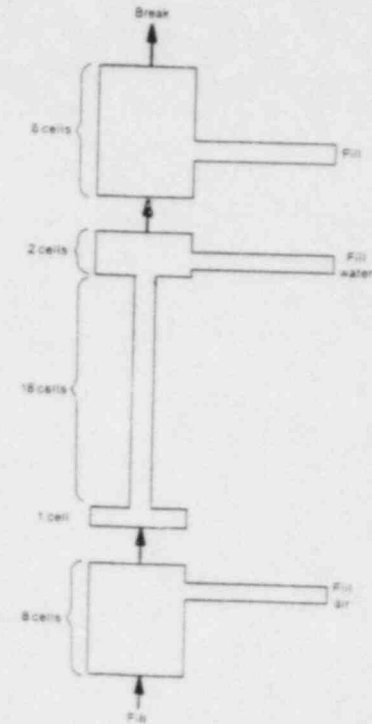
Figure 4.2.2   TRAC-PF1 and TRAC-BD1 Input Model
               Configuration for Dartmouth College
               Single-Tube Tests.
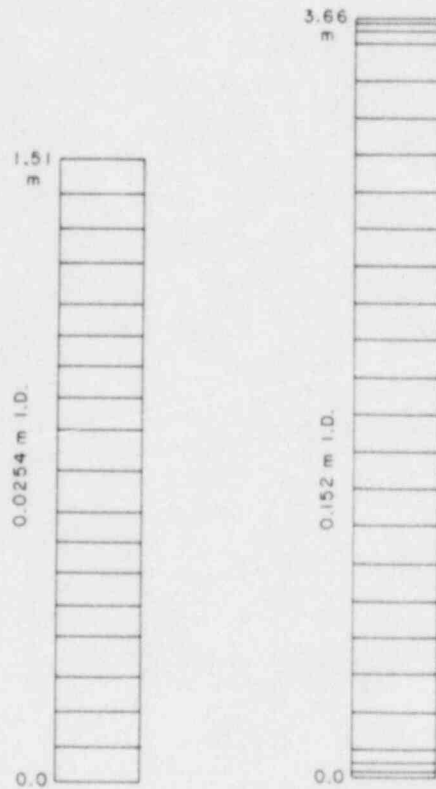
DIFFERENT SCALES
DARTMOUTH COLLEGE TEST
NODALIZATION IN TEST SECTION

Figure 4.2.3   Noding Diagram for the Dartmouth College Test Sections
for TRAC-PF1, TRAC-BD1 and RELAP5/MOD1 Calculations.

For the RELAP5/MODl calculations, the test set up was modeled with four PIPE and three BRANCH components as shown in Figure 4.2.4. The nodalizations for the test sections were exactly the same as for TRAC-PFl and TRAC-BDl calculations and as shown in Figure 4.2.3. In addition, for the smaller-diameter pipe, the upper and lower plenum diameters were gradually reduced at the junction of plena and test pipe. This was done to reduce the sudden area change effects.

The assessment calculations were repeated for different air flow rates. Each produced only one point on the flooding or $\sqrt{j^*_g}$ vs $\sqrt{j^*_f}$ curve. The nondimensional gas and liquid flow rates, j^*_g and j^*_f, are defined as

$$j^*_g = \alpha v_g \sqrt{\rho_g} / \sqrt{(\rho_\ell - \rho_g)gD},$$ (4.2.1)

$$j^*_f = (1 - \alpha)v_\ell \sqrt{\rho_\ell} / \sqrt{(\rho_\ell - \rho_g)gD},$$ (4.2.2)

where α, v, ρ, g, and D are void fraction, phasic velocity, phasic density, acceleration due to gravity, and pipe diameter, respectively.

The liquid flow rate was determined by calculating the liquid inventory in the lower plenum for a given time interval. The computer running time for each calculation varied with the air flow rate and the time period of calculation. The TRAC-PFl small pipe calculation took from 123 to 143 CPU seconds for 15 seconds of transient, whereas, for the large pipe case, it took 173 to 207 CPU seconds for 20 seconds of transient. In contrast, the TRAC-BDl small-pipe calculation took 110 to 220 CPU seconds for 15 seconds of transient while the large pipe calculation took approximately 420 CPU seconds for 9.5 seconds of transient. For RELAP5/MODl, the calculations for the large pipe took approximately 190 CPU seconds for 17 seconds of transient. All calculations were performed on the BNL CDC-7600 computer.

4.2.3 Code Predictions and Comparison with Data

4.2.3.1 Small Tube (0.0254 m I.D.)

TRAC-PFl was applied first to this test. In the initial modeling, the lower plenum was modeled larger than in the test, to minimize the effect of stored water and to stabilize the flow. However, this did not work as the code predicted liquid bridging in the test sections and periodic dumping of water for air flow rates as high as 0.00314 kg/s. In the test, the dumping was observed only at air flow rates below 0.00111 kg/s. The dumping behavior occurred in the test because of bridging (blocking) of the test section with liquid which prevented the flow of air. This led to the accumulation of air in the lower plenum and an increase in the pressure. When the pressure difference between the lower and upper plena exceeded the hydrostatic pressure due to liquid in the upper plenum and the test section, the liquid bridge (or plug) was expelled and the air flow resumed. This behavior was repeated periodically. In the larger lower plenum case, the pressure in this lower
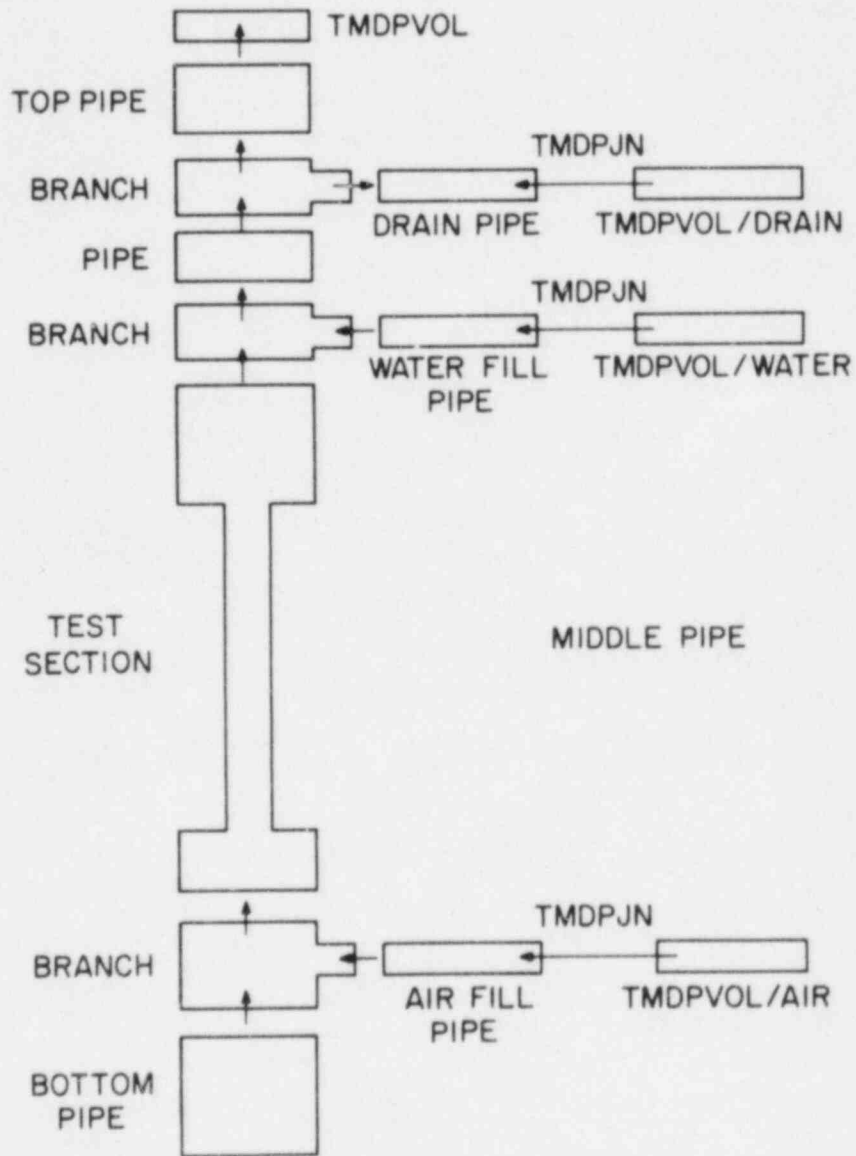
Figure 4.2.4   RELAP5/MOD1 Input Model Configuration for Dartmouth
              College Single-Tube Tests.

plenum took a while to build up, leading to an initially large flow of liquid from the upper plenum which bridged the test section and caused dumping behavior. Hence, the test and the simulation would be sensitive to the lower plenum size. In all final calculations, to be reported here, the actual size of the lower plenum was used.

Figure 4.2.5 shows a comparison of the liquid downflow rates for given air flow rates as predicted by the TRAC-PF1 and TRAC-BD1 codes and the data. TRAC-PF1 results were in good agreement with the data. The code also predicted a dumping behavior for air flow rates less than 0.005 kg/s ($\sqrt{j*_f}$ = 0.241), which is closer to the experimental conditions. The curve through the calculated points showed changes in slope as the air flow rate was increased. This was not in total agreement with the data, and needed further investigation, to be discussed later. TRAC-BD1, on the other hand, predicted dumping at much higher air flow rates. However, it did compute stable countercurrent flow at higher air flow rates, but the liquid downflow rates were highly overpredicted. This behavior of the TRAC-BD1 solution indicated that the interfacial momentum transfer was probably underpredicted by the code. Other possible reasons are inadequate wall friction and a lack of automatic entrance loss at the area changes (e.g., junction between the upper plenum and the test section) in TRAC-BD1. For RELAP5/MOD1 calculations, there were severe instabilities and no useful results were obtained.

4.2.3.2 Large Tube (0.152 m I.D.)

All calculations for this test were performed with a correct size test set-up. Figure 4.2.6 shows the comparison of liquid downflow rates as predicted by TRAC-PF1, TRAC-BD1 and RELAP5/MOD1 with the data for various air injection rates. TRAC-BD1, predicted qualitatively correct behavior, but in most cases overpredicted the liquid downflow rate. On the other hand, TRAC-PF1 predicted anomalous behavior in the range of air flow rates of 0.191 kg/s ($\sqrt{j*_g}$ = 0.47) to 0.103 kg/s ($\sqrt{j*_g}$ = 0.36); the computed liquid filling rate decreased with decreasing air flow rate. However, TRAC-PF1 predicted correct behavior for air flow rates below 0.103 kg/s ($\sqrt{j*_g}$ = 0.36). For RELAP5/MOD1, there was no liquid downflow until the air flow rate was reduced below 0.07 kg/s ($\sqrt{j*_g}$ = 0.3). Calculation below this air flow rate was very unstable. Thus, the RELAP5/MOD1 prediction was in the worst agreement with the data.

4.2.4 Discussion

As mentioned earlier, because of very little entrainment, the Dartmouth College tests are appropriate for assessing the interfacial shear packages used in the advanced codes for countercurrent flow application. Therefore, an attempt will be made to explain the code results as shown in Figures 4.2.5 and 4.2.6 through the interfacial shear used.

TRAC-PF1 employs the Dukler correlation (Dukler, 1980) for the interfacial shear which is expressed as

$$f_i = \{3.04 \log_{10}[4A(1-E)/(1-\alpha)] - 16.16\}^{-2} , \qquad (4.2.3)$$
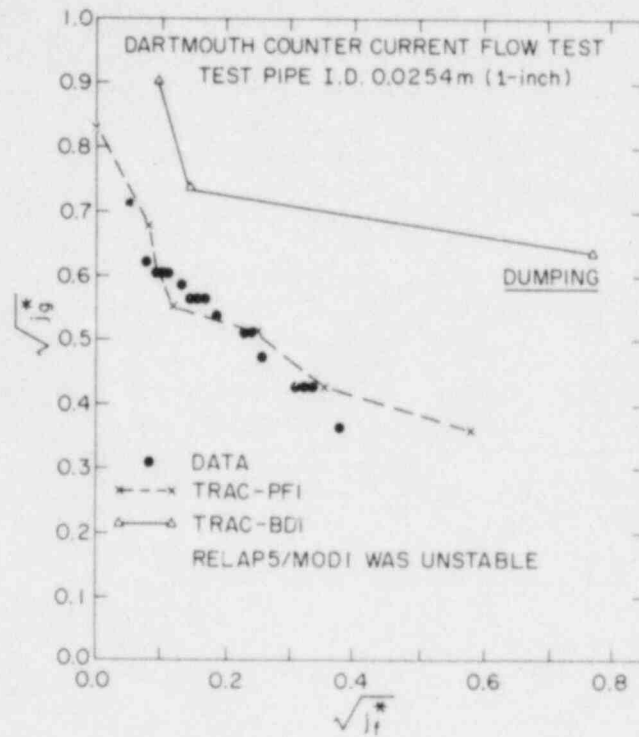
Figure 4.2.5   Comparison Between the Predicted (TRAC-PF1 and TRAC-BD1) and Measured Flooding Curve for Dartmouth College 0.0254 m I.D. Pipe Test.
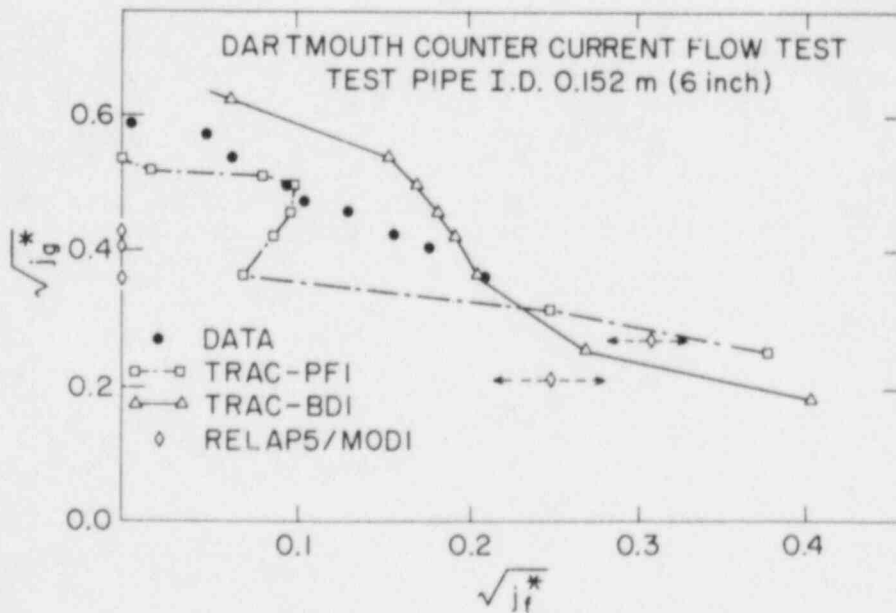
Figure 4.2.6   Comparison Between the Predicted (TRAC-PF1, TRAC-BD1, and RELAP5/MOD1) and Measured Flooding Curve for Dartmouth College 0.152 m I.D. Pipe Test.

where

$$A = Re_g \ (D/0.0508)^{-2} \qquad \text{for } D > 0.0508 \text{ m} ;$$

$$= Re_g \qquad\qquad\qquad \text{for } D \leq 0.0508 \text{ m}.$$

Here α, E, D, and Re_g are the void fraction, entrainment rate, pipe diameter, and the vapor or gas Reynolds number, respectively. Equation (4.2.3) was developed from the University of Houston flooding tests conducted in a 2-inch (0.0508 m) diameter pipe, and it has been plotted in Figures 4.2.7 and 4.2.8 as a function of liquid fraction, α_f, i.e., $(1-\alpha)$, and vapor Reynolds number, Re_g, for two pipe diameters (0.0254 m and 0.152 m). Notice that according to Equation (4.2.3), the shear coefficient, f_i, has discontinuities at certain α_f and Re_g combinations, and it increases with decreasing gas flow rates or gas Reynolds number. In TRAC-PF1, the code developers avoided the discontinuity by imposing an upper limit on the shear coefficient as the larger of 1.2 and 23.53 D. Even with this upper limit, the Dukler correlation has a strong bearing on the TRAC-PF1 prediction of liquid downflow rate and is more dramatic in the case of the 0.152 m I.D. tube. The liquid downflow rate is controlled by the interfacial shear stress which is defined as $f_i v_r^2$. In the case of the TRAC-PF1 prediction, when the air flow rate was decreased, the f_i increased because of thicker film and lower gas Reynolds number. In the air flow rate range of 0.191 kg/s ($\sqrt{j^*_g} = 0.47$) to 0.103 kg/s ($\sqrt{j^*_g} = 0.36$), the f_i increased rapidly as the film thickness approached the film thickness at which the discontinuity occurred. This increase in f_i overcompensated the reduction in v_r (or v_g) resulting in a lower liquid downflow rate as shown in Figure 4.2.6. For air flow rates below 0.07 kg/s ($\sqrt{j^*_g} = 0.3$), the shear coefficient was computed from the second branch of Dukler's correlation where f_i decreased with increasing film thickness. Thus, there was a much faster reduction in interfacial momentum transfer and the liquid filling rate increased sharply, as shown in Figure 4.2.6. Similar behavior was observed for the 0.0254 m I.D. pipe case, although, the effect of discontinuity was milder and was reflected only in terms of change in slopes of $\sqrt{j^*_g}$ vs $\sqrt{j^*_f}$ curve as shown in Figure 4.2.5.

The interfacial shear coefficient in an annular flow regime in TRAC-BD1 was derived from the drift velocity correlation of Ishii (1977) and a distribution parameter given by Andersen and Chu (1982). The interfacial momentum transfer model for the annular flow regime in TRAC-BD1 is as follows:

$$F_{\ell g} = \frac{0.015\alpha(\alpha+a)^2\rho_\ell}{D} \left| \frac{1-\alpha C_o}{1-\alpha} \ v_g - C_o v_\ell \right| \left(\frac{1-\alpha C_o}{1-\alpha} \ v_g - C_o v_\ell \right) , \qquad (4.2.4)$$

where

$$a = \left[\frac{1+75(1-\alpha)}{\sqrt{\alpha}} \ \left(\frac{\rho_g}{\rho_\ell} \right) \right]^{1/2} , \qquad\qquad\qquad (4.2.5)$$
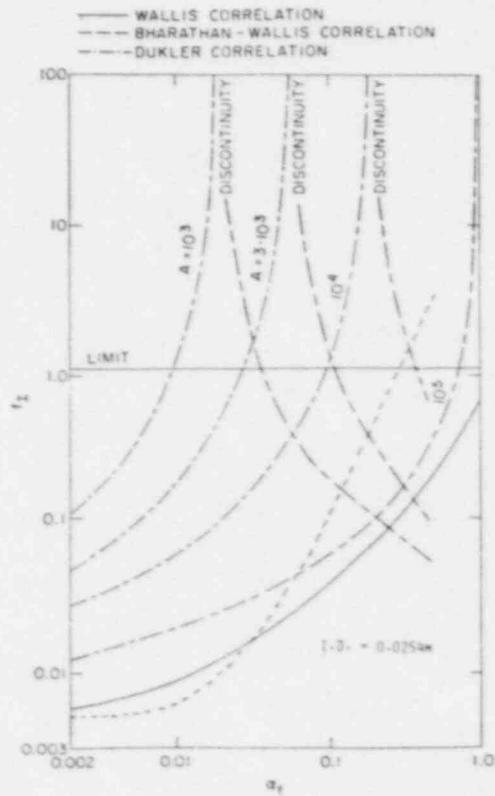
Figure 4.2.7 Comparison of Various Interfacial Shear Correlations for Annular Flows for 0.0254 m I.D. Pipe.
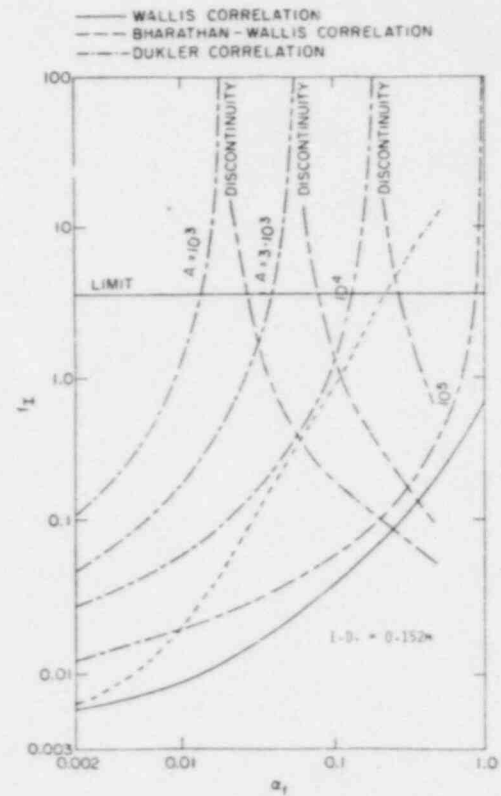
Figure 4.2.8 Comparison of Various Interfacial Shear Correlations for Annular Flows for 0.152 m I.D. Pipe.

and $\qquad C_o = \dfrac{1 + a}{\alpha + a}$. $\hfill (4.2.6)$

Here v_g and v_ℓ are the average gas and liquid velocities in their respective phasic areas, and $F_{\ell g}$ is the interfacial force per unit volume of the gas phase. The interfacial shear coefficient as defined by Dukler (1980) or Wallis (1970) can be obtained from the TRAC-BD1 description as

$$f_i = 0.0075 \sqrt{\alpha}\ [1-75(1-\alpha)]\left| 1 - \frac{1}{a(v_g/v_\ell -1)} \right| (1 - \frac{1}{a(v_g/v_\ell -1)})\ . \qquad (4.2.7)$$

For countercurrent flows, v_g and v_ℓ are of opposite signs; therefore, the last two terms will be greater than 1.0. The variable a is generally small for thin films. For the large tube case (0.152 m I.D.), 'a' varied from 0.0014 to 0.003.

The well-known Wallis correlation (Wallis, 1970) for interfacial shear coefficient in the annular flow regime is

$$f_i = 0.005\ [\ 1+75(1-\alpha)]\ . \qquad (4.2.8)$$

A comparison of expressions for the interfacial shear coefficients in Equations (4.2.7) and (4.2.8) indicates that the TRAC-BD1 model, i.e., Equation (4.2.7), produces a larger interfacial shear stress than the Wallis correlation (Equation 4.2.8). Therefore, the Wallis correlation would produce even larger water downflow rates than that predicted by TRAC-BD1.

In an attempt to suggest a better model for interfacial shear coefficient in annular flow regimes, the Bharathan-Wallis correlation (Bharathan, 1979) was also investigated. This correlation was developed from the Dartmouth College data and had been shown to predict a countercurrent flow limitation superior to the Wallis or Dukler correlation in an earlier simulation of flooding test with 0.0508 m I.D. test section (Popov and Rohatgi, 1983). The Bharathan-Wallis correlation is as follows:

$$f_i = 0.005 + C_{f1}\ \delta^{*C_{f2}}\ , \qquad (4.2.9)$$

where

$$C_{f1} = 0.275\ (10^{9.07}/D^*)\ ,$$

$$C_{f2} = 1.63 + 4.74/D^*\ ,$$

$$\delta^* = \delta/\overline{\sqrt{\sigma/[g(\rho_\ell - \rho_g)]}}\ ,$$

$$\delta = D (1-\sqrt{\alpha})/2 ,$$

$$D^* = D/\sqrt{\sigma/[g(\rho_\ell - \rho_g)]} .$$

Here δ, D, and σ are the film thickness, pipe diameter, and surface tension, respectively. This correlation indicates that f_i depends upon surface tension, but is unaffected by gas or vapor Reynolds number. Comparisons of the Bharathan-Wallis correlation with the Dukler and Wallis correlations are shown in Figures 4.2.7 and 4.2.8 for 0.0254 m and 0.152 m I.D. pipes.

Both the Wallis and the Bharathan-Wallis correlations were incorporated in TRAC-PF1 at BNL. Calculations were performed for the large diameter pipe tests, and the new results along with the original TRAC-PF1 and TRAC-BD1 predictions are shown in Figure 4.2.9. As expected, the Wallis correlation, because of lower interfacial shear coefficient, tends to highly overpredict the liquid downflow rate and seems inappropriate for countercurrent flow situations. The Bharathan-Wallis correlation, on the other hand, tends to underpredict the liquid downflow rate, particularly at higher air upflow rates. However, it does not suffer from any anomalous behavior as depicted by the Dukler correlation for the large diameter pipe.

Similar calculations were performed for the small diameter (0.0254 m I.D.) pipe. From the small and large diameter pipe calculations, it is concluded that a combination of the Dukler and the Bharathan-Wallis correlations is probably required to obtain a good correlation for interfacial shear in the annular flow regime for countercurrent flow applications. The Dukler correlation seems appropriate for the smaller-diameter pipes, whereas the Bharathan-Wallis correlation produces more consistent results for the larger diameter pipes.

For TRAC-BD1, the Kutateladze CCFL correlation was also used for the large diameter pipe tests. As shown in Figure 4.2.10, the use of CCFL correlation improved the TRAC-BD1 prediction for the 0.152 m I.D. pipe tests. However, the code was still predicting larger liquid downflow rates than the experiment. Similar calculations have been performed by the TRAC-BD1 code developers at INEL for the Dartmouth College 0.0254 m I.D. pipe tests. However, to achieve a good agreement with the data, the value of the Kutateladze constant, K, was changed from the standard value of 3.2 to 1.2. This indicates that TRAC-BD1 will require different values for the Kutateladze constant for different experimental apparatus and hardware. Since TRAC-BD1 cannot predict this constant a priori, the built-in Kutateladze correlation must be used with caution.

The RELAP5/MOD1 interfacial shear package could not be assessed because of poor agreement between the code predictions and the data. It is clear that RELAP5 must first have a better flow regime map including an annular-mist regime before the code is applied to CCFL applications. It is our understanding that such a change has been made to the newer version, i.e., RELAP5/MOD2.
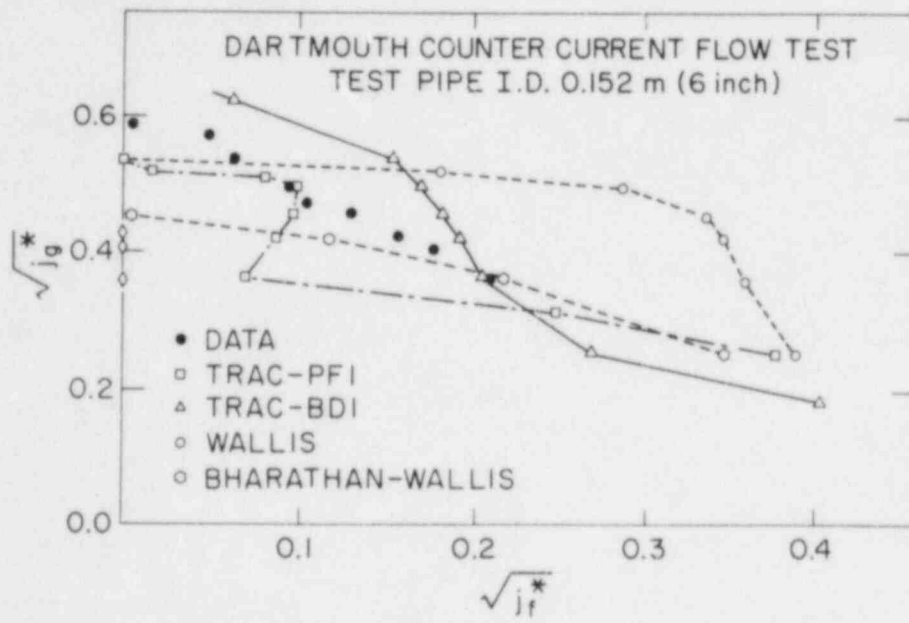
Figure 4.2.9   Flooding Curves Corresponding to Various Interfacial
Shear Correlations for Dartmouth College 0.152 m I.D.
Pipe Test.
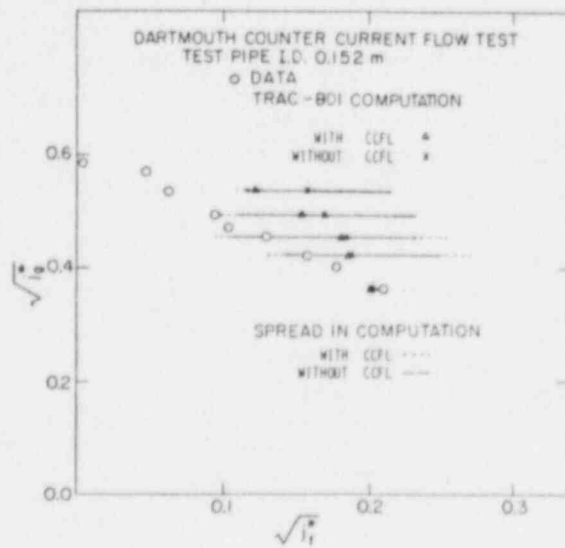
Figure 4.2.10   Comparison of TRAC-BD1 Results With and Without CCFL
Correlation for Dartmouth College 0.152 m I.D. Pipe Test

4.2.5 User Experience

There was no particular difficulty in running the codes for the Dartmouth
College tests. However, RELAP5/MOD1 produced very few useful results because
of severe numerical instabil'ties. The TRAC-PF1 and TRAC-BD1 results were not
very stable either. However, they could, at least, be time averaged and com-
pared to the data. The computer run time statistics for these calculations
are shown in Table 4.2.1.

Table 4.2.1 Typical Computer Run Time Statistics for the Dartmouth
College Single Tube CCFL Test
Computer: BNL CDC-7600

Calculation	TRAC-PF1		RELAP5/ MOD1	TRAC-BD1	
Item	Small Tube	Large Tube	Large Tube	Small Tube	Large Tube
No. of Cells	41	47	49	41	47
Problem Time (s)	29	39	16.8	19	14.7
No. of Time Steps	1496	1774	5388	2428	5312
CPU Time (s)	224	316	190	206	422
CPU-to-Problem Time	7.7	8.1	11.3	10.8	28.7
CPU (s)/Cell/Time Step	3.6×10^{-3}	3.8×10^{-3}	0.7×10^{-3}	2.1×10^{-3}	1.7×10^{-3}

4.3 Dartmouth College Parallel Tube Tests

4.3.1 Test Description

The experimental facility (Clark et al., 1978) as shown in Figure 4.3.1
consisted of an upper plenum which could be connected to a lower collection
chamber by one, two, or three vertical tubes up to 1.52 m in length. The up-
per plenum and lower collection chambers were constructed of 0.33 m I.D. Lu-
cite cylinders. Water was introduced into the upper plenum by means of an an-
nular injection ring to minimize asymmetrical entrance effects in the tubes.
A drain was installed to provide a constant water level of approximately 0.1 m
in the upper plenum for all tests. The upper portion of the plenum was open
to the atmosphere through a disentrainment device designed to minimize splash-
ing during operation.

The lower chamber was sealed at both ends and was 0.71 m in depth. A
drain was provided to expel water accumulated during testing, and a port in

water source →

disentrain-
ment device

annular
water injector

variable head
drain

pressure
tap

parallel tubes

pressure
transducer

pressure
tap

accumulator

pressure
regulator

air
injector

graduated
scale

rotameters

compressor

drain
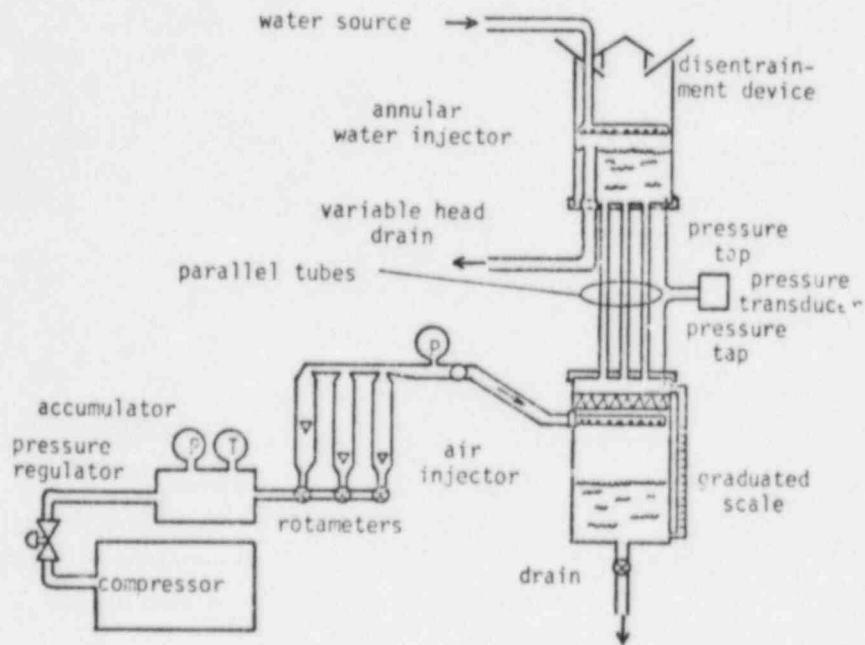
Figure 4.3.1 Schematic of Dartmouth College Parallel Tube Test
Facility.

the side of the chamber accepted an air injection system. An aluminum honey-comb baffle was installed above the air injector to reduce asymmetrical entrance effect in the tubes being tested. All tubes tested were machined with square edges at both ends and were mounted vertically in the apparatus with the end surfaces aligned flush with the end plate surfaces of the upper and lower chambers.

During the experiment, the air flow rate was changed stepwise. After each step, a sufficiently long time was allowed for the flow to establish. The air flow rate was changed either in the ascending or descending order with the only requirement that none of the tubes was completely filled with water downflow. Therefore, throughout the experiments each tube remained in either a countercurrent flow or a pure air upflow regime. After a steady-state condition was achieved, the pressure drop across the tubes, i.e., the pressure difference between the top of the lower chamber and the bottom of the upper plenum, the air flow rate, and the intergrated water downflow rate were measured. The water downflow rate was measured by means of a graduated scale installed in the lower chamber. All experiments were conducted at near-atmospheric pressure and room temperature. The details of the experiments can be found in (Clark et al., 1978).

The test series with three parallel tubes each of 0.0254 m I.D. and 1.52 m length was chosen for simulation with TRAC-PF1 (Version 7.0) and TRAC-BD1 (Version 12.0). The RELAP5/MOD1 code was not applied to these tests because of its poor prediction of the single tube tests discussed in Sections 4.1 and 4.2.

4.3.2 Input Models

The test section was modeled primarily using the VESSEL module of TRAC-PF1 and TRAC-BD1. One radial ring and three 120° azimuthal sectors were used in both models. For TRAC-PF1, the axial flow area in each azimuthal sector was reduced to that for 0.0254 I.D. tube, and no communication across the azimuthal cell boundaries was allowed. Thus, three distinct parallel tubes were created within the VESSEL module of TRAC-PF1.

For TRAC-BD1, three test pipes were modeled with three one-dimensional CHAN (or CHANNEL) components. The nodalizations of both TRAC-PF1 and TRAC-BD1 input models were the same, and as an example, the TRAC-BD1 nodalization is shown in Figure 4.3.2. The upper and lower parts of the VESSEL did represent the upper and lower plena of the test apparatus. Several PIPE, BREAK, and FILL components were attached to the VESSEL to complete the model.

Water was introduced into the upper plenum between Cell Junctions 5 and 6 horizontally in a radial direction at a rate exceeding the conservatively estimated free-fall water downflow rate in a channel. The excess water was allowed to leave the upper plenum through a drain pipe (not shown in Figure 4.3.2) connected at Cell 7. Thus, a constant water level was maintained. The air entering the upper plenum through the vertical channels was allowed to leave through PIPE 2 and/or the drain pipe at Cell 7. Atmospheric pressure was specified at BREAK 1 representing the top of the test apparatus.
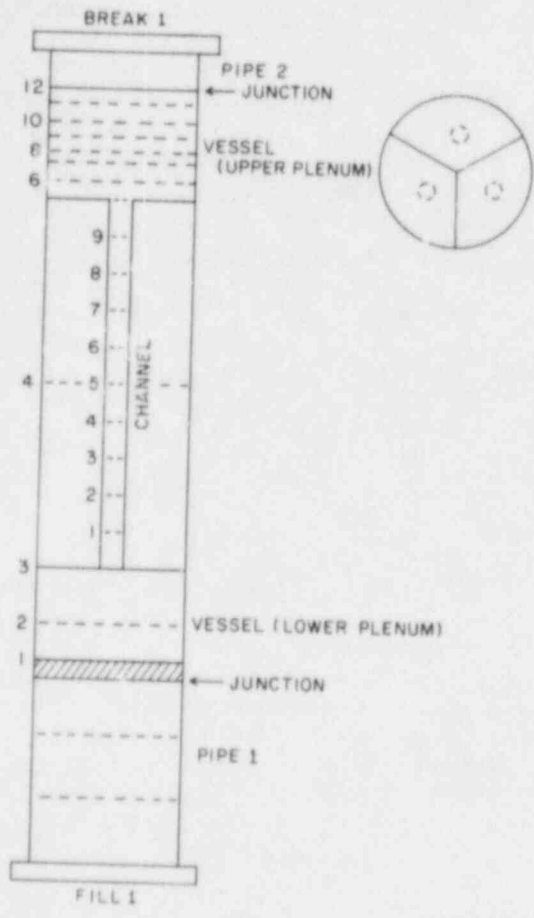
Figure 4.3.2 TRAC-BD1 Noding Diagram for the Dartmouth College
Parallel Tube Test.

Air was injected into the lower plenum vertically at Cell Junction 2 using a FILL component. PIPE 1 and FILL 1 shown in Figure 4.3.2 were not present in the experimental facility, but were added for the convenience of computation. The code had to be run for a certain period of time for each operational point (with fixed air flux) until a stable condition was reached. During this time, water collected in the lower plenum could fill it up, thus changing the flow conditions at the entrance of the tube. During the experiment, the lower plenum was periodically drained by means of a manually operated valve. This drainage was simulated by attaching PIPE 1 at the bottom of the lower plenum where the water was collected without altering the tube entrance conditions.

Another difficulty related to the size of the lower plenum had to be overcome. Since the air volume in the lower plenum would affect the time response of the system, an air shield (or restriction) was placed between the lower plenum and PIPE 1 (shaded area in Figure 4.3.2). In order to drain the water down, but at the same time keep the air from diffusing into the drain pipe (PIPE 1), a very high value of the additional friction loss coefficient for the air was used. Thus, the effective lower plenum volume in the model was kept the same as in the experiment.

4.3.3 Code Predictions and Comparison With Data

The TRAC-BD1 code was first run to simulate a very slow transient with the dimensionless air flux changing with time as

$$\frac{d(J^*_g/J^*_{g,o})}{dt} = - 0.006 \text{ s}^{-1} \tag{4.3.1}$$

where $J^*_{g,o}$ is the initial nondimensional value of the air flux. This was done to account for any possible history effect in establishing a stable operating condition. Later, additional calculations with constant air fluxes were run using the code's restart capability. Figure 4.3.3 shows the paths for the slow transient (solid line) as well as the runs made with fixed air fluxes (dashed lines). The TRAC-BD1 results showed that each point on the slow transient can indeed be regarded as a quasi-steady-state calculation.

Since the water downflow rates during these experiments were not reported, only the data on overall pressure drop across the test section were available for code comparison. Figure 4.3.4 shows the TRAC-BD1 results and the measured nondimensional pressure drop, ΔP^* vs J^*_g. These are defined as

$$\Delta P^* = - \left(\frac{\Delta P}{L} + \rho_g g \right) / [g(\rho_\ell - \rho_g)] . \tag{4.3.2}$$

$$J^*_g = (Q_{g,total}/A_{total}) \rho_g^{1/2} [Dg(\rho_\ell - \rho_g)]^{-1/2} . \tag{4.3.3}$$
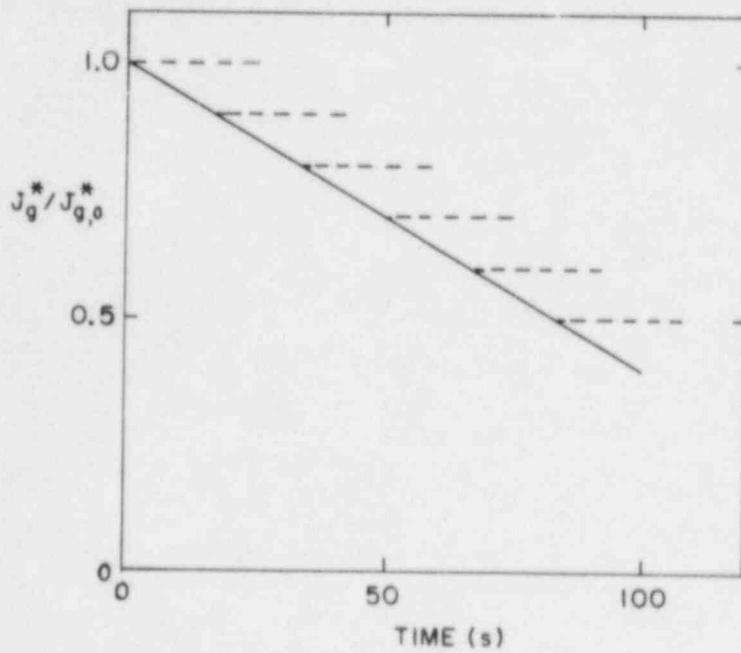
Figure 4.3.3 Variation of Air Flow Rate for TRAC-BD1 Calculation.
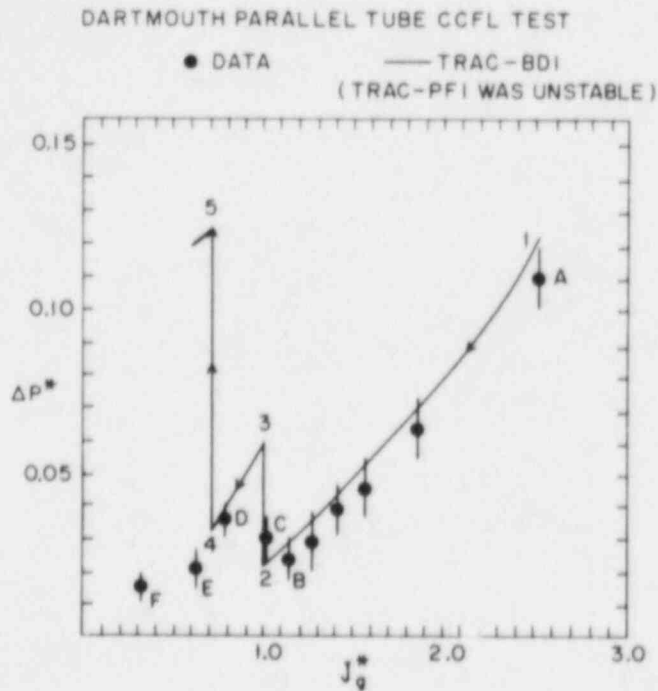
Figure 4.3.4 Comparison Between the Measured and TRAC-BD1 Pressure
Drop for the Dartmouth College Parallel Tube Tests.

In the above equations, ΔP, L, $Q_{g,total}$, A_{total}, and D represent the measured pressure difference between the lower and upper plena, tube length, total volumetric gas flow through all three tubes, total tube flow area, and tube inside diameter, respectively. Standard symbols are used for the phasic densities and the acceleration due to gravity.

In Figure 4.3.4, the alphabets A-B-C-D-E represent the experimental path as the air flow rate was decreased in steps, whereas the numbers 1-2-3-4-5 denote the TRAC-BD1 results. For J^*_g greater than approximately 1.0, the code prediction is in close agreement with the data (see Paths A-B and 1-2). This is to be expected since in this region only air flowed through all the pipes and no water was able to flow down. This also confirms that TRAC-BD1 correctly predicts the wall friction due to single phase gas flow.

As the air flow rate was decreased further, i.e., $J^*_g < 1.0$, according to TRAC-BD1, water started to flow down through one of the pipes while only air continued to flow up through the two remaining pipes. In the experiment, however, there was two-phase countercurrent annular flow in one pipe and single-phase air upflow in two pipes. This corresponds to Point C in Figure 4.3.4. Notice that the nondimensional pressure drop ΔP^* increased as the flow pattern changed from Point B to C. A change in flow pattern was also observed in the calculation (Point 2 to 3). However, instead of having one pipe in the countercurrent annular flow regime, TRAC-BD1 calculated the pipe to be in a low-void ($\alpha \approx 5\%$) two-phase downflow regime, and the other two pipes in the single-phase air upflow regime. This resulted in higher air flow rates through the air-filled pipes and caused higher ΔP^* (see Path 4 to 5), which was in contradiction with the experimental path D-E. Calculations could not be continued below J^*_g of approximately 0.5 because of the code failure in numerics.

In short, some qualitative aspects of the experiments were predicted by TRAC-BD1. However, there were significant disagreements between the code prediction and the experimental data regarding ΔP^* and flow pattern below J^*_g of approximately 1.0 when water starts to flow down through one or more tubes.

The TRAC-PF1 results for these tests were even more discouraging. Calculations were performed to obtain steady states for various nondimensional air flow rates (J^*_g) ranging from 3.9 to 0.39. No stable results were obtained for any air flow rate. The results indicated considerable difficulty in convergence for both high and low air flow rates and took an extremely long running time. As an example, the void fraction, pressure, air velocity, and liquid velocity at the top of the three pipes for the nondimensional air flow rate (J^*_g) of 1.974 are shown in Figure 4.3.5. Generally, air could not penetrate through the water in the upper plenum in the beginning, and the lower plenum pressure started to increase. At some point (usually about 0.2 to 0.4 bar above the atmospheric pressure), air violently penetrated the water above one of the test pipes and entrained most of the water in that cell. The air velocity in the pipe increased rapidly (up to the order of 500 m/sec) and the pressure in the pipe decreased substantially below the atmospheric pressure. Finally, the calculational time step decreased to a very small value (in the order of 0.1 msec) because of the high gas flow rate, and the CPU-to-
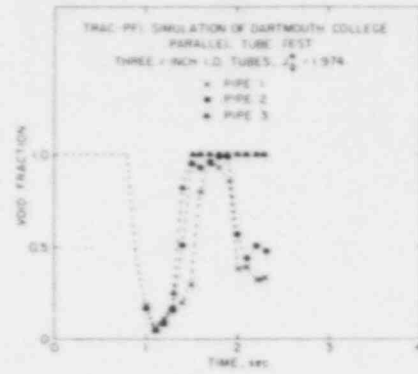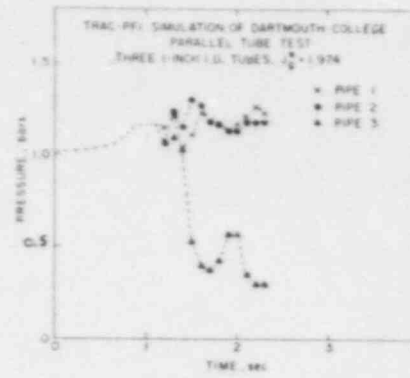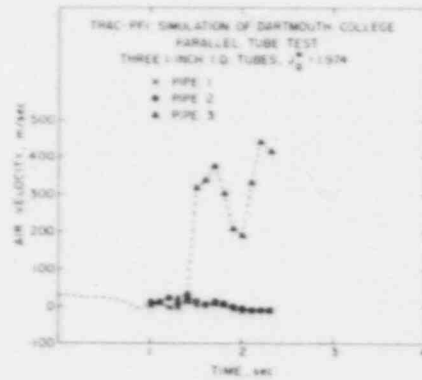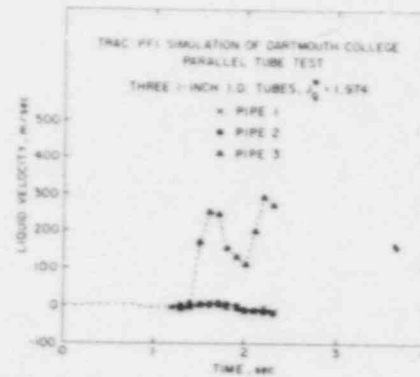
Figure 4.3.5 TRAC-PF1 Prediction of (a) Void Fraction, (b) Pressure, (c) Air Velocity, and (d) Water Velocity at the Top of the Pipes for J_g^* of 1.974.

real time ratio increased to a prohibitively high value (in the order of 2000). This is equivalent to more than a half hour of computer time for each second of real time. At this point, the calculation was usually terminated, either because of exceedingly small time steps (0.1 msec) or because the pressure was out of range in the water property table.

Other calculations were performed beside those mentioned above by changing several parameters, such as the mode and location of injection of water and minimum time step, etc. However, these calculations also failed. For example, one calculation was run with the lower and upper plena divided into three independent sections (by setting the azimuthal flow area to zero), which is equivalent to running three independent pipe tests; similar dumping behavior was obtained. In another calculation, the minimum time step was further reduced to 0.01 msec. However, this minimum time step was immediately reached and the calculation stopped.

From experience gained from calculations of the Dartmouth College single-tube tests (see Section 4.2), it appears that the TRAC-PF1 code sometimes calculates exceedingly high interfacial shear coefficients for large-diameter pipes. The difficulty in these calculations may be due to a very high interfacial shear calculation in the upper plenum which is essentially a large-diameter pipe. It is suggested that these parallel-tube tests be simulated again with the newer version of the code, i.e., TRAC-PF1/MOD1 (Liles et al., 1983).

4.3.4 Discussion

In order to better understand the CCFL phenomenon in a multitube system, let us examine the fundamental differences between a single- and a parallel-tube CCFL operation. Figure 4.3.6 shows the typical ΔP^* vs J^*_g curve for countercurrent flow in a single 0.0254 m I.D. vertical tube connecting two plena. For $J^*_g > 1.0$, no water can flow down, and only air flows upward. Therefore, ΔP^* decreases as J^*_g is decreased from a value higher than 1.0 (Part C of Figure 4.3.6). As J^*_g is decreased below 1.0, water starts to flow down and a countercurrent, rough-film annular flow regime develops in the tube. Since the interfacial friction increases as the liquid film thickens, the pressure drop increases with the decrease in the air flow rate. This is Part B of Figure 4.3.6, where the Wallis-type correlation (Wallis, 1970) for interfacial friction in the annular flow regime is valid. As the air flow rate is decreased further ($J^*_g < 0.5$), the liquid film becomes smoother or wavy, and the pressure drop starts to decrease with the decrease in the air flow rate. This is Part A of Figure 4.3.6. Although the flow is still in the countercurrent annular flow regime, no established correlation for interfacial shear is available for this region.

For a single-tube J^*_g-controlled experiment, it is possible to traverse all parts of the curve shown in Figure 4.3.6. However, in a multitube system, where only the total J^*_g can be controlled, but not J^*_g through each tube, stable operation in Part B is not possible. Therefore, in the 3 tube system discussed earlier, one tube starts to operate in Part A, whereas two tubes continue to operate in Part C as soon as the total J^*_g is decreased
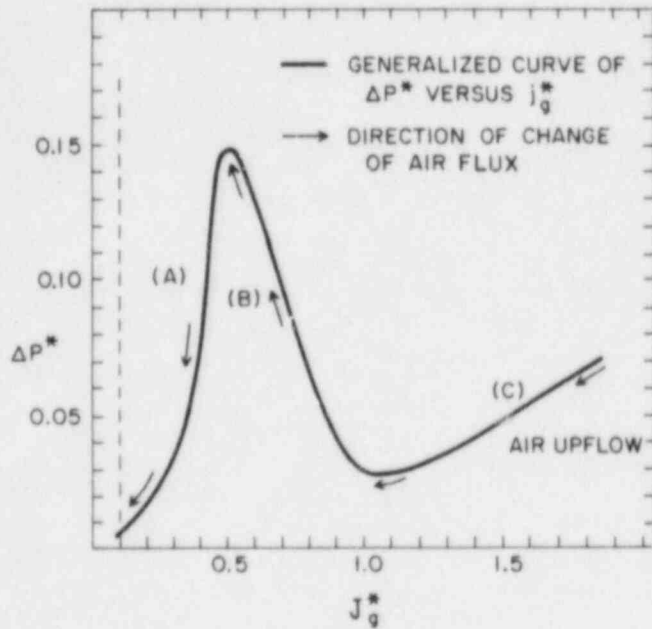
Figure 4.3.6 A Typical ΔP^* vs. J_g^* Curve for Counter-Current Flow in a Single Vertical Tube (Approximate Data for 0.0254m I.D. Tube).

below 1.0. It must be reiterated that the flow regime in the tube operating in Part A is still in the countercurrent annular flow regime and not in the low-void downflow regime. TRAC-BD1, however, predicted a low-void mixture flowing down in one tube as soon as the J^*_g is decreased below 1.0. The code essentially uses a Wallis-type correlation for the annular flow regime which increases the interfacial shear as water starts to flow down. This tends to increase the ΔP^* and reduce the air flow rate through that tube. Since the code does not have any correlation to describe Part A of Figure 4.3.6, the calculation eventually stabilizes when the tube becomes almost water filled and a very low-void two-phase mixture flows down. As a result, the air flow rate through the other two tubes increases significantly (~50%) and the total ΔP^* across the tubes jumps appreciably (from Point 2 to 3 in Figure 4.3.4). Therefore, it is apparent that unless the interfacial shear package can be modified to include Part A of Figure 4.3.6, the code will not be able to predict the multitube CCFL data.

TRAC-PF1 will also require interfacial shear correlations appropriate for Part A of Figure 4.3.6. However, even the present shear package for Part B of Figure 4.3.6 needs improvement for large-diameter pipes.

4.3.5 User Experience

There was no particular difficulty in running the TRAC-BD1 code for this multitube experiment except at $J^*_g < 0.5$ when the code stopped because of numerical difficulties. TRAC-PF1 showed more instabilities and usually failed after a few seconds of problem time. The TRAC-PF1 time step sizes became exceedingly small which resulted in a very high CPU-to-real time ratios as shown in Figure 4.3.7. The run time statistics for the TRAC-BD1 calculation are shown in Table 4.3.1.

Table 4.3.1   TRAC-BD1 Computer Run Time Statistics For
Dartmouth College Parallel-Tube Test

Computer: BNL CDC-7600

No. of Cells:	144 (33 in Vessel, 30 in Channels, 81 in Pipes)
Problem Time:	6200 s (mostly single-phase air)
No. of Time Steps:	17710
CPU Time:	6629 s
CPU-to-Problem Time:	1.07
CPU (s)/Cell/Time Step	2.5×10^{-3} s
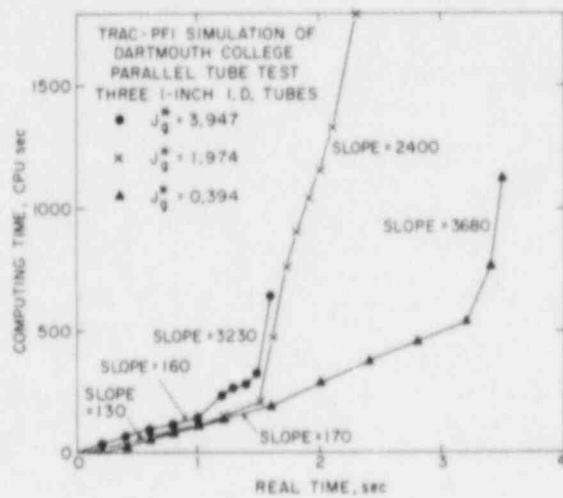
Figure 4.3.7   TRAC-PF1 Computer Run Time on BNL CDC-7600
for Dartmouth College Parallel Tube Test
Simulation.

4.4 Summary and Conclusions

The advanced codes, namely, TRAC-PF1, TRAC-BD1, and RELAP5/MOD1 were applied to several air-water "flooding" or CCFL tests conducted at the University of Houston and Dartmouth College. The University of Houston experiments were particularly useful for assessing the liquid entrainment inception point, whereas the Dartmouth College tests were more appropriate for assessing the interfacial shear package for the countercurrent annular flow regime. The Dartmouth College parallel tube tests were also useful for understanding the differences between the single- and multi-tube CCFL operations.

For the single-tube CCFL tests, TRAC-PF1 and TRAC-BD1 yielded much better results than RELAP5/MOD1 which allowed very little liquid downflow until the gas upflow rate was very small. Inclusion of an annular-mist flow regime is needed in RELAP5/MOD1 as the first step of improving the code prediction. (It is our understanding that such a step has been taken for the newer version of RELAP5, i.e., RELAP5/MOD2.)

For the parallel-tube CCFL tests, only TRAC-BD1 predicted qualitatively reasonable results. TRAC-PF1 was unable to produce any stable result, and RELAP5/MOD1 was not applied to this test because of its poor prediction of the single-tube tests.

The following conclusions can be drawn from the results presented in Sections 4.1 through 4.3:

1. For situations where liquid is injected in the middle of a test channel, the CCFL phenomenon is greatly influenced by the liquid entrainment inception and rate. In such cases, TRAC-BD1 tends to predict the best agreement with data. Thus, the TRAC-BD1 entrainment inception and rate correlations seem to be reasonable. TRAC-PF1, on the other hand, predicts an early liquid entrainment which results in lower liquid downflow rates. Therefore, TRAC-PF1 entrainment model/correlation needs improvement.

2. For situations where liquid flows down from an upper plenum, the interfacial shear seems to be the dominant parameter for the CCFL phenomenon. In such cases, TRAC-PF1 produced the best agreement with data for small pipe diameters (~0.025 m I.D.). Thus, the Dukler correlation for interfacial shear seems reasonable for small diameter pipes or channels. However, for large diameter pipes (~0.15 m I.D.), TRAC-PF1 produced anomalous behavior because of the discontinuities in the Dukler correlation. In this case, the Bharathan-Wallis correlation may be used.

3. The interfacial shear coefficient used in the TRAC-BD1 code overpredicts the liquid downflow rate. Use of the Kutateladze CCFL correlation tends to improve the prediction. However, the Kutateladze constant in the CCFL correlation has to be adjusted to achieve a good prediction. It seems that a combination of Dukler correlation (for small diameter pipe) and Bharathan-Wallis correlation (for large diameter pipe) should produce a better interfacial shear correlation for the countercurrent annular flow regime.

4. A good prediction of single-tube CCFL data does not guarantee a similar success for the parallel tube CCFL data. For example, TRAC-PF1 produced good agreement with the Dartmouth College 0.0254 m I.D. single tube data. However, it could not even produce a stable result for the parallel tube experiments conducted in three 0.0254 m I.D. tubes. Also, the interfacial shear package must include correlations valid for the entire countercurrent annular flow regime, i.e., wavy-transition-rough film regimes, to enable a code to adequately predict the parallel tube CCFL phenomenon.

5. The RELAP5/MOD1 flow regime map for high void fractions must be changed to include an annular-mist regime before the code can be expected to produce reasonable results for CCFL applications. Such a change has been made in RELAP5/MOD2.

5. SIMULATION OF POST-CHF EXPERIMENTS

The post-CHF heat transfer plays an important role in determining the peak clad temperature for both PWR and BWR accident situations. Thus, assessment of the post-CHF models that are being used in the reactor safety codes is of utmost importance. In the present effort, only one post-CHF experiment conducted in an 8x8-rod bundle at Oak Ridge National Laboratory (ORNL) was simulated with TRAC-PF1 (Version 7.0), TRAC-BD1 (Version 12.0), and RELAP5/MOD1 (Cycle 14) codes. Needless to say, simulation of more post-CHF experiments would have been highly desirable, but could not be performed because of resource limitations.

5.1 ORNL Rod Bundle Test

5.1.1 Test Description

A series of high pressure and high temperature steady-state experiments (Mullins et al., 1982) were conducted with water flowing vertically upward through an 8x8-rod bundle with rod diameter and rod pitch typical of PWRs with 17x17 fuel assemblies. A cross section of the test assembly is shown in Figure 5.1.1. There were four unheated rods in the bundle; the axial and radial power profiles were uniform. Two flow measurement sites were positioned at each end of the test section containing the rod bundle. Heated rod sheath temperatures were measured at 30 axial locations in different groups of rods at each axial level. There were a number of differential pressure measurement stations intended for tracking the two-phase mixture level.

The experiments were conducted in the following manner. In the beginning of each steady-state run, the inlet flow was established and the loop conditions were adjusted to provide the prescribed inlet fluid temperature and pressure. The bundle power was then ramped up until the dryout was established at a predetermined axial position in the bundle. After the rod surface temperature and operating pressure were stabilized, the steady-state operating point was assumed to be reached.

Test number 3.07.9H, with the following operating conditions was selected for the assessment purpose:

System pressure:	88.9 bar
Mass flux:	256 kg/m^{2}s
Inlet liquid velocity:	0.326 m/s
Inlet liquid temp.:	537.3°K
Bundle power:	2.733 MW
Average heat flux:	417 kW/m^2

The test was simulated with all three codes, namely, TRAC-BD1 (Version 12.0), TRAC-PF1 (Version 7.0), and RELAP5/MOD1 (Cycle 14).
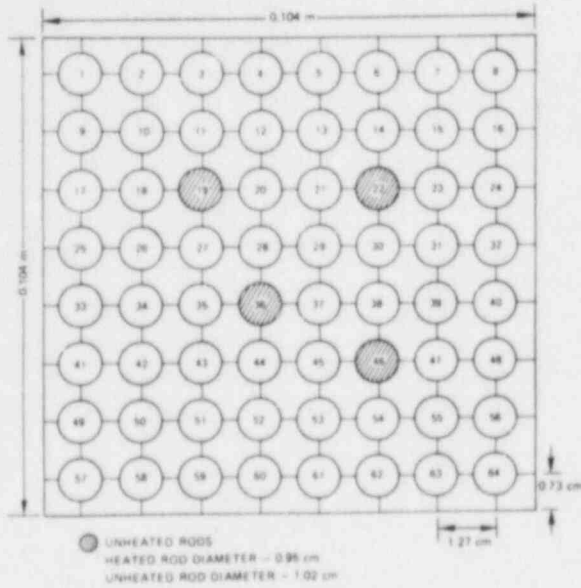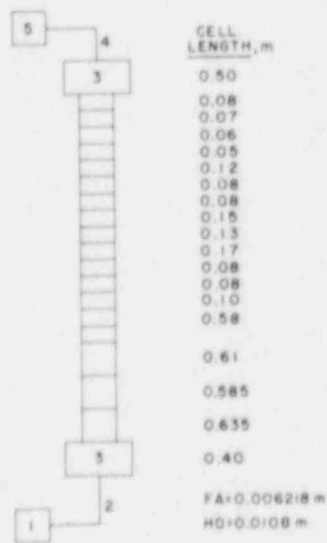
Figure 5.1.1 Cross-Section of ORNL Rod Bundle.

Figure 5.1.2 RELAP5/MOD1 Noding Diagram for the ORNL
Rod Bundle Test.

5.1.2 Input Models

In the case of TRAC-BD1, the rod bundle was modeled with the code's CHAN-NEL component using 17 axial cells such that the cell centers coincide with the thermocouple locations. The cell sizes varied from 0.06 to 0.635 m. The CHANNEL component was placed in a four-cell VESSEL module to represent the lower and upper plena of the test section. Constant flow rate and pressure boundary conditions were applied at the VESSEL's entrance and exit, respectively. The Biasi critical quality-boiling length correlation (Phillips et al., 1981b), and the maximum of the homogeneous nucleation temperature, and the Iloeje correlation (Iloeje et al., 1973) for the minimum stable film boiling temperature (T_{MSFB}) were selected as the user options. The calculation was run in a transient mode in order to activate the CHF and post-CHF heat transfer logic which are suppressed for a steady-state calculation. A quasi-steady-state was reached after approximately 64 seconds of the problem time.

In the case of TRAC-PF1, the rod bundle was modeled with a one-dimensional CORE component, and the Biasi CHF correlation (Biasi et al., 1967) and T_{MSFB} from the homogeneous nucleation temperature were used. Constant flow rate and pressure boundary conditions were applied through the FILL and BREAK components at the CORE entrance and exit, respectively.

The RELAP5/MOD1 model of the test section consisted of a combination of PIPE, TIME DEPENDENT VOLUME, and TIME DEPENDENT JUNCTION components. The heated rods were represented using a cylindrical heat structure model. An example of nodalization is shown in Figure 5.1.2 for the RELAP5/MOD1 code. The code uses the W-3 critical heat flux correlation package which includes the Hsu-Beckner correlation (1977), and the modified Zuber correlation (Smith and Griffith, 1976). The nodalization for all three input models was the same, and all three codes were run in the transient mode until a quasi-steady-state condition was reached.

5.1.3 Code Predictions and Comparison with Data

All three codes have some differences in their wall heat transfer and vapor generation models, which are reflected in the code predictions of major thermal-hydraulic parameters. However, as only the rod surface temperatures were measured, the other computed fluid variables such as void fraction, liquid, and vapor temperature could not be verified with the data; therefore, only a code-to-code comparison was performed for these variables. Figure 5.1.3 shows a comparison of the predicted rod surface temperature with the experimental data averaged over a number of heated rods. TRAC-BD1 showed good agreement with the data and correctly predicted the onset of CHF. However, both RELAP5/MOD1 and TRAC-PF1 predicted an early CHF condition which led to an overprediction of the rod surface temperature.

Subsequent to the CHF location, the rod surface temperature rapidly increased because of deterioration of the heat transfer process. This was due to a combination of lower heat transfer coefficient, and increased vapor superheating. Figure 5.1.4 shows the predicted vapor temperatures along the channel. TRAC-BD1 and TRAC-PF1 both predicted substantial vapor superheating above the CHF location. The RELAP5/MOD1 code, on the other hand, predicted
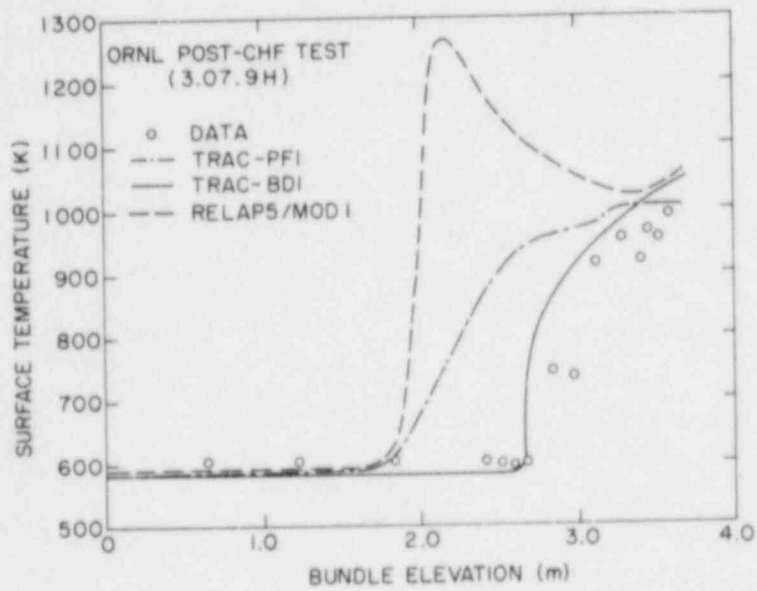
Figure 5.1.3 Comparison Between the Measured and Predicted Rod
Surface Temperature for ORNL Test 3.07.9H.
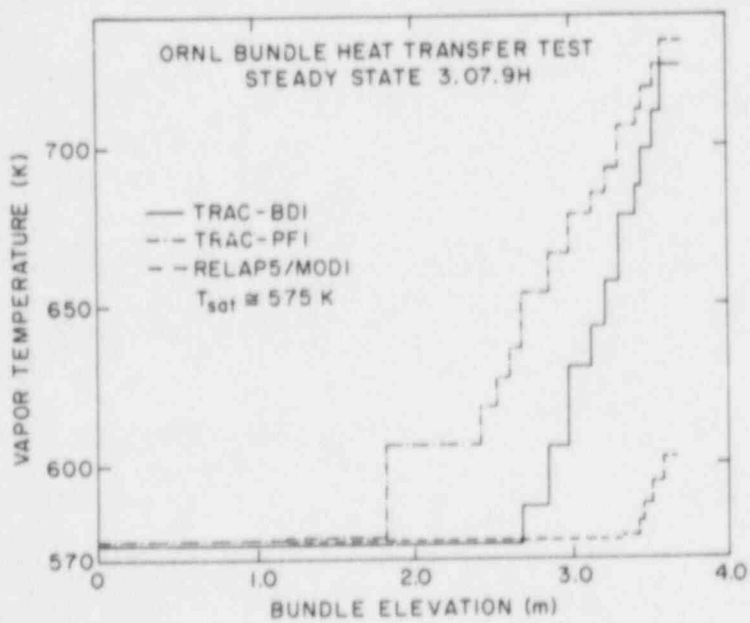
Figure 5.1.4 Various Predictions for the Vapor Temperature for
ORNL Test 3.07.9H.

almost no vapor superheating as long as some liquid was present in the mixture. This is in contradiction with the reality, particularly for the low mass flux used in the selected test. In such cases, the vapor-to-liquid heat transfer is low enough to create a significant vapor superheating as calculated by TRAC-BD1 and TRAC-PF1. This vapor superheating causes the actual wall temperature to increase continuously as shown in Figure 5.1.3. RELAP5/MOD1 did not capture this trend because of the high vapor generation rate which kept the vapor temperature close to saturation until almost all the liquid was evaporated. Therefore, the RELAP5/MOD1 model for vapor generation in the post-CHF regime needs improvement.

5.1.4   Discussion

Since all three codes used different CHF correlations, it is not surprising that the predicted CHF locations are different. Within the limitation of this assessment, the TRAC-BD1 CHF correlation seems to be the best.

At the post-CHF region, both TRAC-PF1 and TRAC-BD1 predicted increasing vapor superheating. This is to be expected since at low mass fluxes, the interfacial heat transfer between the vapor and liquid is rather poor. Thus, the actual vapor generation rate should be significantly less than the equilibrium phase change rate resulting in a significant vapor superheating. RELAP5/MOD1 did not predict this because of its high vapor generation rate. Clearly, the RELAP5/MOD1 models for the post-CHF region need improvement.

5.1.5   User Experience

There was no difficulty in running any of the computer codes for this particular test. The run time statistics are provided in Table 5.1.1

Table 5.1.1 Computer Run Time Statistics for the ORNL Post-CHF
Test Simulation

Computer: BNL CDC-7600

Calculation Item	TRAC-PF1	RELAP5/MOD1	TRAC-BD1
No. of Cells	19	19	19
Problem Time (s)	100	100	65
No. of Time Steps	603	12801	5054
CPU Time (s)	54.7	357	483
CPU-to-Problem Time	0.55	3.6	7.4
CPU (s)/Cell/Time Step	4.8×10^{-3}	1.5×10^{-3}	5.0×10^{-3}

5.2 Summary and Conclusions

Because of resource limitations, only one post-CHF experiment was simulated with the TRAC-PF1, TRAC-BD1 and RELAP5/MOD1 codes. From the results presented in Section 5.1.3, the following conclusions can be drawn:

1. The CHF correlation used in the TRAC-BD1 code, i.e., the Biasi critical quality-boiling length correlation, seems to be adequate. Other correlations as used in TRAC-PF1 and RELAP5/MOD1 tend to predict an early CHF which results in an overprediction of wall temperature in the post-CHF region.

2. RELAP5/MOD1 tends to overpredict the vapor generation rate at the post-CHF region. This results in almost no vapor superheating until all the liquid droplets are evaporated in the RELAP5/MOD1 calculation. TRAC-BD1 and TRAC-PF1, on the other hand, calculate a significant vapor superheating which is closer to reality. Thus, the RELAP5/MOD1 model for vapor generation in the post-CHF regime should be improved.

6. SIMULATION OF STEAM GENERATOR EXPERIMENTS

The steam generator is one of the more important pieces of equipment in the pressurized water reactor (PWR) system. It is here that heat generated in the reactor core is transferred into the secondary side. Thus, the thermal-hydraulics behavior of the primary side greatly depends on the performance of the steam generator during many transients, including the operational transients and small-break LOCA. Even during the reflood stage of a large-break LOCA, the steam generator heat transfer (from secondary to primary) determines the steam venting capacity and thus influences the core cooling.

In the present assessment effort, two types of steam generator experiments were simulated with TRAC-PF1 (Version 7.0) and RELAP5/MOD1 (Cycle 14) codes. First, two series of operational transients conducted in a 19-tube B&W once-through steam generator (OTSG) were simulated. Next, two tests conducted in the FLECHT-SEASET U-tube steam generator were simulated. Conditions in these latter tests were those expected during the reflood phase of a large break LOCA. The assessment results of these two different experiments will be discussed separately.

6.1 B&W Once-Through Steam Generator Tests

6.1.1 Test Description

The test apparatus was a laboratory steam generator which was a single-pass countercurrent vertically oriented shell and tube heat exchanger, consisting of 19 tubes, 5/8 inch in nominal diameter (0.628 inch in outside diameter and 0.0365 inch in wall thickness), spaced on a triangular pitch of 7/8-inch centers. The tube bundle was enclosed in a hexagonal shell 3.935 inches across flats, and was held in place by 16 tube support plates spaced at approximately 3 ft intervals. The distance between the lower and the upper tube sheets was 52 ft 1-3/8 inch. To simulate the standard B&W Once-Through Steam Generators (OTSG), a steam bleed line was installed at an elevation of 32 ft 3/8 inch from the lower tube sheet. Thus, some steam from the bundle region could mix with the feedwater, and raise its temperature close to saturation. On the other hand, by simply closing the valve in the bleed line one could simulate the Integral Economizer Once-Through Steam Generators (IEOTSG).

A variety of transient experiments were conducted in both the OTSG and IEOTSG configurations. Two test series were simulated at BNL using the TRAC-PF1 and RELAP5/MOD1 codes, one for each of the IEOTSG and OTSG configurations.

a) Test Series 68-69-70 where the load was increased from 15% to 25% by stepping up the steam valve opening with the IEOTSG configuration.

b) Test Series 28-29 which simulated a loss of feedwater transient with the OTSG configuration.

In both cases, the operating pressures and temperatures were representative of the full-scale plant conditions, and all the pertinent variables at the primary and secondary sides were measured. These included the pressure, flow

rate, inlet and exit fluid temperature at the primary side, and the feedwater flow rate and temperature, steam pressure and temperature, and differential pressure at the secondary side. The data are proprietary to B&W, and the measurement uncertainties were not available in the data report (Loudin and Oberjohn, 1976).

6.1.2   Input Models

For TRAC-PF1, the test apparatus was modeled by using the once-through option of the STEAM GENERATOR component (STGEN) for TRAC. The secondary TEE connection available in the TRAC-PF1 STGEN module was used to simulate the aspirator of the OTSG.

However, since only one secondary TEE is provided in the STGEN module, it cannot be used for both the aspirator and the auxiliary feedwater connection for possible use in analyzing other transients such as the Rancho Seco Overcooling Transient. Therefore, another input deck was prepared by connecting two STGEN modules in series with a TEE component in between as shown in Figure 6.1.1. Results of these two inputs were compared to ensure that they produced similar results. The boundary conditions were imposed by a set of FILL and BREAK components at the inlet and exit of the primary and secondary sides.

For RELAP5/MOD1, the steam generator was modeled by assembling PIPES, BRANCHES, and HEAT STRUCTURES as well as JUNCTIONS. The time dependent junction and volumes provided the boundary conditions for both the primary and secondary sides.

Several different nodalizations for the tube region were studied for each test series for each code. In all cases, the primary side had two more cells than the secondary side to represent the inlet and outlet plena. This is required by TRAC. The number of active nodes in the primary and secondary sides were increased from 5 to 10 to 20 to 40. In all cases, the cell lengths were uniform and the active length of the steam generator was 15.9 m. Four radial nodes were employed in the tube wall for heat conduction calculations. A steady state was established for each test series. The transient was then initiated by changing the boundary conditions.

6.1.3   Code Predictions and Comparison With Data

The results of the TRAC-PF1 simulation of IEOTSG (Test Series 68-69-70) were considerably better than those of the TRAC-PD2 as shown in Figure 6.1.2. The simulation of OTSG (Test Series 28-29) with TRAC-PF1, also showed stable results for both the steady-state and the transient calculations (Figure 6.1.3).

The RELAP5/MOD1 (Cycle 14) results were also significantly improved over the earlier calculation with Cycle 1 of the same code for both the IEOTSG and OTSG tests.

Figure 6.1.4 compares the RELAP5/MOD1 and TRAC-PF1 results for the IEOTSG test (Series 68-69-70) with the experimental data. (The vertical scale is
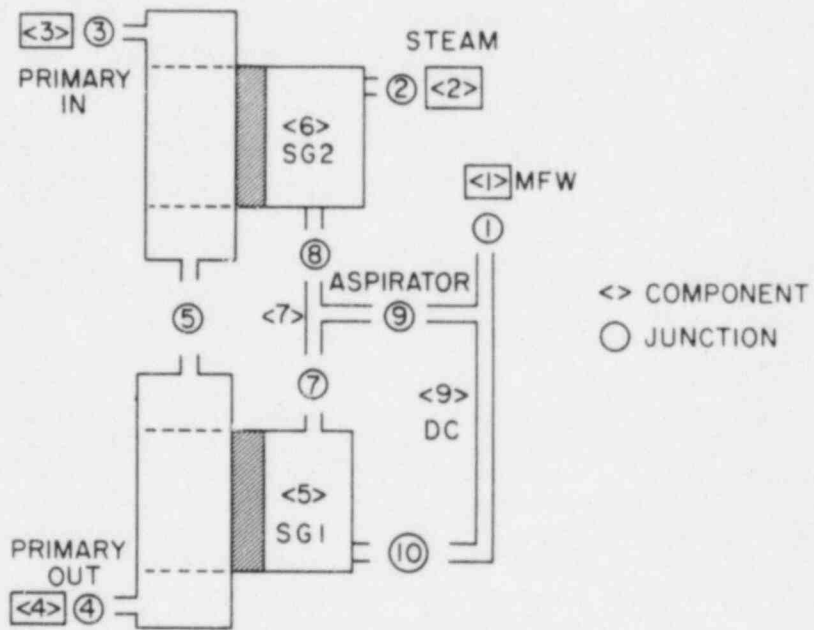
Figure 6.1.1   Representation of a Once-Through Steam Generator
With Two TRAC-PF1 STGEN Modules.
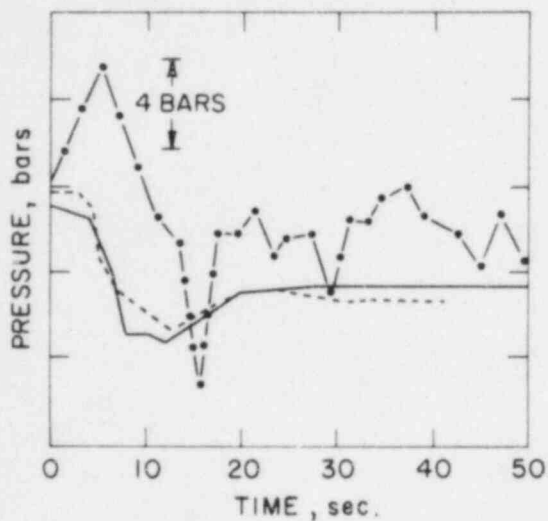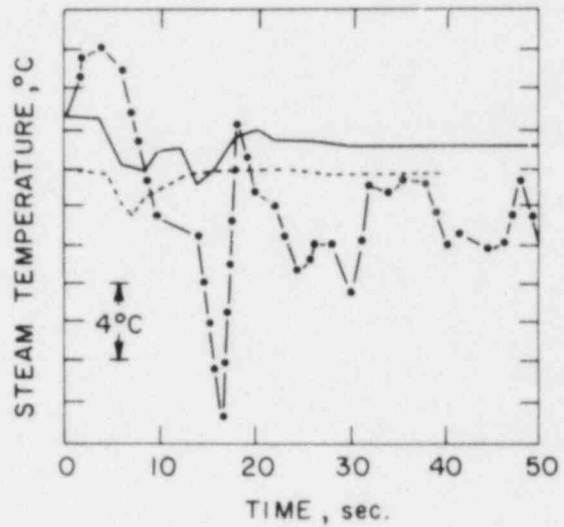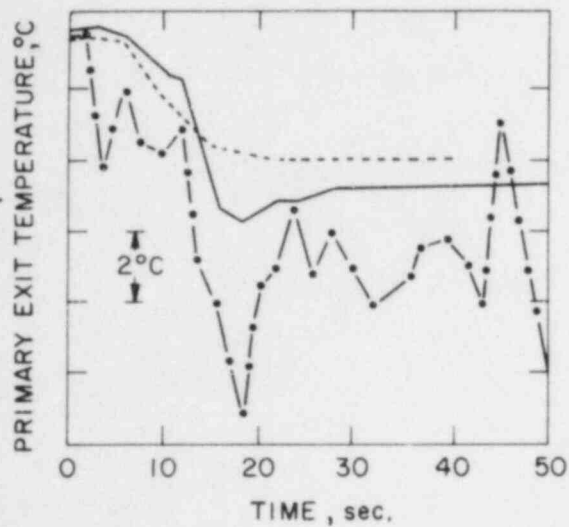
Figure 6.1.2   Comparison of TRAC-PF1 and TRAC-PD2 Predictions
With Experimental Data of IEOTSG Test Series 68-69-70.
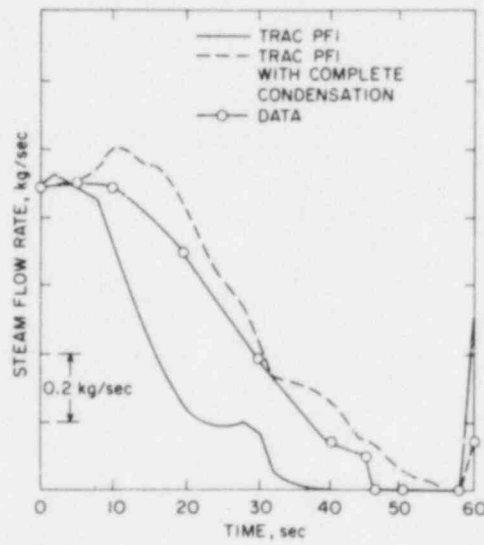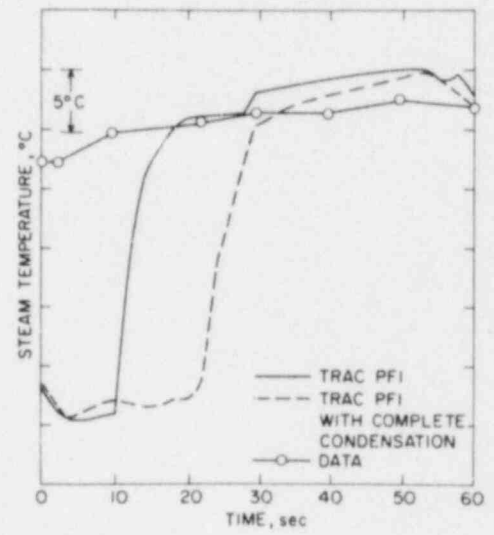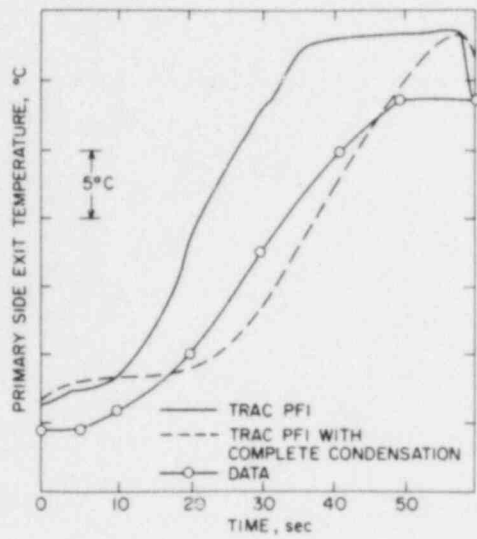
Figure 6.1.3 Comparison of TRAC-PF1 Predictions With Experimental
Data of OTSG Test Series 28-29.
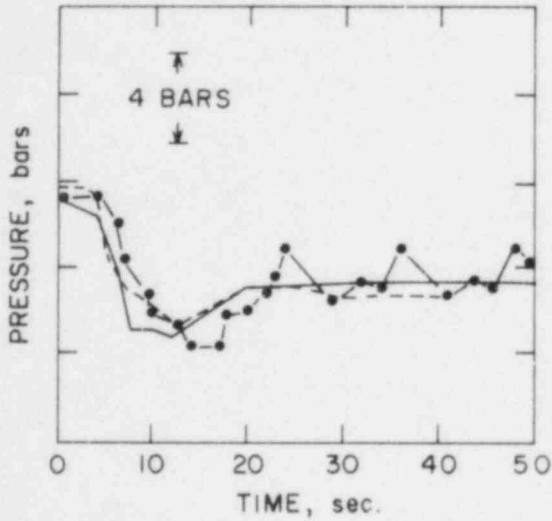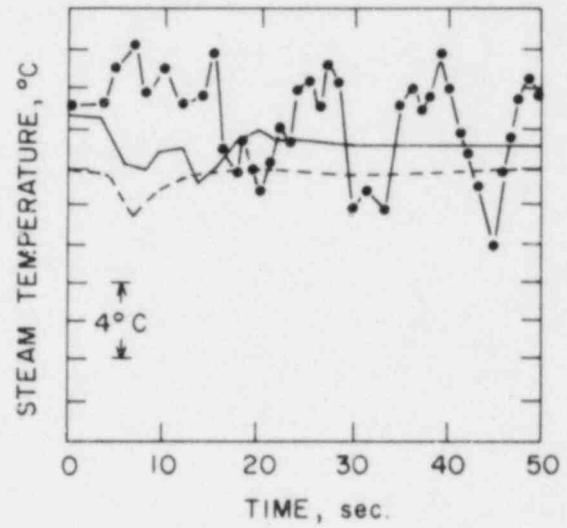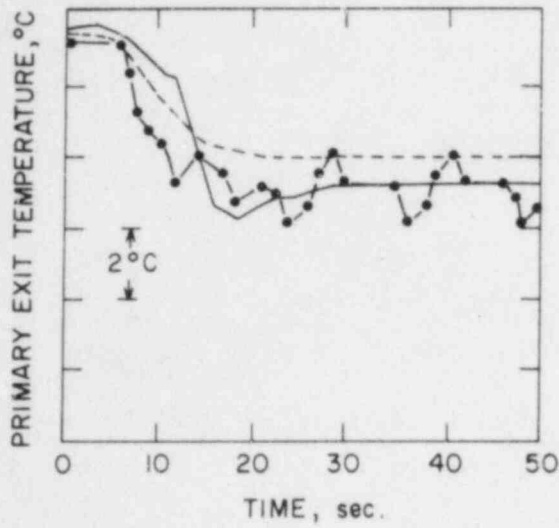
Figure 6.1.4 Comparison of Predicted Primary Exit Temperature, Secondary Exit Steam Temperature, and Secondary Pressure With Experimental Data of IEOTSG Test Series 68-69-70.

withheld in all figures presented in this section because the data are B&W proprietary.) Both calculations were performed using 10 cells or nodes in each side of the steam generator. Both codes showed good agreement with the experimental data, although the RELAP5/MOD1 results still showed some oscillations.

Figure 6.1.5 shows the comparison of the RELAP5/MOD1 and TRAC-PF1 results with OTSG (Series 28-29) test data. Note that the TRAC-PF1 code was slightly modified to ensure complete condensation of aspirated steam in the downcomer during steady state. This will be discussed later.

6.1.4   Discussion

In the previous calculation with the TRAC-PD2 code, significant oscillation was observed during both steady-state and transient calculations even in cases where 40 nodes were used for each side of the steam generator for both the OTSG and IEOTSG configurations. However, with TRAC-PF1 (Version 7.0) the oscillation was virtually eliminated in both the steady-state and transient calculations even with only 10 nodes.

Although TRAC-PF1 showed stable results for the steady state of the OTSG test (Series 28), a substantial portion of the recirculated steam into the downcomer through the aspirator (steam-mixer valve in the test) remained as vapor even at the bottom of the downcomer. Therefore, the fluid entering the tube region still contained a significant amount of voids even though the liquid was substantially subcooled. This was contrary to both expectation and reality. As a result, the initial water inventory in the downcomer was significantly less than that in the test, and consequently, the computed exit steam flow rate decreased faster than the test flow rate during the transient. This effect of condensation (or lack of sufficient condensation) was confirmed when the calculation was repeated with the interfacial condensation rate increased by a factor of 10^4 to ensure complete condensation. The calculated results were now very close to the experimental data, as shown in Figure 6.1.3.

The simulation for the OTSG test was repeated using two STGEN modules as shown in Figure 6.1.1. This configuration may be necessary when both the aspirator and auxiliary feedwater connections are needed since the TRAC-PF1 (Version 7.0) provides only one external connection from the secondary side which can be used only for the aspirator or for the auxiliary feedwater connection. The results, as shown in Figure 6.1.6, were almost identical to those where only one STGEN module was used, and the computing times were close. This indicates that, if needed, one may use the configuration with two STGEN modules without incurring any significant penalty in either computer time or accuracy. Calculations for both the tests were repeated with different numbers of nodes to study the effect of the nodalization. The results for OTSG are given in Figure 6.1.7. They showed some improvement as the number of nodes increase, but not enough to justify the increased computing time. It is, therefore, recommended that 10 nodes be used for cases such as feedwater transient where the steam generator thermal performance is important; otherwise, 5 nodes can be used for other cases.
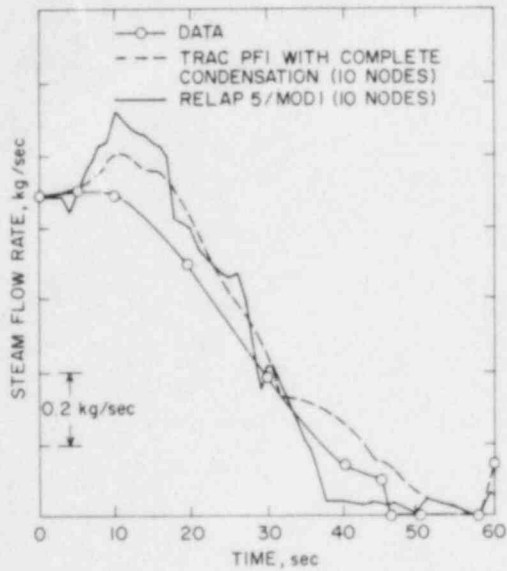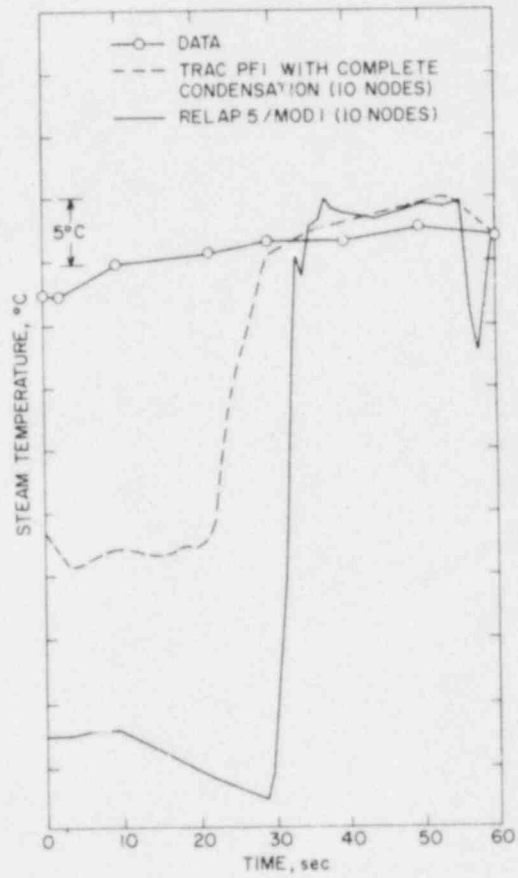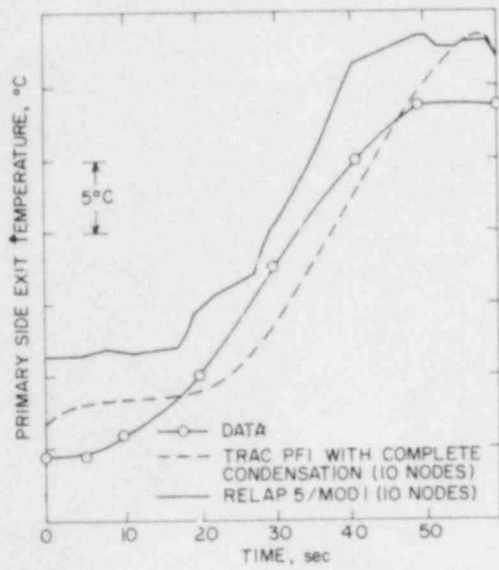
Figure 6.1.5 Comparison Between the Measured and Predicted Primary
Exit Temperature, Secondary Exit Steam Temperature, and
Flow Rate for B&W OTSG Test 28-29.
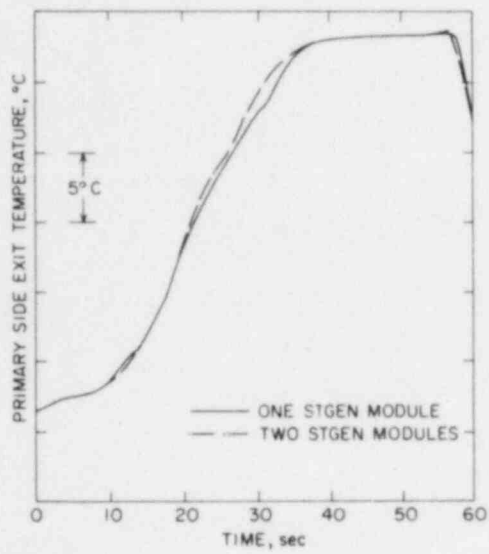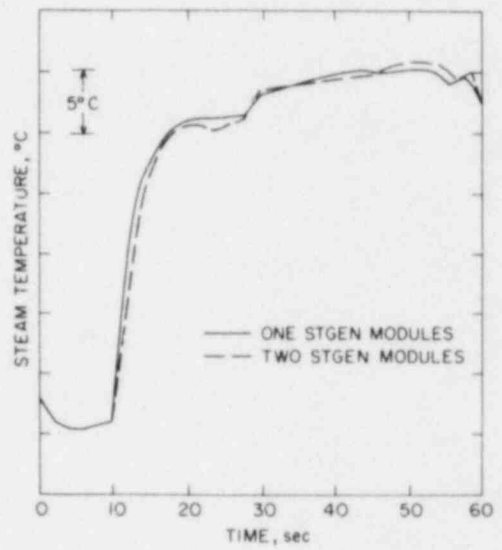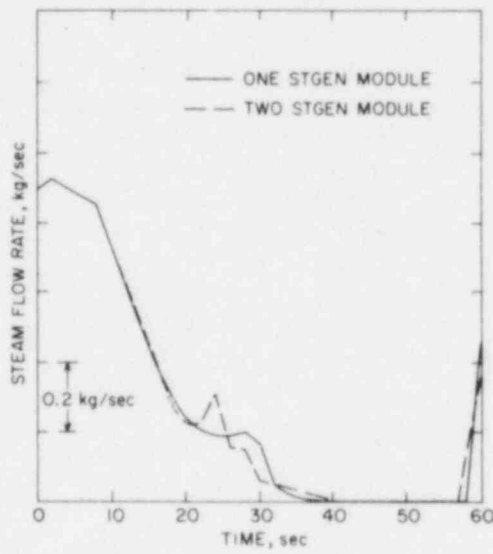
Figure 6.1.6   Comparison Between TRAC-PF1 Calculations With One and
Two STGEN Modules for OTSG Test Series 28-29.
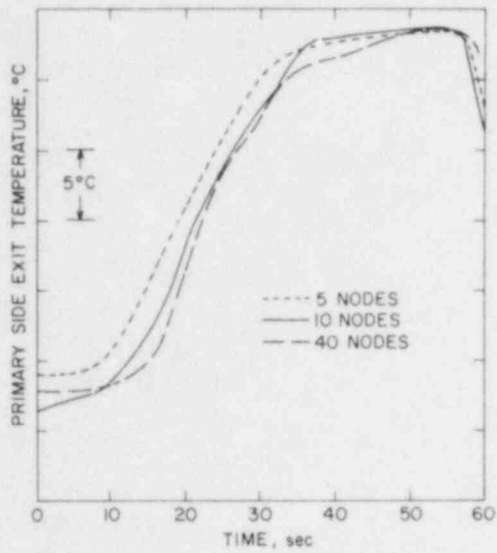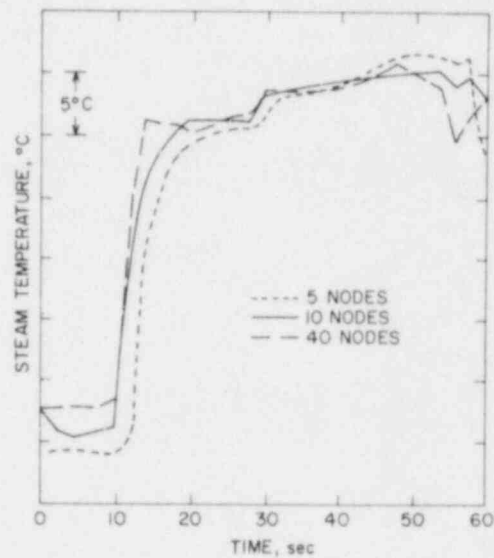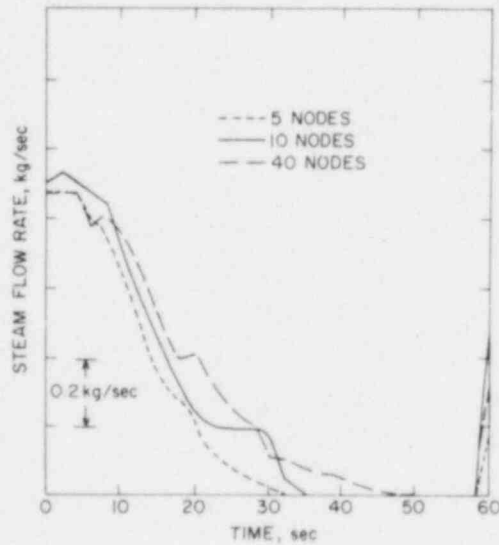
Figure 6.1.7 TRAC-PF1 Predictions for OTSG Test Series 28-29 With Various Nodalizations.

The results for the IEOTSG simulation (Test Series 68-69-70) with RELAP5/MOD1, as given in Figure 6.1.4, showed good agreement with the data, but still showed some oscillations. This calculation was, therefore, repeated with the maximum time step limited to 0.01 second. This reduced the magnitude of oscillation considerably as shown in Figure 6.1.8. However, the computer running time increased by a factor of 10. Also, the secondary side pressure prediction was worse than the original calculation.

To study the effect of nodalization, the IEOTSG calculation was repeated with the RELAP5/MOD1 code using 40 cells in each side of the steam generator. The results shown in Figure 6.1.9 indicate some improvement in stability, but the calculated pressure for the 40-node case was much worse than the 10-node case.

In Figure 6.1.5, the RELAP5/MOD1 and TRAC-PF1 results are compared with the OTSG (Series 28-29) test data. Note that the TRAC-PF1 code was slightly modified to ensure complete condensation of aspirated steam in the downcomer during steady state. For both calculations 10 nodes were used in each side of the steam generator. The RELAP5/MOD1 results indicate a slightly lower overall primary-to-secondary side heat transfer than the results obtained with TRAC-PF1 and the experimental data. This manifests itself in the higher primary side exit temperature and lower secondary side exit steam temperature. It should be mentioned that at steady state, RELAP5/MOD1 did not predict any superheating of steam, whereas both the experiment and TRAC-PF1 indicated significant superheating. This agrees with the observation made in Section 5.1 with respect to the RELAP5/MOD1 post-CHF model. The secondary side exit flow rate was, however, predicted reasonably well by the RELAP5/MOD1 code.

6.1.5   User Experience

The TRAC-PF1 (Version 7.0) code ran without major difficulty for both OTSG and IEOTSG tests. However, RELAP5/MOD1 (Cycle 14) needed more careful attention to the maximum time step and stringent time step control option (e.g., Option 2 in the case of OTSG calculation) to suppress the oscillation. The computer run time statistics are shown in Table 6.1.1.

6.2   FLECHT-SEASET U-Tube Steam Generator Tests

6.2.1 Test Description

A schematic of the FLECHT-SEASET steam generator test facility is presented in Figure 6.2.1. It can be seen that a boiler and water supply tank are connected to the hot leg side of the inlet plenum. The boiler supplies the steam while the water is entrained at the mixer box to send a variety of two-phase flow situations to the steam generator which will resemble conditions that exist in the primary system during reflood. Figure 6.2.1 also shows the steam generator model to be well instrumented with steam probes, tube wall thermocouples, fluid thermocouples, flowmeters, and pressure transducers to establish the exact state of the fluid so that the code predictions could be compared against the data. A detailed description of the facility has been published (Howard et al., 1980) which establishes the data credibility along with the experimental procedures.
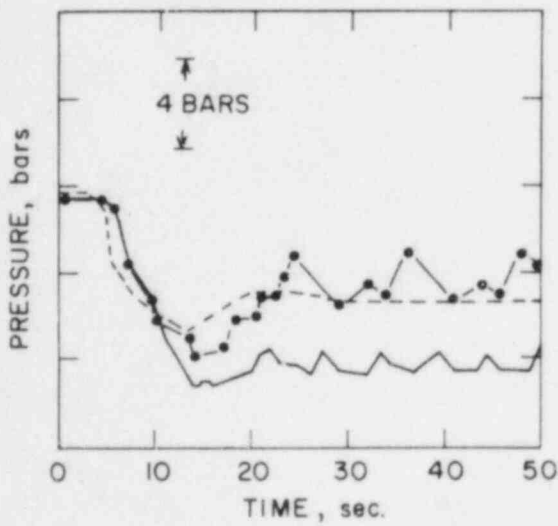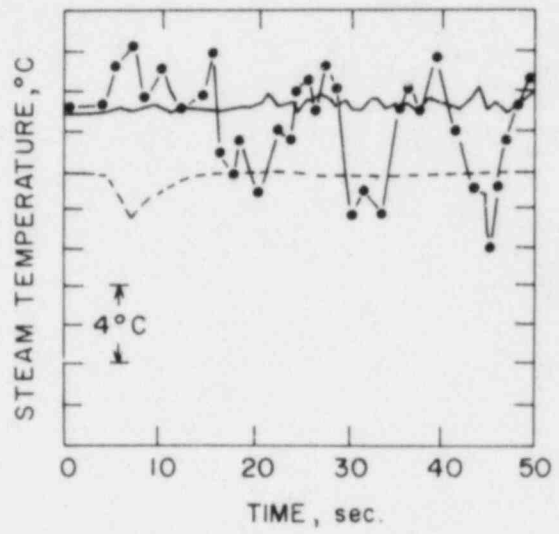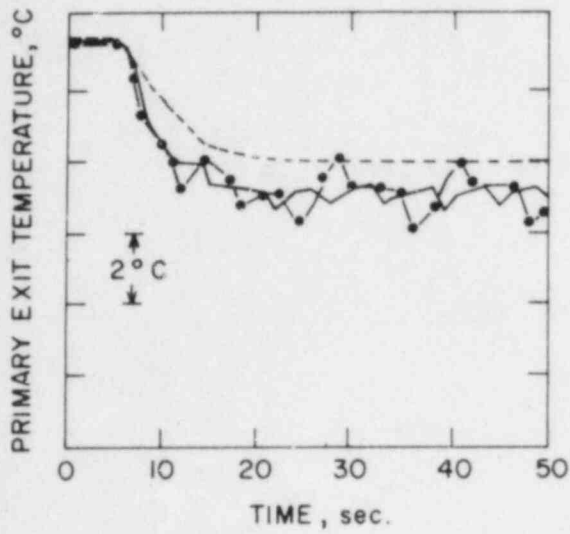
Figure 6.1.8 Comparison of RELAP5/MOD1 Calculations With Two
Different Maximum Time Steps for IEOTSG Test Series
68-69-70.
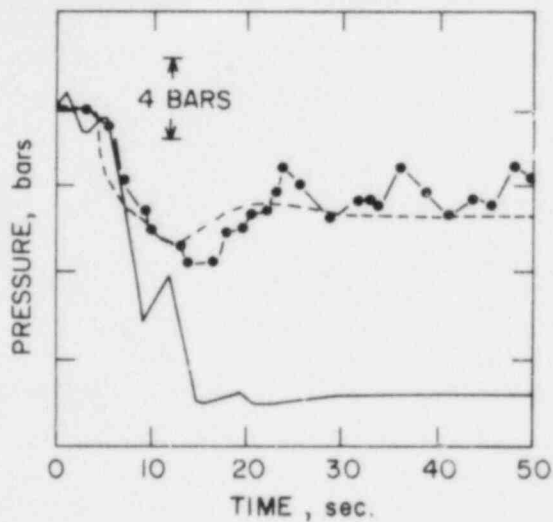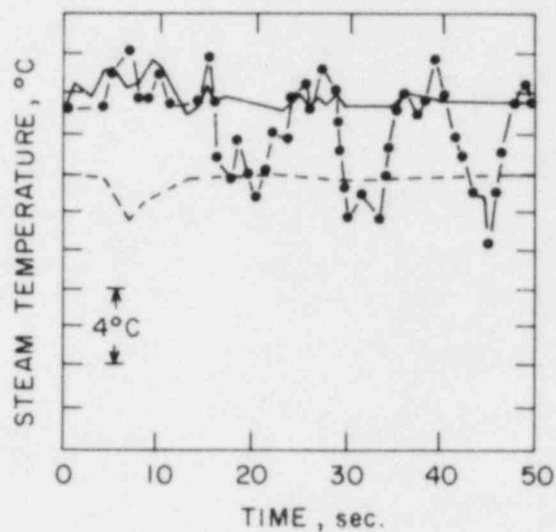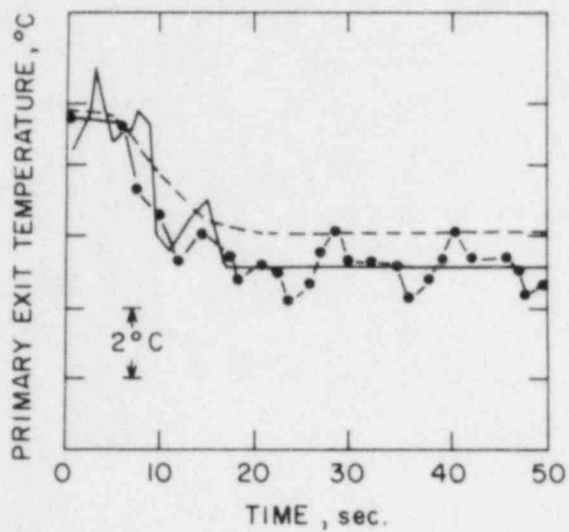
Figure 6.1.9 Comparison of RELAP5/MOD1 Calculations With Two
Different Nodalizations for IEOTSG Test Series
68-69-70.
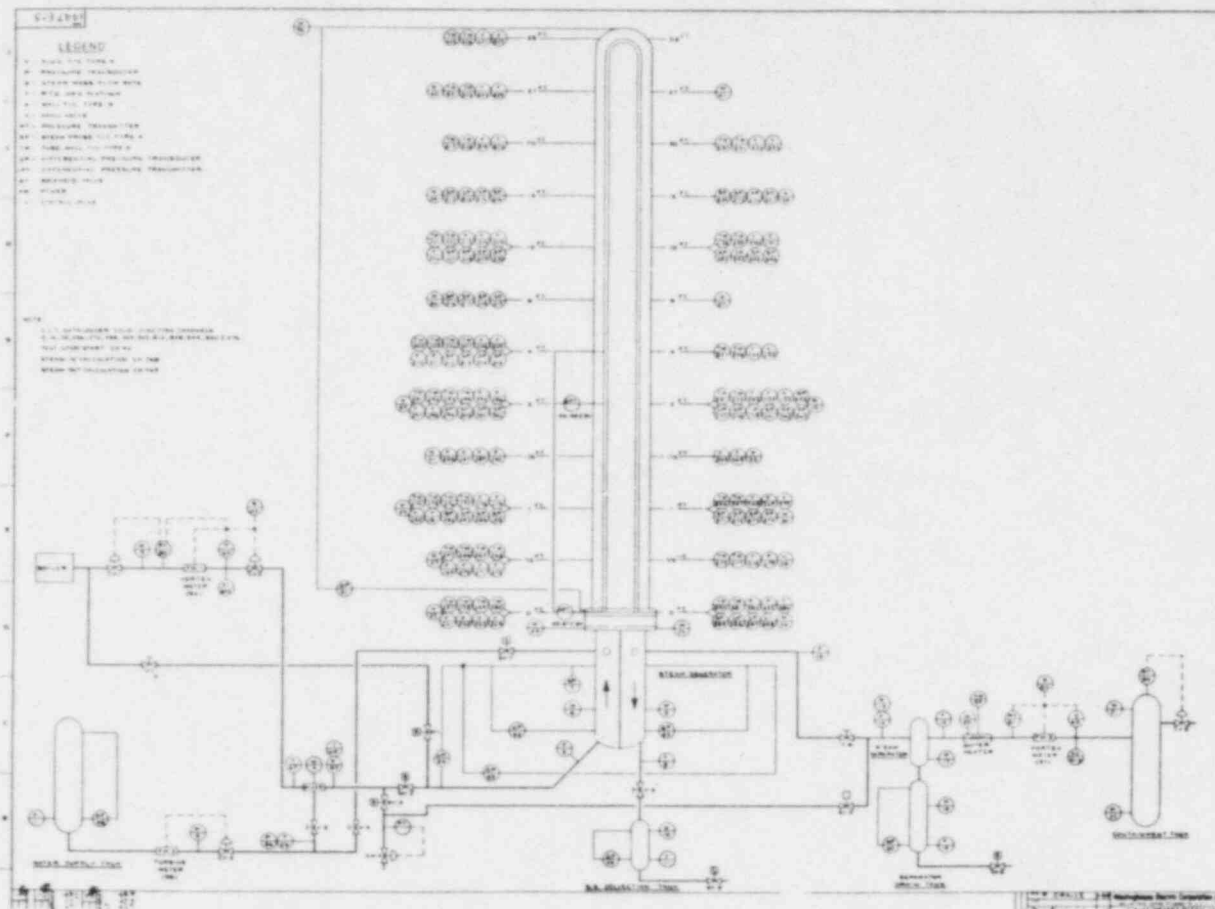
Figure 6.2.1 Schematic of the FLECHT-SEASET Steam Generator Test Facility.

Table 6.1.1 Computer Run Time Statistics for the B&W Model
Steam Generator Test Simulation

Computer: BNL CDC-7600

| Calculation | TRAC-PF1 | | RELAP5/MOD1 | |
Item	IEOTSG Series 68-69-70	OTSG Series 28-29	IEOTSG Series 68-69-70	OTSG Series 28-29
No. of Cells	22	32	22	32
Problem Time (s)	50	60	50	60
No. of Time Steps	255	296	400	485
CPU Time (s)	21	42.3	12	18.5
CPU-to-Problem Time	0.42	0.71	0.24	0.31
CPU(s)/Cell/Time Step	3.7×10^{-3}	4.5×10^{-3}	1.4×10^{-3}	1.2×10^{-3}

The steam generator itself consisted of a lower plenum split in half, a U-tube bundle, and a cylindrical shell. The bundle had 33 tubes each of 0.0222 m I.D., of which 32 were operational. The height of the steam generator was 10.7 m above the tubesheet with an inside diameter of 0.32 m. The facility was instrumented with a large number of thermocouples to measure the shell wall, tube wall, secondary side fluid, and the primary side steam temperatures. Also, several flowmeters at various locations provided enough differential pressure and pressure transducers to establish the state of the experiment at any given time.

The tests were run by feeding steam and water into a mixing chamber which generated a high-void two-phase mixture in the hot leg. The established mist-flow conditions in the primary side remained constant during the test. Hence, the primary, or tube side, of the steam generator was receiving fluid at steady-state conditions while the real transient was the cooldown of the water on the shell side of the steam generator. The secondary, or shell side, was initially filled up to a level which covered the tubes with high pressure stagnant water that cooled down slowly during the test corresponding to the heat transfered from the secondary to the primary fluid.

Tests ID=21806 and ID=22010 were simulated with both TRAC-PF1 (Version 7.0), and RELAP5/MOD1 (Cycle 14). The operating conditions for these tests are given in Table 6.2.1.

Table 6.2.1 Operating Conditions for the Simulated FLECHT-SEASET
Steam Generator Tests

	Test Averaged Boundary Conditions					Secondary Side Initial Conditions	
TEST ID	Steam Flow kg/s	Steam Temp. °K	Water Flow kg/s	Water Temp. °K	Flow Quality	Average Temp. °K (above 0.3 m)	Pressure MPa (topmost level)
21806	0.045	421.2	0.181	401.2	0.20	544.2	5.69
22010	0.182	427.2	0.045	398.2	0.80	546.7	5.75

6.2.2 Input Models

To predict tests ID=21806 and ID=22010, the TRAC-PF1 and RELAP5/MOD1
codes modeled the test facility as shown in Figures 6.2.2 and 6.2.3, respec-
tively. Great care was taken to make sure that both codes used exactly the
same options and geometrical data (i.e., the cells in both input decks were
identical). Since both input decks are identical, except for the differences
in the component names, only the TRAC-PF1 model will be described, with dif-
ferences noted when applicable.

TRAC-PF1 modeled the test facility as shown in Figure 6.2.2. The hot leg
was represented by a TEE component so that the two-phase steam-water mixture
could be supplied as mass flow rate boundary conditions by the two FILL compo-
nents seen in Figure 6.2.2. The steam generator models of TRAC, called STGEN,
had 22 cells in the primary with 12 levels on the secondary side. This number
of cells was necessary to center some cells with the instrumentation locations
and to keep a cell length consistency throughout the steam generator. The two
FILL components in the secondary side of STGEN are required, but are set to
zero mass flow rate since the secondary side was stagnant. In RELAP5/MOD1,
the code does not have a steam generator model per se, but one is built with
PIPE components that achieve the same purpose.

The final boundary condition to be discussed in the nodalization is the
BREAK (or SNGLJUN-TMDPVOL combination of RELAP5) component seen in Figure
6.2.2 at the primary side exit plenum. The BREAK was used to provide a pres-
sure boundary condition. The pressure was determined by backing out the data
from the mixer chamber pressure and two differential pressures between the hot
leg and the exit plenum.

The last topic to be discussed in the modeling of the FLECHT-SEASET steam
generator is the problem with the energy stored in the 3200 kg of metal above
the tubesheet. The 500 kg of Inconel 600 in the tube bundle can easily be
handled by TRAC-PF1 since this is built into the STGEN component. But the
2700 kg of steam generator shell wall which represents a source of about 30%
of the total energy released during both tests cannot be simulated in the

TRAC-PF1 (7.0)
NODALIZATION

FILL

STGEN

FILL

FILL

BREAK

FILL

TEE

FILL
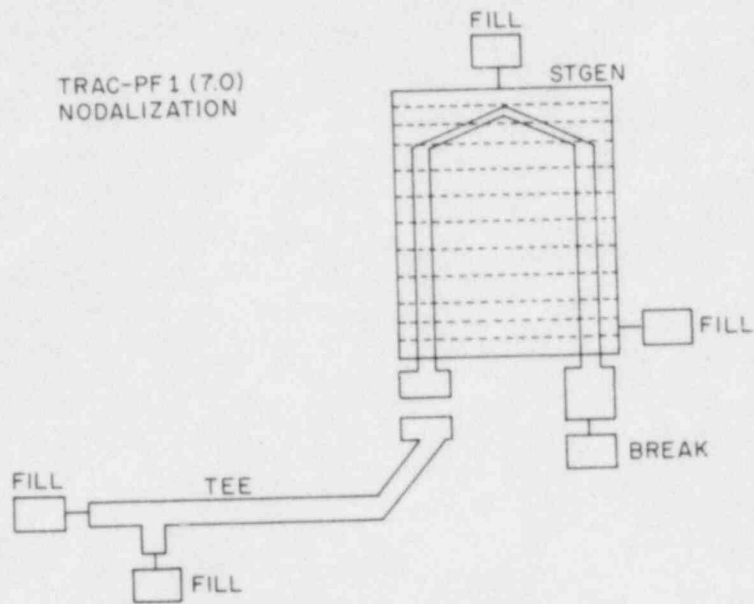
Figure 6.2.2   TRAC-PF1 Nodalization for the FLECHT-SEASET
Steam Generator Tests.

PIPE

RELAP5/MOD 1 (CY14)
NODALIZATION

SNGLJUN

SNGLJUN

TMDPVOL

TMDPJUN

TMDPVOL

BRANCH

PIPE

TMDPJUN

TMDPVOL
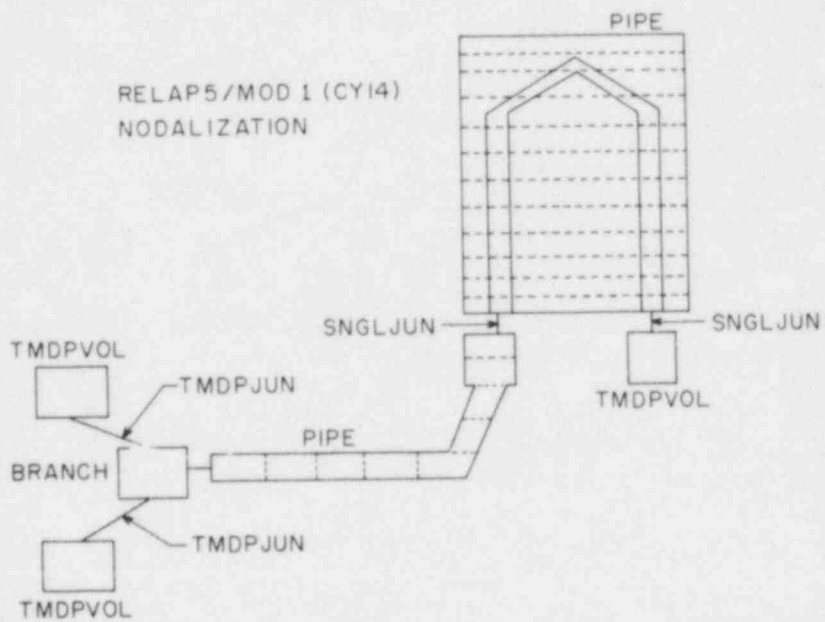
Figure 6.2.3   RELAP5 Nodalization for the FLECHT-SEASET
Steam Generator Tests.

STGEN component of TRAC-PF1. It should be noted that for a typical full-scale U-tube steam generator the internal surface area to volume ratio is ~1.4 m^{-1} while that for the FLECHT-SEASET steam generator was ~37.0 m^{-1}. Therefore, it is not as critical to model the steam generator shell in the typical full-scale U-tube steam generator because the released energy would represent a fraction much less than the 30% present in the FLECHT-SEASET steam generator. However, if the code is to be used to model thermal-hydraulic experiments in the reduced-scale facilities such as the FLECHT-SEASET steam generator, the energy stored in the shell wall should be a representable option.

This problem was circumvented by adding an equivalent water volume to the steam generator secondary side water. This additional water had the same amount of energy as the shell wall, and was determined from

$$M_s \, c_{p,s} \, T_s = M_w \, c_{p,w} \, T_w \qquad\qquad (6.2.1)$$

where
  M_s = mass of steam generator shell wall

  M_w = mass of equivalent water

  $c_{p,s}$ = heat capacity of shell wall

  $c_{p,w}$ = heat capacity of water

  T_s = initial temperature of shell wall

  T_w = initial temperature of water

After a hand calculation, the volume of additional water turned out to be 0.31 m^3.

This assumption of adding the equivalent water mass to represent the shell wall was justified from experimental data as well as from RELAP5/MOD1 calculations. It is seen from Figure 6.2.4 that the experimental values of the steam generator secondary side fluid temperature, and the steam generator shell wall temperature followed each other. At this point, it is important to note that the test results have never shown any radial temperature distributions on any horizontal plane. Thus, the comparison of the two codes with the data was justified since the data and codes were both one dimensional. This trend was followed throughout the steam generator test except below the 0.6096 m (2 ft) level (see Figure 6.2.5) where the most rapid changes were taking place.

The result of not simulating the steam generator shell wall with TRAC-PF1 is presented in Figure 6.2.6. Comparisons of other predicted variables showed the same type of difference. Finally, to place this method of treating the steam generator shell on a more solid ground, RELAP5/MOD1 (Cycle 14) was used for the same test (i.e., ID=21806) and was run three times. First, it was run ignoring the stored energy in the shell wall. Second, it was run with heat slabs representing the shell wall. This is possible with RELAP5, but not with TRAC. And finally, RELAP5 was run with the equivalent water mass. Figure 6.2.7 illustrates the conclusion from these runs. The simulations with the
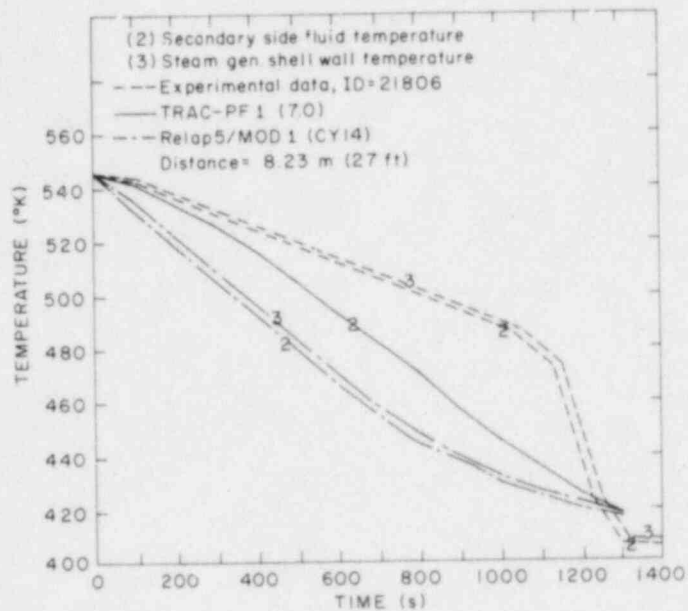
Figure 6.2.4 Secondary Side Fluid and Shell-Wall
Temperature at 27 ft Elevation for
FLECHT-SEASET Steam Generator Test
ID=21806.
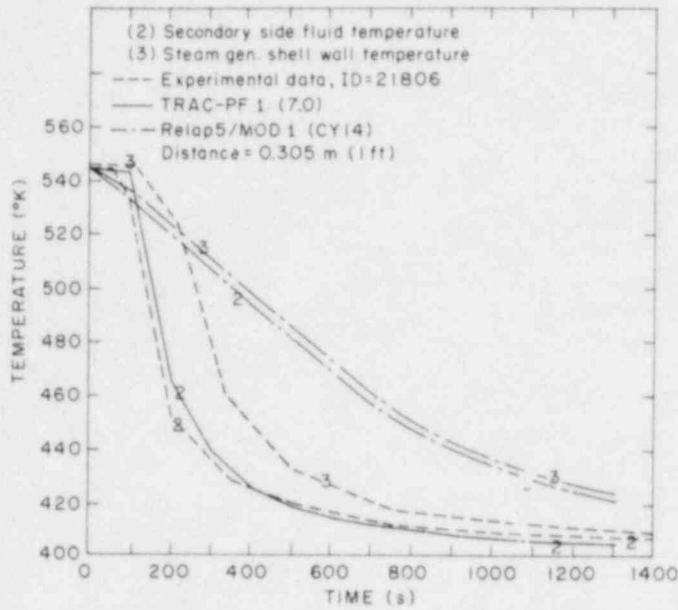
Figure 6.2.5 Secondary Side Fluid and Shell Wall Temperature at 1 ft Elevation for FLECHT-SEASET Steam Generator Test ID=21806.
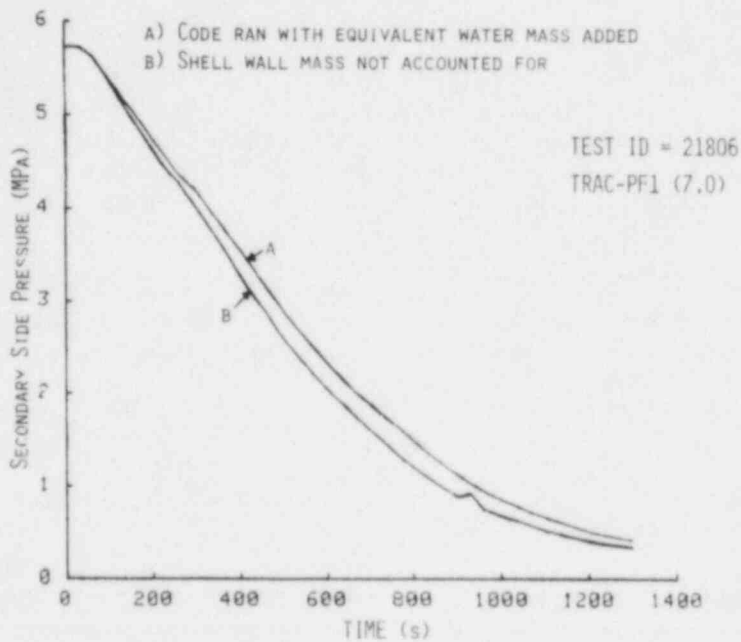
Figure 6.2.6 TRAC-PF1 Secondary Side Pressure for ID=21806 With and Without the Equivalent Water Mass for the Steam Generator Shell Wall.

heat slabs representing the shell wall and the water equivalence of steel yielded the same result while showing the same magnitude of improvement as found in the TRAC-PF1 prediction (see Figure 6.2.6). Also, many other parameters showed the same result. Consequently, the equivalent water approach was used for simulation of tests ID=21806 and ID=22010 with TRAC-PF1.

6.2.3   Code Prediction and Comparison with Data

6.2.3.1   Test ID = 21806

The TRAC-PF1 (Version 7.0) predictions for FLECHT-SEASET test ID=21806 are presented in Figures 6.2.8 through 6.2.14. The overall performance of the code can be judged from Figure 6.2.8 which shows the pressure at the top cell in the secondary side of the steam generator. It may be inferred that the code predicted the correct heat transfer from the secondary to primary side for the initial 300 s and then it began to overpredict the heat removed from the steam generator, as verified by the exit steam temperature in Figure 6.2.9, and the secondary side pressure in Figure 6.2.8. While the code did predict the secondary fluid temperature quite well for the first cell (see Figure 6.2.5) of the steam generator, this was the exception and not the rule. In Figure 6.2.4 the code predicted a lower secondary side fluid temperature, meaning that the heat transfer from secondary to primary was overestimated. Also the entrained droplets (see Figure 6.2.10) did not transverse the U-tube until the heat transfer rate decreased around 900 s (which is indicated by the change in slope for the TRAC prediction in Figure 6.2.8). Finally, in Figures 6.2.11 through 6.2.14 the predicted secondary side fluid and primary side steam temperatures are compared with the experimental values at various times. These results show that the top part of the steam generator is considerably cooler than expected which was caused by the larger heat flux predicted by TRAC-PF1. For the lower part, i.e., up to approximately 5 m, the secondary side temperature was first underpredicted (Figure 6.2.11), then overestimated (Figures 6.2.12 and 6.2.13), and by 1178 s it was again underpredicted (Figure 6.2.14). This came about because the code initially predicted the inlet side of the tube bundle to be in the transition boiling heat transfer regime, causing a higher wall heat flux than the expected film boiling situation above the quench front that was found experimentally. As already mentioned, the data showed a quench front moving up the tubes, causing a sharp knee in the wall and the secondary side temperature as an initial film boiling event was transformed into a nucleate boiling situation. The code, however, did not predict the correct turn around temperatures and times, as seen in Table 6.2.2, which caused the overprediction seen in Figures 6.2.12 and 6.2.13 for the secondary side fluid temperature. Finally, the code did approach the correct end result as the secondary side fluid temperature approached the primary side inlet fluid conditions.

The results of RELAP5/MOD1 for test ID=21806 are also presented on Figures 6.2.8 through 6.2.14. Figure 6.2.8 shows that the secondary side pressure is greatly underpredicted, while Figure 6.2.10 shows that RELAP5/MOD1 overpredicted the droplet carry over. Also in Figure 6.2.9 RELAP5/MOD1 exit steam temperature showed oscillations with a magnitude of almost 200 K. This was caused by the wall heat transfer mode switching alternately between the
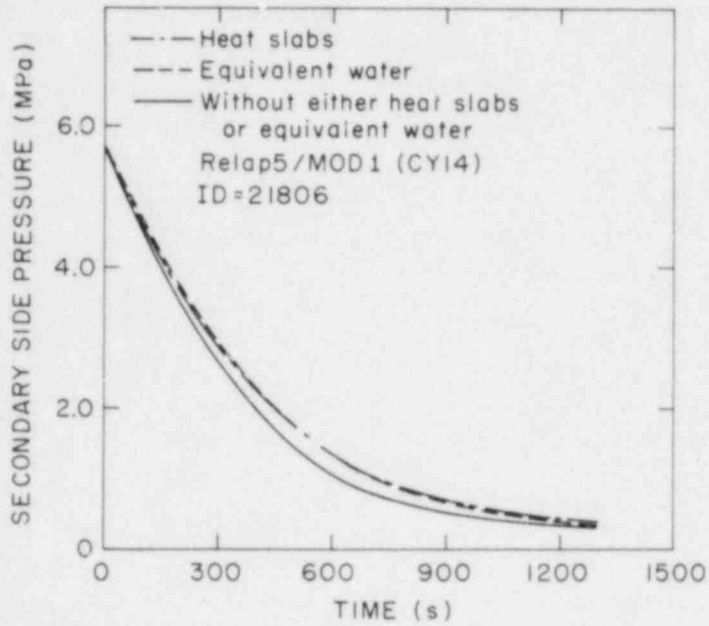
Figure 6.2.7   RELAP5/MOD1 Secondary Side Pressure for ID=21806
With Various Modeling for the Steam Generator Shell
Wall.
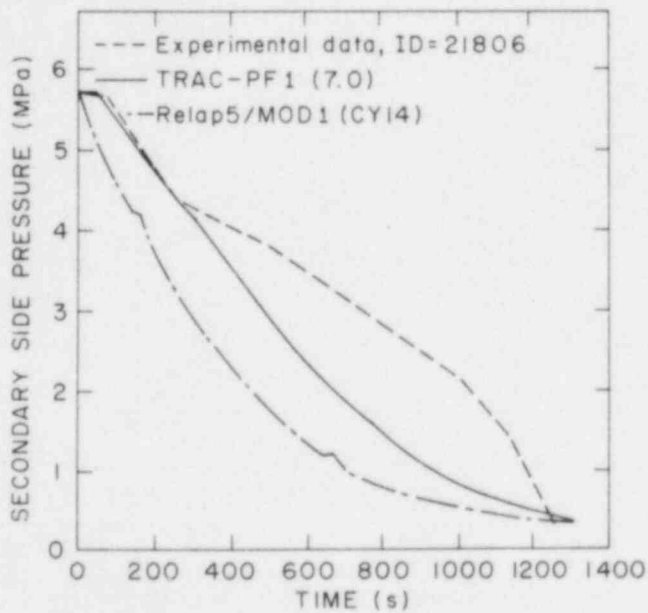
Figure 6.2.8   Comparison Between the Measured and Predicted
Secondary Side Pressure for ID=21806.

Figure 6.2.9   Comparison Between the Measured and Predicted
Primary Side Exit Steam Temperature for ID=21806.
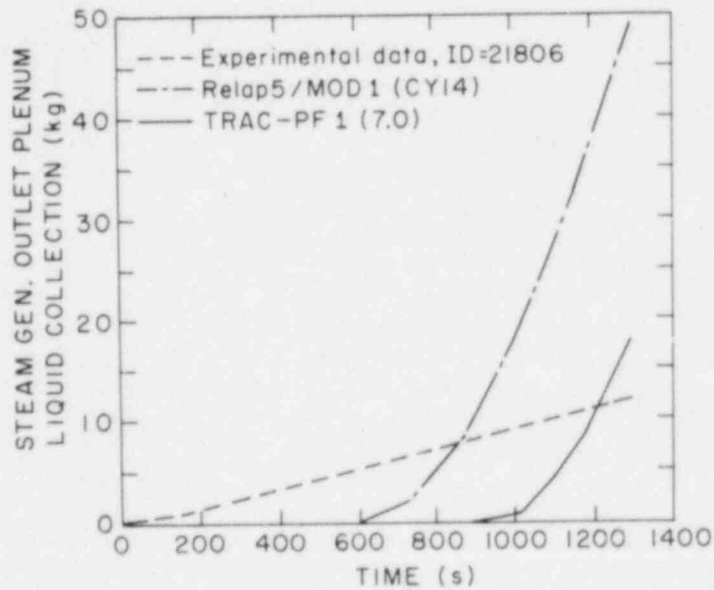
Figure 6.2.10 Comparison Between the Measured and Predicted
Liquid Mass at the Primary Side Outlet Plenum
for ID=21806.

forced convection of superheated vapor at medium flow using high flow correlations (i.e., heat transfer mode 18) and forced convection from superheated vapor to wall (i.e., heat transfer mode 22). These oscillations were found to be the direct result of the code taking too large a time step which allowed too much energy to be transferred during the time step. These oscillations stopped when the maximum time step was reduced. However, the results of the prediction were not changed, although the computer run time was significantly increased.

Other problems with the RELAP5/MOD1 calculations are easily detected in Figures 6.2.11 through 6.2.14, where primary and secondary fluid temperatures are presented. In Figure 6.2.11, for example, RELAP5/MOD1 predicted a straight fluid temperature profile in the secondary side with a drop and sudden rise at the top of the steam generator. The straight section corresponds to the saturation temperature, and is caused by bubble formations in the lower levels which caused mixing to take place. The top three cells, where a drop and then a sudden rise in the secondary side temperature were calculated, were predicted to be filled with water only ($\alpha=0$); two lower cells with subcooled water and the top cell with saturated water. This was not confirmed experimentally, and the calculated void fraction profile is, of course, non-physical. It is suspected that there are some FORTRAN or coding errors which need to be corrected by the code developers.

Finally, the results for ID=21806 indicate that RELAP5/MOD1 has a high interfacial mass transfer rate, particularly at high void fractions. In Figure 6.2.11, the code predicts the primary steam temperature to remain at the saturation temperature until the void fraction reaches unity. Then, and only then, does the code start to calculate superheated steam conditions. However, Figure 6.2.10 shows that during the experiment water was being collected in the outlet plenum although the steam was superheated (see Figure 6.2.11).

6.2.3.2 Test ID=22010

The results of this test simulation are presented in Figures 6.2.15 through 6.2.19. The secondary side pressure, shown in Figure 6.2.15, again indicates that TRAC-PF1 overpredicts the amount of energy transferred from the secondary side to the primary. This fact is also observed in Figure 6.2.16, which shows the exit steam temperature to be overpredicted.

In Figure 6.2.17 through 6.2.19, the experimental values of the secondary side fluid temperature, along with the primary side steam temperatures, are compared with the predicted values at various times. These figures demonstrate that TRAC-PF1 overpredicted the heat transfer throughout the run. Also, it should be noted in Figure 6.2.17, that the code predicted the primary side temperatures to be higher than the secondary side which is the heat source. This, of course, is believed to be generated by the numerical scheme and/or the time-step control.

Finally, the experimental data showed that the liquid did reach the outlet plenum with the result of 1.5 $\pm$ 0.7kg of water being carried over by 675 s

Figure 6.2.11 Comparison Between the Measured and Predicted
Primary Side Fluid Temperatures for Test ID=21806
at 338 s.

Figure 6.2.12 Comparison Between the Measured and Predicted
Primary Side Steam and Secondary Side Fluid
Temperatures for Test ID=21806 at 670 s.

Figure 6.2.13 Comparison Between the Measured and Predicted
Primary Side Steam and Secondary Side Fluid
Temperatures for Test ID=21806 at 842 s.

Figure 6.2.14   Comparison Between the Measured and Predicted Primary Side Steam and Secondary Side Fluid Temperatures for Test ID=21806 at 1178 s.

and 3.1 + 0.7 kg by 1300 s. TRAC-PF1 did not predict any liquid carryover. This could also be the result of greater secondary-to-primary heat transfer in the calculation. The code not only vaporized the droplets which entered the primary tubes, but it also did not predict the observed quench front propagation as shown in Table 6.2.2. Furthermore, the code predicted oscillations between the transition boiling regime and convection to single-phase vapor regime for the first 5 m of the U-tube bundle for the entire run, while the rest of the steam generator stayed in the convection to single-phase vapor heat transfer regime.

The last calculation to discuss is the RELAP5/MOD1 results of test ID = 22010. These results are also plotted on Figures 6.2.15 through 6.2.19 with the TRAC-PF1 predictions to facilitate comparison.

In Figure 6.2.15 the secondary side pressure is overpredicted by RELAP5/MOD1, probably because of the high prediction of the primary steam temperature near the top of the steam generator. In Figures 6.2.17 through 6.2.19, the RELAP5/MOD1 steam temperature exceeds the secondary side temperature which resulted in a higher secondary side temperature in RELAP5/MOD1. This generated excess steam in the secondary side causing the overpressurization seen in Figure 6.2.15. Also, it should be noted that for the primary temperature to exceed the secondary temperature a violation of the second law of thermodynamics has taken place, which is believed to be the result of an inadequate time step control. This can be stated because the test was rerun for a short time with a smaller maximum time step which stopped the primary side temperature from exceeding the temperature of the secondary side; but, it did not significantly change the prediction. However, the run time was significantly increased. Finally, in Figure 6.2.16, the primary exit steam temperature suggests that more energy was removed from the steam generator in the RELAP5/MOD1 calculation than was observed experimentally. Since the temperatures of the top levels were predicted to be higher than the data, the excess energy was removed from the lower levels (see Figures 6.2.17 through 6.2.19).

RELAP5/MOD1 also overpredicted the vapor generation rate in the primary side. No droplet traversed the U-tube in the RELAP5 prediction, whereas the experimenters collected 1.5 + 0.7 kg of water at 675 s and 3.2 + 0.7 kg of water at 1300 s in the outlet plenum. Again, as in test ID = 21806, the code shows that while it is in a two-phase flow situation the primary side remains at saturation temperature (see Figures 6.2.17 through 6.2.19) until all the droplets are vaporized; then, and only then, did the energy go into superheating the vapor. Also, because of the overprediction of the vapor generation rate, no quench front was developed in the tubes although it was expected (see Table 6.2.2).

6.2.4   Discussion

The FLECHT-SEASET steam generator test IDs 21806 and 22010 were two adequate tests for code assessment since the data showed the results to be essentially one-dimensional as both TRAC-PF1 and RELAP5/MOD1 are for the steam generator model. Hence, the following will attempt to summarize the major attributes discovered during these test simulations.
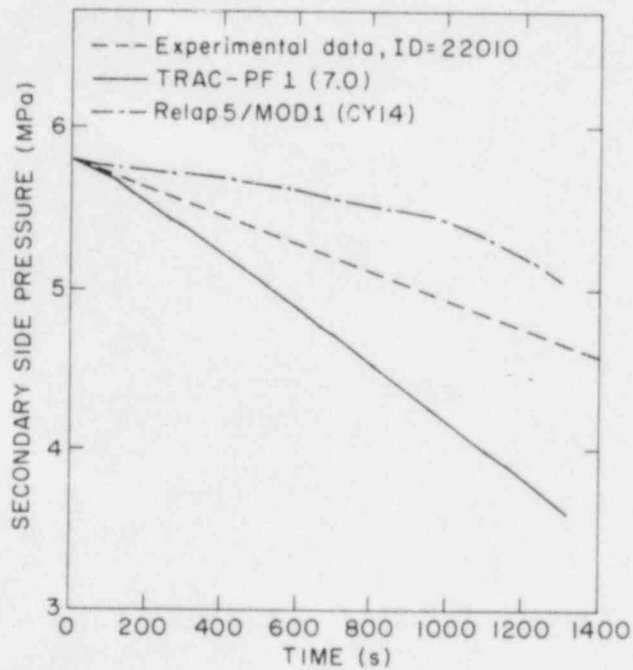
Figure 6.2.15 Comparison Between the Measured and Predicted
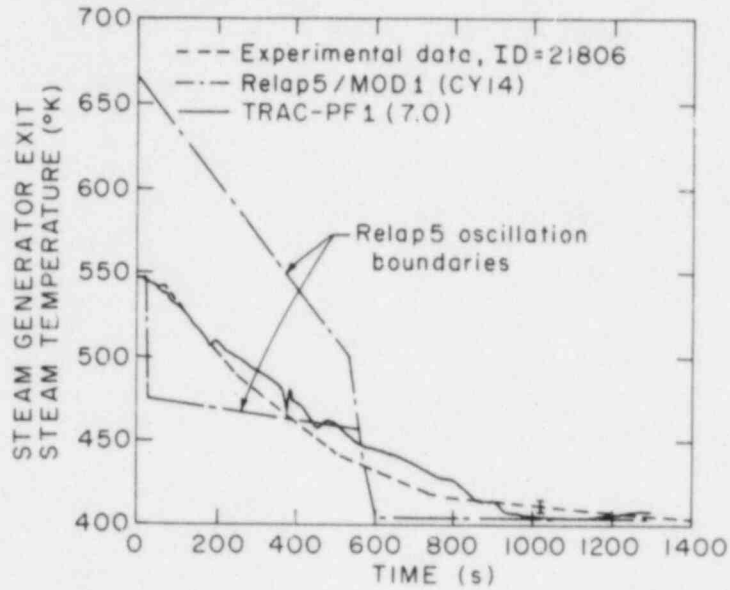Secondary Side Pressure for Test ID=22010.
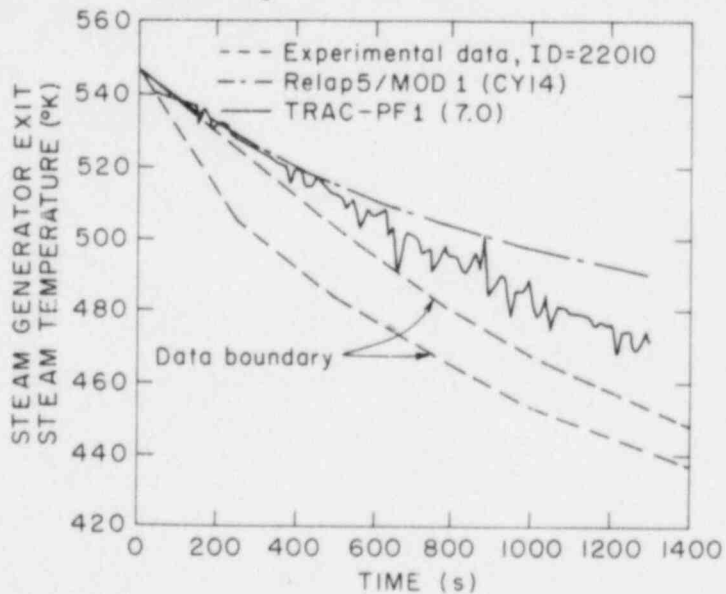
Figure 6.2.16 Comparison Between the Measured and Predicted
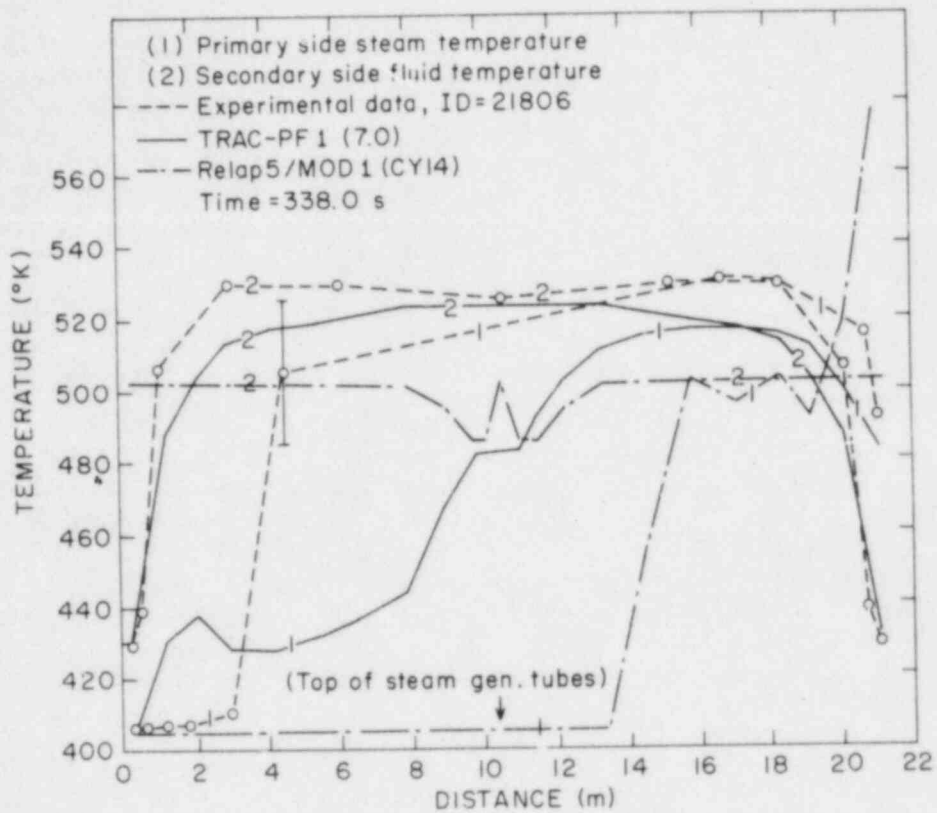Primary Side Exit Steam Temperature for
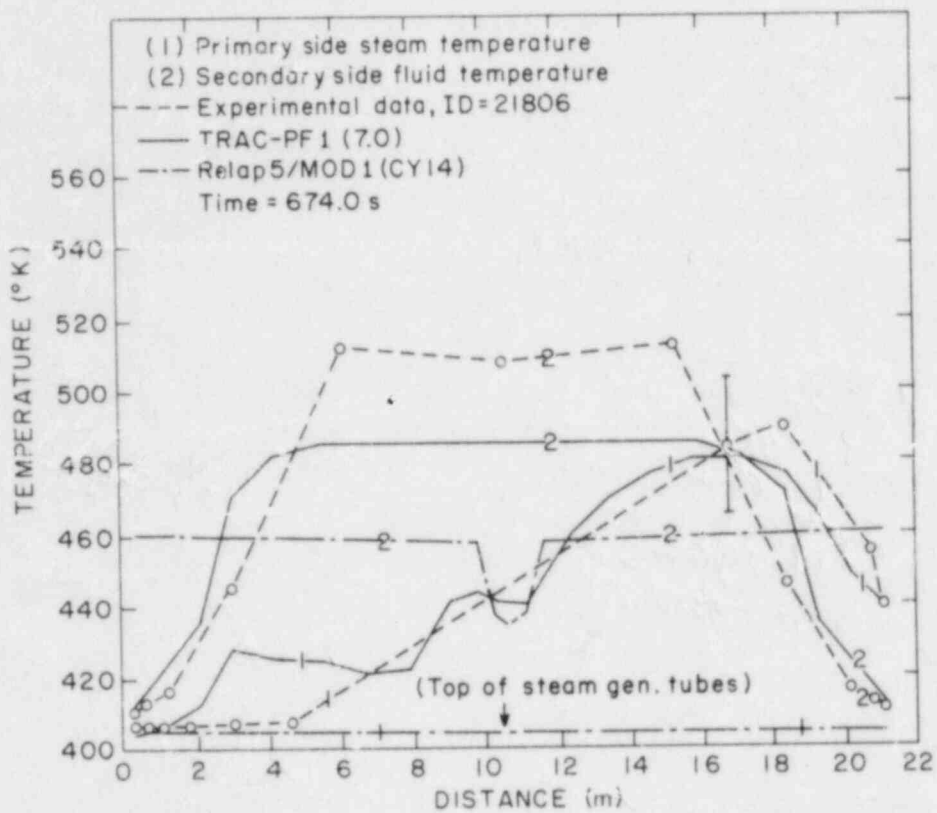Test ID=22010.
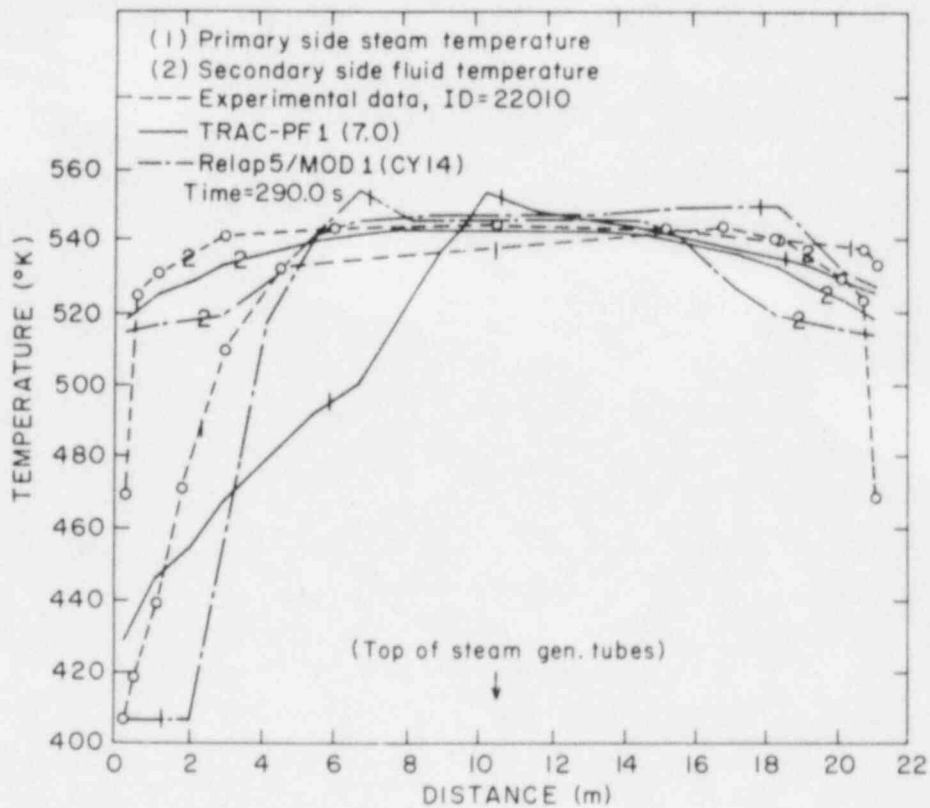
Figure 6.2.17   Comparison Between the Measured and Predicted Primary
                 Side Steam and Secondary Side Fluid Temperatures for
                 Test ID=22010 at 290 s.
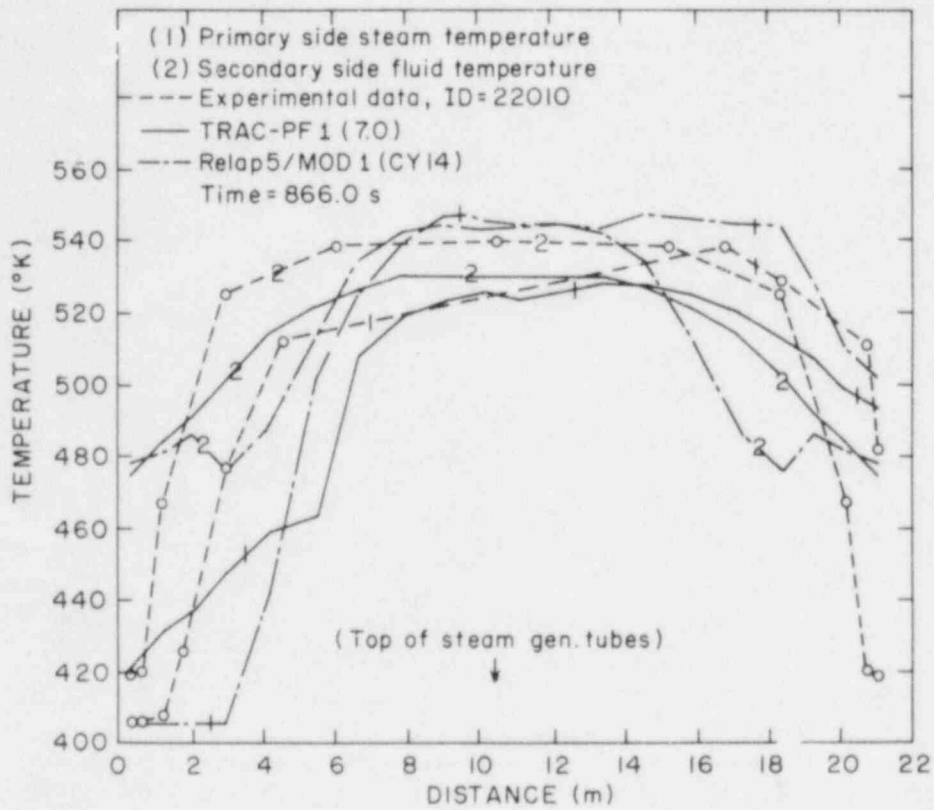
Figure 6.2.18   Comparison Between the Measured and Predicted Primary
                Side Steam and Secondary Side Fluid Temperatures for
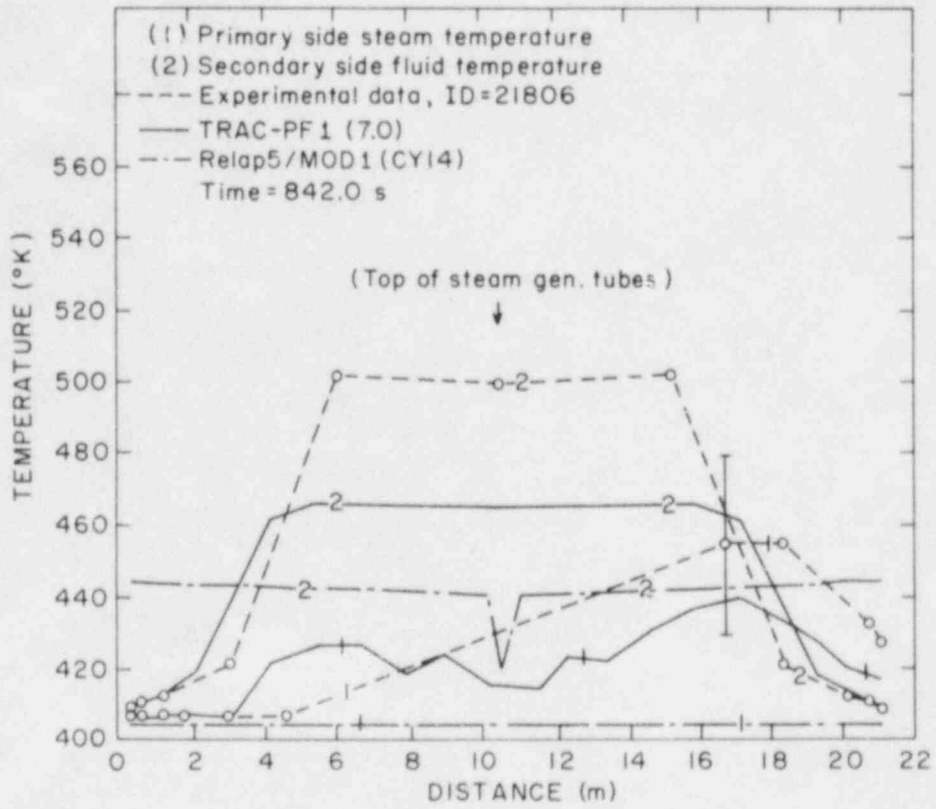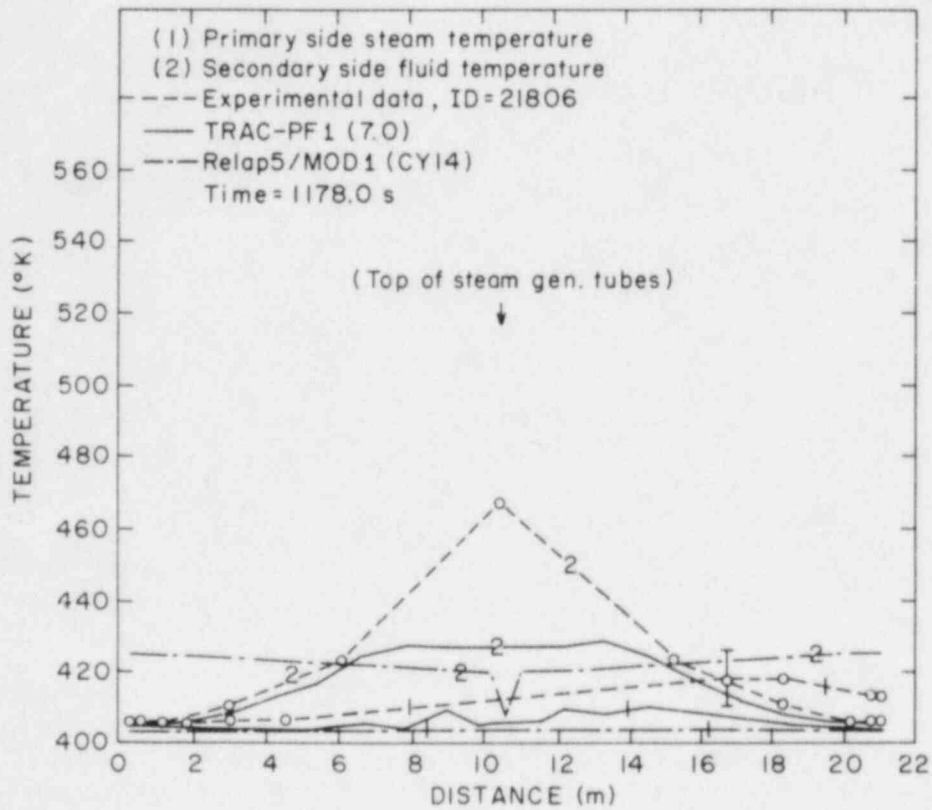   Test ID=22010 at 866 s.
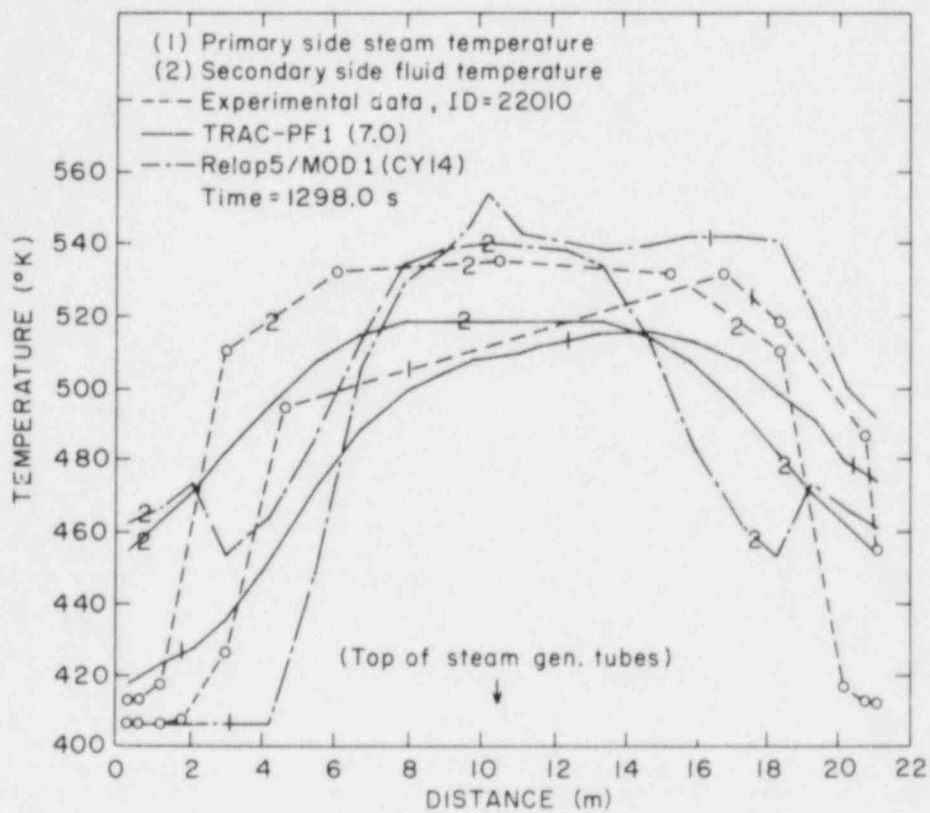
Figure 6.2.19 Comparison Between the Measured and Predicted Primary
Side Steam and Secondary Side Fluid Temperatures for
Test ID=22010 at 1298 s.

Table 6.2.2   Quench Time and Temperature Comparison for TRAC-PF1 (Version 7.0)
Predictions and FLECHT-SEASET Steam Generator
Tests ID=21806 and ID-22010

Test	Location (m)	Data		TRAC-PF1			
				First Appearance of Nucleate Boiling		Fully Established Nucleate Boiling	
		Time(s)	Time(°K)	Time (s)	Time(°K)	Time (s)	Time (°K)
21806	0.3048	102*	533	131	475	398	420
	1.2192	302	520	398	460	610	423
	3.0486	580	514	797	438	908	420
22010	0.3048	183	527	No Quench Predicted			
	1.2192	788	502	"	"	"	

* Values were averaged for a level.

In the primary side, TRAC-PF1 did predict a nonequilibrium situation, i.e., superheated steam in the presence of water droplets, as was found in the experiment. RELAP5/MOD1, however, did not predict superheated temperatures until all the droplets were evaporated. This implies that RELAP5 overestimated the interfacial heat and mass transfer rates at high void fractions or dispersed-droplet regimes. It should be pointed out that neither code for either test predicted the droplet carryover accurately. Furthermore, a quench or liquid film front, recorded in the primary side, was not predicted accurately by either code for both tests. Finally, both codes, particularly RELAP5/MOD1, occasionally predicted higher primary side temperature which was caused by an inadequate time step control. This was clearly demonstrated by rerunning RELAP5/MOD1 with smaller time steps as the above problem including numerical oscillations were alleviated. This demonstrates that the time-step control of RELAP5/MOD1 is not as restrictive as it should be.

In conclusion, both TRAC-PF1 and RELAP5/MOD1 codes overpredicted the heat transfer from the secondary side to the primary, although the overall prediction of TRAC-PF1 was better than that of RELAP5/MOD1. Also, neither code predicted the droplet carryover or the quench front advancement accurately. Finally, RELAP5/MOD1 clearly needs improvement in the dispersed droplet regime, time-step control, and prediction of void fraction profiles.

6.2.5 User Experience

There was no particular difficulty in simulating the FLECHT-SEASET steam generator tests with TRAC-PF1. The time step control of TRAC-PF1 is adequate and no special attention is needed for the maximum time step as long as it is

reasonable (~1 s). However, TRAC-PF1 cannot model the heat transfer from, or to, the shell wall. This is of no great concern when modeling a full-scale steam generator, since the internal surface-area-to-volume ratio in that case is rather small. However, it could be of concern while modeling a tall-but-skinny test facility such as the FLECHT-SEASET steam generator.

The RELAP5/MOD1 code had several problems which were noted during the simulation of the FLECHT-SEASET steam generator tests. First, the time-step control is very important for the RELAP5/MOD1 code. If large oscillations appear in a prediction, the first thing that should be performed is to rerun a part of the transient using a small maximum time step to determine if a large maximum time step caused the problem. Finally, the nonphysical void profiles predicted in the calculations demonstrated that some coding error must exist in the code which should be corrected. The computer run time statistics for the base calculations are shown in Table 6.2.3.

Table 6.2.3 Computer Run Time Statistics for FLECHT-SEASET
U-Tube Steam Generator Test Simulation
Computer: BNL CDC-7600

Calculation Item	TRAC-PF1		RELAP5/MOD1	
	Test ID = 21806	Test ID = 22010	Test ID = 21806	Test ID = 22010
No. of Cells	46	46	46	46
Problem Time (s)	1300	1300	1300	1300
No. of Time Steps	31022	7048	42322	167370
CPU Time (s)	4419	1115	2568	9271
CPU-to-Problem Time	3.40	0.86	1.98	7.13
CPU(s)/Cell/Time-Step	3.1×10^{-3}	3.4×10^{-3}	1.3×10^{-3}	1.2×10^{-3}

6.3 Summary and Conclusions

Both TRAC-PF1 (Version 7.0) and RELAP5/MOD1 (Cycle 14) were used to simulate operational transients in OTSG and IEOTSG configurations, and large break LOCA conditions in the FLECHT-SEASET U-tube steam generator. From the results presented in Sections 6.1 and 6.2, the following conclusions can be drawn:

1. TRAC-PF1 produced a more stable result for the integral economizer once-through steam generator (IEOTSG) heat transfer than its predecessor, TRAC-PD2, and yielded reasonable results for a load change transient.

2. For a loss-of-feedwater transient in a once-through steam generator (OTSG), TRAC-PF1 underpredicted the exit steam flow rate. This was caused by the lower initial water inventory due to a lower rate of condensation of the aspirated steam. An increase in the condensation rate improved the result, indicating that the direct-contact condensation rate in TRAC-PF1 is underestimated.

3. A noding study showed that approximately 10 nodes in each side of the steam generator are adequate for TRAC-PF1 for transients such as loss-of-feedwater.

4. RELAP5/MOD1 (Cycle 14) results are also slightly improved over those of Cycle 1 for the same IEOTSG tests. However, the RELAP5/MOD1 results still suffer from numerical instability, and thus, restrictions on the maximum time steps are necessary for the RELAP5/MOD1 calculation. This is valid for both once-through and U-tube steam generator simulation.

5. For RELAP5/MOD1, use of more nodes does not necessarily lead to better agreement with the experimental data.

6. Although RELAP5/MOD1 produced reasonable results for the OTSG loss-of-feedwater transient, it fails to predict the initial super-heated steam condition at the exit of the secondary side. Consequently, the total primary-to-secondary heat transer at steady state is underpredicted by as much as 10%.

7. For large-break LOCA conditions, both TRAC-PF1 and RELAP5/MOD1 tend to overpredict the secondary-to-primary heat transfer. The actual nonequilibrium effects are also underpredicted by both codes (although more so by RELAP5/MOD1). Thus, the codes would tend to exaggerate the steam-binding effects and would tend to predict slower core reflood.

8. Both TRAC-PF1 and RELAP5/MOD1, particularly RELAP5/MOD1, tend to overpredict the vapor-to-droplet heat transfer in the dispersed droplet regime. Improvement in this area is needed.

9. RELAP5/MOD1 also produced an anomalous void profile in the secondary side of the FLECHT-SEASET U-tube steam generator which indicated some errors in the code (either FORTRAN or in interfacial shear).

10. TRAC-PF1 should have the capability to model the steam generator shell wall. Although not of utmost importance for full-scale plant, this capability might be necessary for modeling tall-but-skinny model steam generators.

7. SIMULATION OF NATURAL CIRCULATION EXPERIMENTS

During many abnormal transients in LWRs, the reactor coolant pumps are tripped either to avoid pump cavitation or to mitigate any adverse consequences of the transient. The reactor system may, therefore, operate in a natural circulation mode for many cases. Thus, it is essential that the advanced safety codes accurately predict the reactor behavior under the natural circulation condition.

In the present assessment effort, three series of natural circulation tests conducted in the FRIGG loop (Nylund et al., 1968) were simulated with TRAC-PF1 (Version 7.0) and RELAP5/MOD1 (Cycle 14). The main objective was to evaluate the codes' capability in predicting the natural circulation flow rate for a given core or bundle power.

7.1 FRIGG Loop Tests

7.1.1 Test Description

FRIGG loop natural circulation tests (Nylund et al., 1968) were performed in a steam-water loop with a test section simulating the Marviken boiling heavy water reactor fuel assembly. The test section included a vertical electrically heated rod bundle with uniform radial and axial power distributions mounted in a 0.159 m diameter shroud as shown in Figure 7.1.1. The heated length of the bundle was 4.37 m; it contained 36 rods whose outside diameters were 0.0138 m. In addition, the bundle had 8 spacers with known (or measured) form loss coefficients.

A series of runs were conducted with different vessel inlet throttling. During each run, the pressure at the inlet and exit of the loop (around 50 bar), and the inlet water subcooling (a few degrees for each series of runs) were kept constant. The electrical power applied to the bundle (Q) was changed stepwise in order to obtain a relationship between the power and the natural circulation flow rate through the bundle.

The following three series of experiments with different entrance loss coefficients were simulated with TRAC-PF1 and RELAP5/MOD1:

a) Run Nos. 301017 - 301022 with entrance loss coefficient, K_{ent} = 4.5,

b) Run Nos. 301001 - 301016 and 301044 - 301047 with K_{ent} = 14.0, and

c) Run Nos. 301023 - 301030 with K_{ent} = 19.0.

The first and the last set of experiments were interrupted because of technical problems with the facility so that the rod bundle power was not raised to the level of the critical heat flux condition. However, for the second set, the power was raised until the CHF condition was reached at the exit of the bundle.

7.1.2 Input Models

For TRAC-PF1, the experiments were modeled using the one-dimensional CORE component for the vessel and rod bundle, PIPEs for the riser and downcomer, and two BREAKs to impose constant pressure boundary conditions at the downcomer entrance and riser exit (see Figure 7.1.2). The CORE had 16 axial levels with cell lengths of approximately 0.275 m. Twenty seven cells were used for the downcomer pipe with cell lengths varying from 0.25 to 0.86 m, and the riser pipe was represented by five cells 0.11 to 0.45 m in length. To model the loop geometry more accurately, the code's NAMELIST data capability was used to specify the elevations of the cell centers (IELV=1). The effects of rod bundle spacers were taken into account with additive loss coefficients (IKFAC=0).

Steady-state calculations with various bundle powers were run with the loop initially filled with single-phase water. In all cases, the code reached a steady state. However, during the steady-state calculations, TRAC-PF1 does not check for the critical heat flux condition. Therefore, the assessment of the CHF correlation used in TRAC-PF1 has been based on the constitutive relations package and the results are discussed later.

Two minor errors, found in the homogeneous friction factor option and in the annular friction factor option, were corrected at BNL, and the assessment calculations were performed with the corrected version of TRAC-PF1.

For RELAP5/MOD1, three PIPE components, one for the vessel with the electrically heated rod bundle, one for the riser pipe attached at the top of the vessel, and one for the downcomer pipe supplying subcooled water into the bottom entrance of the vessel, were used to simulate the test facility. The nodalization of the components was kept identical to that of the TRAC-PF1 modeling, as discussed earlier. The only difference was that the constant pressure boundary conditions at the entrance of the downcomer, and at the exit of the riser were specified using the RELAP5/MOD1 TIME DEPENDENT VOLUME components instead of the TRAC-PF1 BREAK components shown in Figure 7.1.2. The vessel with rod bundle was divided into 16 axial levels with cell lengths approximately equal to 0.275 m. Twenty seven volumes were used for the downcomer pipe with cell lengths varying from 0.25 to 0.86 m, and the riser pipe was represented by five cells 0.11 to 0.45 m in length. The effects of the rod bundle spacers were taken into account by additive loss coefficients.

Since RELAP5/MOD1 did not have a steady-state calculational capability, the code was run using the transient option starting with the loop filled with single-phase water. A few key variables in different places of the loop, namely, the void fraction, liquid and vapor phasic velocities, pressure, and loop mass flow rates, were closely monitored in order to determine whether a steady state was achieved.

7.1.3 Code Predictions and Comparison With Data

TRAC-PF1 had two options for wall friction: (a) homogeneous friction factor, and (b) annular flow friction factor. The first and the third set of experiments with bundle entrance loss coefficients of 4.5 and 19.0, respectively, were simulated with the homogeneous friction factor option only and the

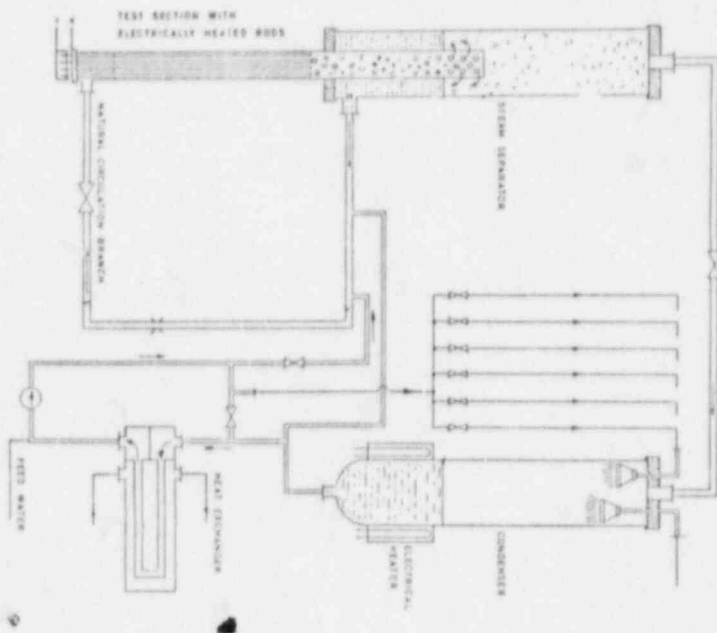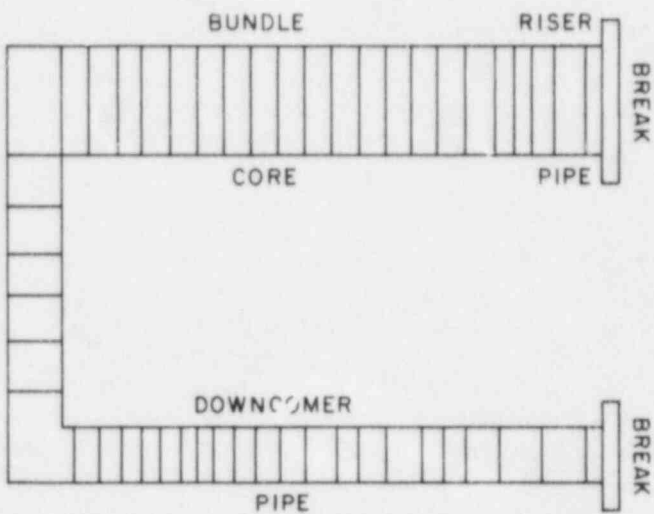Figure 7.1.1 Schematic of the FRIGG Loop.

Figure 7.1.2 Nodalization for the FRIGG Natural Circulation Tests.

results are presented in Figure 7.1.3 as bundle mass-flux vs power. It is seen that the predicted mass-fluxes were considerably larger than the experimental values and the predicted mass flux vs power curves did not have maxima as found in the experiment.

The second set of experiments with a bundle entrance loss coefficient of 14.0 has been simulated using both the homogeneous and the annular friction factor options available in TRAC-PF1. The results are shown in Figure 7.1.4. Although the code with the annular friction factor option produced results in better agreement with the data than with the homogeneous friction factor option, the bundle mass-flux was still overpredicted in both calculations. The possible reasons for this discrepancy are discussed later in Section 7.1.4.

The corresponding RELAP5/MOD1 results are shown in Figures 7.1.5 and 7.1.6. It can be seen that for all three sets of runs the loop mass flow rate was overpredicted. Moreover, the trend of the G vs Q curve, i.e., the presence of a maximum at a certain power was not predicted by the code.

As the bundle power was being increased, the RELAP5/MOD1 calculations showed difficulties in converging to a steady state (crosses in Figure 7.1.6). However, no burnout or CHF condition was predicted by the code. Therefore, the instabilities had to be due to some numerical or time-step control problems rather than the CHF condition which was the case in the experiment.

As mentioned earlier, for the second set of experiments with $K_{ent} = 14.0$, the power was raised until the CHF condition was reached at the bundle exit. Comparisons between the experimental wall heat flux and the code calculated critical heat fluxes are shown in Figures 7.1.7 and 7.1.8 as a function of bundle power. It can be seen that neither TRAC-PF1 nor RELAP5/MOD1 was able to predict the CHF condition. For TRAC-PF1, which used the Biasi correlation based on round tube data, the bundle power must be raised further to predict the CHF, whereas RELAP5/MOD1 would completely miss the CHF since the correlation used (W-3) was not applicable to the FRIGG loop natural circulation conditions. On the other hand, the Condie-Bengston CHF correlation (Condie, 1978) used in the RELAP4/MOD7 code was found to be successful in predicting the CHF condition as shown in Figures 7.1.7 and 7.1.8. Thus, correlations applicable to the low flow rod bundle situations should be incorporated in TRAC-PF1 and RELAP5/MOD1 for prediction of CHF condition in the natural circulation mode.

7.1.4   Discussion

There might be two reasons for the discrepancies between the code predictions and experimental data as shown in Figures 7.1.3 through 7.1.6. First, the interfacial shear package which influences the void fraction in the bundle could change the driving or gravity head, and thus produce higher loop mass flow rate than the data. On the other hand, underprediction of the two-phase friction losses including the form losses would also result in an overprediction of the loop mass flow rate.

Figure 7.1.3 Comparison Between the Measured and TRAC-PF1 Bundle Mass Fluxes for K_{ent}=4.5 and K_{ent}=19.0.

Figure 7.1.4 Comparison Between the Measured and TRAC-PF1 Bundle Mass Fluxes for K_{ent}=14.0.
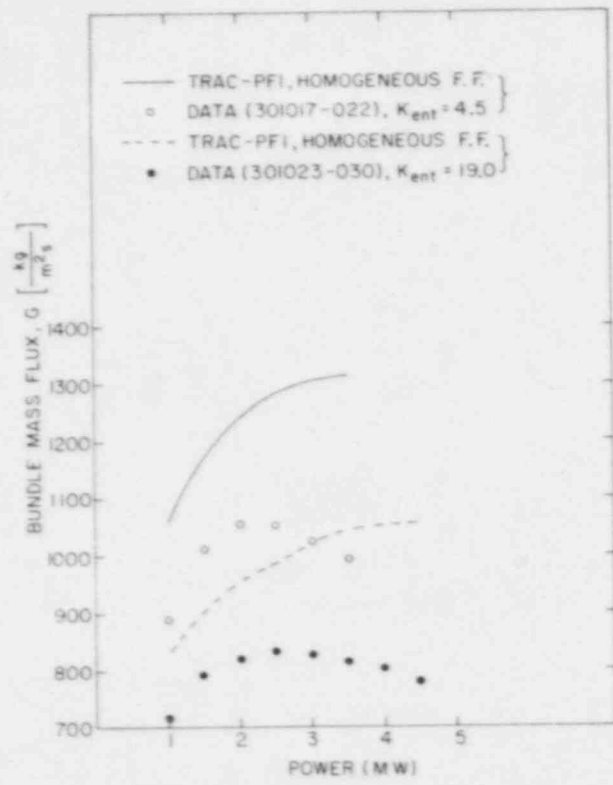
Figure 7.1.5 Comparison Between the Measured
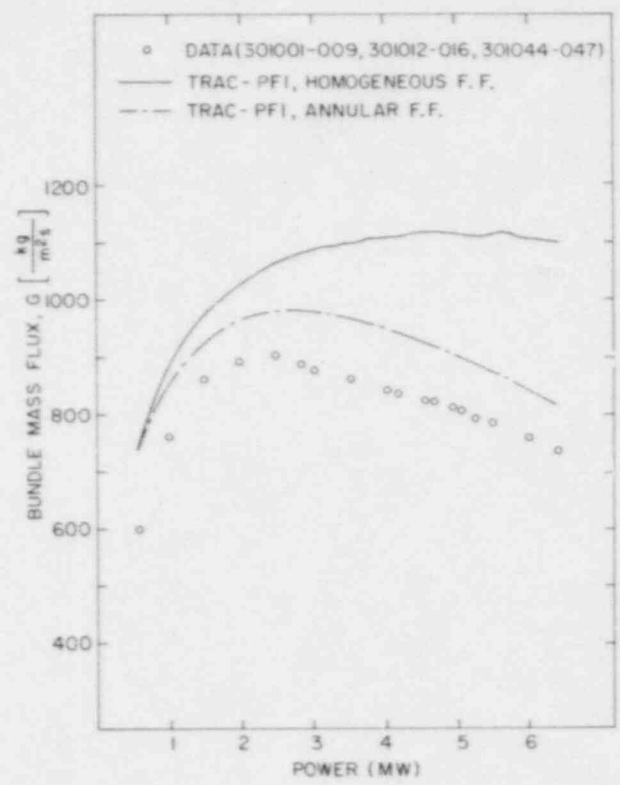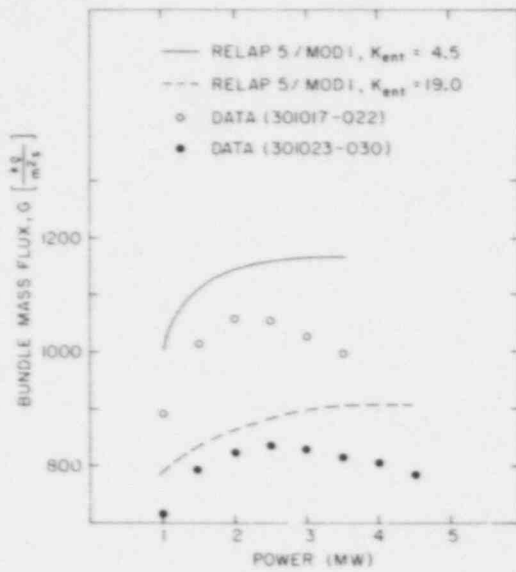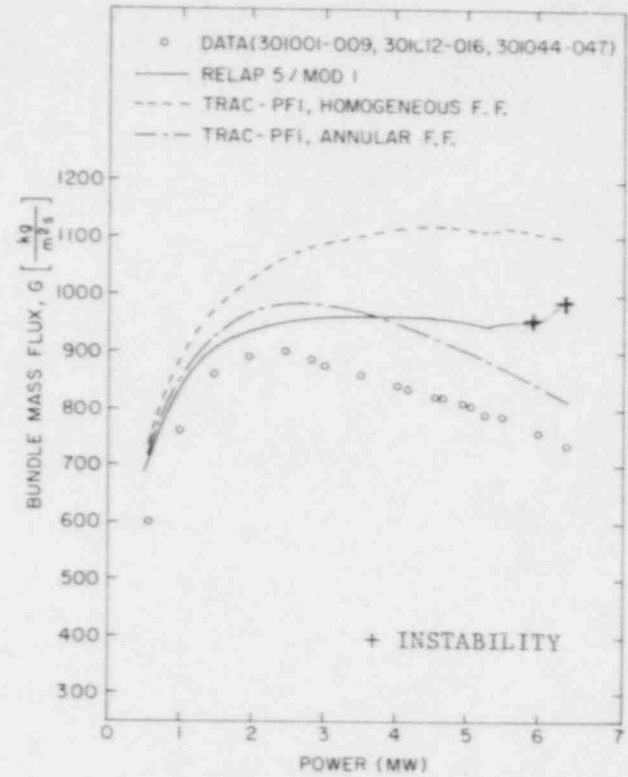and RELAP5 Bundle Mass Fluxes for
K_{ent}=4.5 and K_{ent}=19.0.

Figure 7.1.6 Comparison Between the Measured
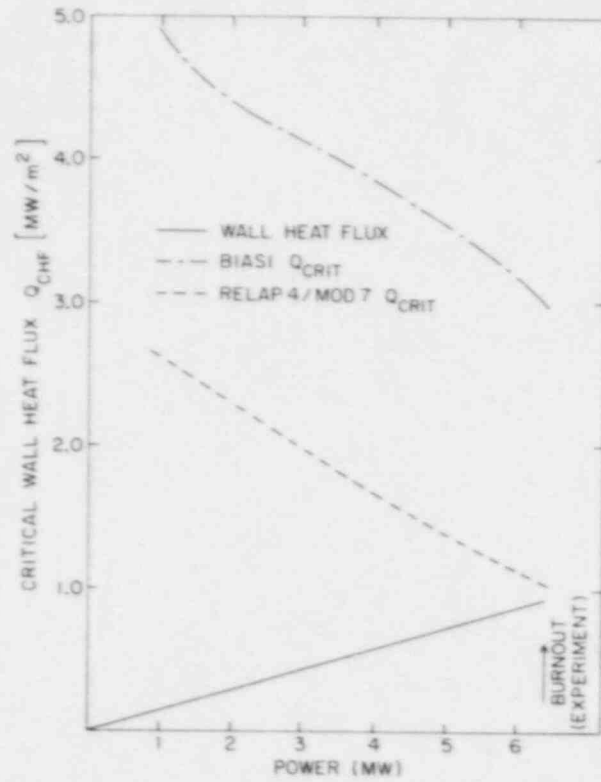and RELAP5 Bundle Mass Fluxes
for K_{ent}=14.0.

Figure 7.1.7 Comparison Between the Measured and Predicted Power for CHF or Burnout.
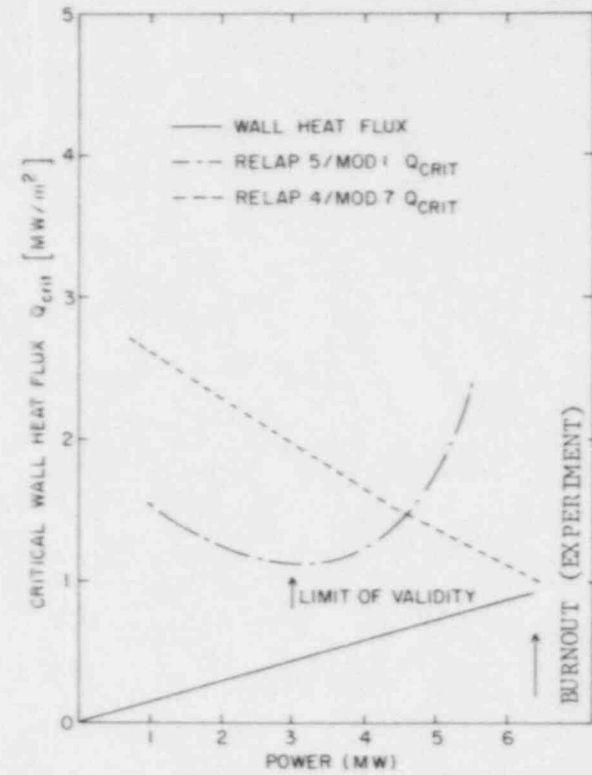
Figure 7.1.8 Comparison Between the Measured and Predicted Power for CHF or Burnout.

Let us first consider the bundle mass flux vs interfacial friction + void fraction + driving head dependence. In the course of the sensitivity studies, the TRAC-PF1 code was run twice for Run No. 301046 (Q = 6 MW) with artificially increased and decreased values of interfacial friction. The resultant void fraction profiles are shown in Figure 7.1.9. In the first case, the code's two-fluid model was virtually collapsed to the homogeneous flow model and, as it was expected, values of void fraction were higher than those in the original run (Curves 1 and 2 in Figure 7.1.9). In the second case, a decrease in the interfacial shear led to an increased slip and lower values of void fraction (Curve 3 in Figure 7.1.9). However, the predicted mass fluxes showed an unexpected trend. For the first case, the bundle mass-flux dropped despite an increase in the void fraction and the driving head. For the second case, the predicted mass-flux increased even when the void fraction and the driving head dropped. The situation was even more puzzling after the same sensitivity studies were performed for Run 301005 with a lower bundle power of 2.86 MW. The trends for mass-flux were completely reversed.

Although surprising at first sight, these results have been qualitatively and, to a certain degree, quantitatively explained using the integrated momentum equation written for the homogeneous equilibrium flow for the FRIGG loop. It is to be mentioned that in the course of the present investigation, a simple computer program based on the latter approximation was written and run as a fast scoping tool for sensitivity studies.

The sensitivity studies proved that the disagreement between the TRAC predictions and the data seen in Figures 7.1.3 and 7.1.4 cannot be explained in terms of the interfacial friction. Variations in the bundle mass-flux were not large enough even for extremely large variations in the interfacial friction which was increased by 1000 times and decreased by 10 times in the sensitivity studies. In view of the above conclusions, it is believed that the two-phase friction calculations were the cause of the disagreement. It should be pointed out that there is a large difference in values of the two-phase friction coefficients based on the homogeneous and the annular friction factor options in TRAC-PF1. As an example, Figure 7.1.10 shows the friction coefficient $C_{f\ell}$ vs the flow quality x for the FRIGG bundle geometry at G = 1000 kg/m^2s, p = 50 bar, T_ℓ = T_{sat}. It is clear that for the annular flow friction factor which produces a larger friction with the increases in flow quality (or bundle power) is a more appropriate option in the natural circulation mode, even though the actual flow pattern may not resemble an annular flow at the lower void fractions.

The above discussion is also valid for the RELAP5/MOD1 code, although the code has no user option for the two-phase friction factor.

7.1.5 User Experience

There was no particular difficulty in running either TRAC-PF1 or RELAP5/MOD1 for the FRIGG loop natural circulation tests. However, the user must ensure that the heights of the vertical components and the form losses are correctly incorporated in the input deck. Some oscillations in the RELAP5/MOD1 calculations were also observed. Typical computer run time statistics for these test simulations are given in Table 7.1.1.
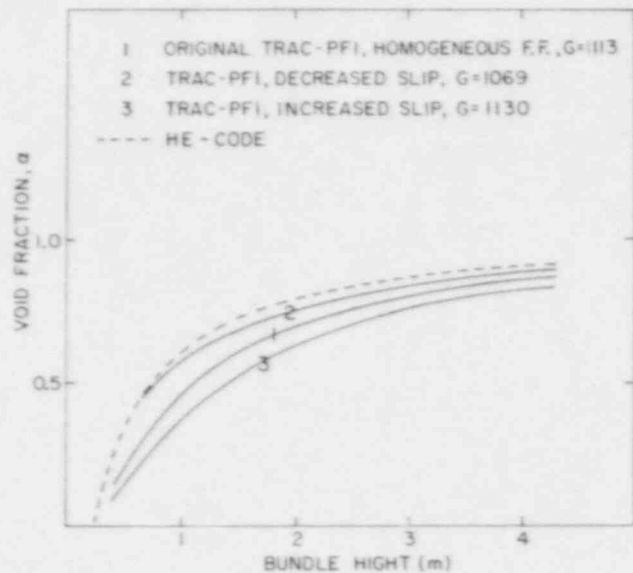
Figure 7.1.9 TRAC-PF1 Axial Void Fractions
for Various Interfacial Shear
or Slip.
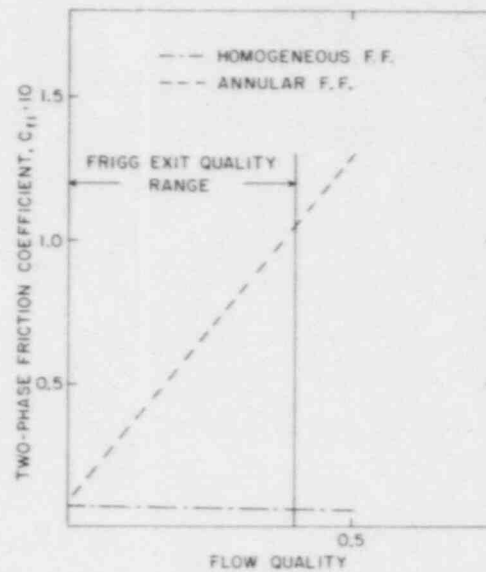
Figure 7.1.10 Comparison Between TRAC-PF1 Homo-
geneous and Annular Flow Friction
Factors.

Table 7.1.1 Typical Computer Run Time Statistics for FRIGG
Loop Natural Circulation Test Simulation

Computer: BNL CDC-7600

Calculation Item	TRAC-PF1	RELAP5/MOD1
No. of Cells	48	48
Problem Time (s)	11.3	40
No. of Time Steps	296	451
CPU Time (s)	47.2	20.6
CPU-to-Problem Time	4.2	0.52
CPU (s)/Cell/Time Step	3.3×10^{-3}	0.95×10^{-3}

7.2 Summary and Conclusions

From the results presented in Section 7.1, the following conclusions are drawn:

a) For TRAC-PF1:

1. TRAC-PF1, with either the homogeneous or the annular two-phase friction factor option, overpredicted the loop mass flow rate. However, the results obtained with the annular friction factor option have been closer to the data both qualitatively and quantitatively.

2. Sensitivity studies showed that the interfacial shear is not responsible for the disagreement between the code predictions and the data.

3. An investigation showed that TRAC-PF1 would overpredict the power needed to experience a CHF condition in the FRIGG bundle. This is due to the use of the Biasi critical flux correlation which was developed only from the round tube data.

b) For RELAP5/MOD1:

1. The bundle mass-flux has been overpredicted for all three sets
    of experimental runs. The overprediction is believed to be due
    to underestimation of the two-phase wall friction and form
    losses.

2. The experimentally observed trend for the bundle mass flux, G,
    vs the bundle power Q, was not predicted by the code.

3. The RELAP5/MOD1 critical heat flux correlation has been found
    to be inadequate for the tests under consideration since the
    correlation was derived for a different range of major param-
    eters.

4. Further efforts should be directed toward improving the numeri-
    cal stability of RELAP5/MOD1.

8. OVERALL SUMMARY, CONCLUSIONS AND RECOMMENDATIONS

Independent assessment of the TRAC-PF1 (Version 7.0), RELAP5/MOD1 (Cycle 14), and TRAC-BD1 (Version 12.0) codes has been performed using various separate-effect tests. The tests simulated can be grouped in the following six categories:

1. Critical flow tests (Moby-Dick nitrogen-water, BNL flashing flow, Marviken Test No. 24).

2. Level swell tests (GE large vessel test).

3. Countercurrent Flow Limiting (CCFL) tests (University of Houston, Dartmouth College single- and parallel-tube tests).

4. Post-CHF tests (Oak Ridge rod bundle test).

5. Steam generator tests (B&W 19-tube model S.G. tests, FLECHT-SEASET U-tube S.G. tests).

6. Natural circulation tests (FRIGG loop tests).

TRAC-PF1 and RELAP5/MOD1 were applied to all the above categories; however, because of resource limitations, TRAC-BD1 was applied only to the CCFL and post-CHF tests.

Useful results were obtained for all TRAC-PF1 calculations except for the Dartmouth College parallel-tube CCFL tests. RELAP5/MOD1 did not produce any useful result for the Moby-Dick nitrogen-water tests and the code was not applied to the parallel-tube CCFL tests because of its poor prediction of the single-tube CCFL tests. TRAC-BD1 produced useful results for both CCFL and post-CHF tests.

Regarding the computer run time, both TRAC-PF1 and TRAC-BD1 took approximately 3 ms of CPU time (in the BNL CDC-7600) per cell per time step. RELAP5/MOD1, in that respect, was faster because it took approximately 1 ms per cell per time step. However, RELAP5/MOD1 usually took smaller time steps than TRAC-PF1, and thus, the CPU-to-real time ratio of these two codes was quite comparable. Sometimes, the RELAP5/MOD1 maximum time step had to be restricted to avoid numerical instabilities. In those cases, RELAP5/MOD1 was actually more expensive to run than TRAC-PF1.

From the results presented in Chapters 2 through 7, the following conclusions and recommendations are drawn for each code:

8.1 Conclusions and Recommendations for TRAC-PF1

1. For two-component two-phase critical flow without phase change, TRAC-PF1 can be expected to produce stable results for all void fractions, which is an improvement over the TRAC-P1A code. However, the results are sensitive to the friction factor option selected for

calculation. The homogeneous friction factor option overpredicts the mass flow rate by ~15 to 22%, whereas the annular friction factor option underpredicts the same by ~5 to 12%. It is recommended that the same single-phase friction factor be used for both the homogeneous (NFF=1) and the annular (NFF=2) flow friction factor options.

2. For single-component (i.e., water) two-phase flow with phase change, TRAC-PF1 may significantly underpredict the subcooled critical flow rate by as much as 25% as shown in the BNL flashing test simulations. An accurate flashing delay model seems to be a necessary (although not sufficient) condition for achieving better agreement with the subcooled critical flow data. Simulation of Marviken Test No. 24 also supports this conclusion.

3. The choking option of TRAC-PF1 seems to be reasonable for subcooled critical flow through short nozzles if "correct" upstream boundary conditions are provided.

4. TRAC-PF1 needs a more accurate flashing delay model for the bulk or pipe flow. The present delay model in the choked flow formulation cannot predict the early pressure undershoot observed in the experiment. This undershoot and the corresponding liquid superheat could be important in determining the vapor generation rate later in the transient.

5. TRAC-PF1 tends to overpredict the void fraction below the mixture level and the level swell during a rapid depressurization transient. A high interfacial shear in TRAC-PF1 is believed to be partially responsible for the higher void fraction and the higher level swell rate.

6. For situations where liquid is injected in the middle of a test channel, the CCFL phenomenon is greatly influenced by the liquid entrainment inception and rate. In such cases, TRAC-PF1 predicts an early liquid entrainment which results in lower liquid downflow rates. Therefore, TRAC-PF1 entrainment model/correlation needs improvement.

7. For situations where liquid flows down from an upper plenum, the interfacial shear seems to be the dominant parameter for CCFL phenomenon. In such cases, TRAC-PF1 produced good agreement with data for small pipe diameters (~0.025 m I.D.). Thus, the Dukler correlation for interfacial shear seems reasonable for small-diameter pipes or channels. However, for large diameter pipes (~0.15 m I.D.), TRAC-PF1 produced anomalous behavior because of the discontinuities in the Dukler correlation. In this case, the Bharathan-Wallis correlation may be used.

8. A good prediction of single-tube CCFL data does not guarantee similar success for the parallel-tube CCFL data. For example, TRAC-PF1

produced good agreement with the Dartmouth College 0.0254 m I.D. single-tube data. However, it could not even produce a stable result for the parallel-tube experiments conducted in three 0.0254 m I.D. tubes. Also, the interfacial shear package must include correlations valid for the entire countercurrent annular flow regime, i.e., wavy-transition-rough film regimes, to enable TRAC-PF1 to adequately predict the parallel-tube CCFL phenomenon.

9. TRAC-PF1 cannot accurately predict the low flow CHF conditions, as evidenced from the ORNL post-CHF and FRIGG loop tests. Correlations other than the Biasi CHF correlation, which was based on single-tube data, should be investigated. However, TRAC-PF1 does calculate vapor superheating in the post-CHF regime.

10. TRAC-PF1 produces a more stable result for integral economizer once-through steam generator (IEOTSG) heat transfer than its predecessor, TRAC-PD2, and yielded reasonable results for a load change transient.

11. For a loss-of-feedwater transient in a once-through steam generator (OTSG), TRAC-PF1 underpredicted the exit steam flow rate. This was caused by the lower initial water inventory due to a lower rate of condensation of the aspirated steam. An increase in the condensation rate improved the result, indicating that the direct-contact condensation rate in TRAC-PF1 is underestimated.

12. A noding study showed that approximately 10 nodes in each side of the steam generator is adequate for TRAC-PF1 for transients such as loss-of-feedwater.

13. For large-break LOCA conditions, TRAC-PF1 tends to overpredict the secondary-to-primary heat transfer. The actual nonequilibrium effects are also somewhat underpredicted by TRAC-PF1. Thus, the code would tend to exaggerate the steam-binding effects and would tend to predict slower core reflood.

14. TRAC-PF1 should have the capability of modeling the steam generator shell wall. Although not of utmost importance for a full-scale plant, this capability might be necessary for modeling tall-but-skinny model steam generators.

15. TRAC-PF1 with either homogeneous or the annular two-phase friction factor option overpredicted the loop mass flow rate during natural circulation condition. However, the results obtained with the annular friction factor option have been closer to the data, both qualitatively and quantitatively.

8.2 Conclusions and Recommendations for RELAP5/MOD1

1. For single-component (i.e., water) two-phase flow with phase change, RELAP5/MOD1 may significantly underpredict the subcooled critical

flow rate by as much as 25% as shown in the BNL flashing test simulations. An accurate flashing delay model seems to be a necessary (although not sufficient) condition for achieving better agreement with the subcooled critical flow data. Simulation of Marviken Test No. 24 supports this conclusion.

2. For the RELAP5/MOD1 choking model, the short nozzles should be treated as zero-volume area changes to obtain good agreement with data, even though this contradicts the reality. Also, the RELAP5/MOD1 choking model seems to be sensitive to nodalization.

3. RELAP5/MOD1 needs a more accurate flashing delay model for the bulk or pipe flow. The present delay model in the choked flow formulation cannot predict the early pressure undershoot observed in the experiment. This undershoot and the corresponding liquid superheat could be important in determining the vapor generation rate later in the transient.

4. RELAP5/MOD1 predictions for average void fraction, level swell rate, and break flow rate during level swell due to rapid depressurization seem reasonable. However, the code underpredicts the vessel pressure and produces an irregular axial void fraction profile. It seems that the interfacial shear package of RELAP5/MOD1 needs re-examination and improvement.

5. There seems to be no need to represent a converging-diverging discharge nozzle with a zero volume junction for the RELAP5/MOD1 calculation, as suggested by the RELAP5 code developers.

6. The RELAP5/MOD1 flow regime map for high void fractions must be changed to include an annular-mist regime before the code can be expected to produce reasonable results for CCFL applications. At present, RELAP5/MOD1 cannot predict the CCFL situation even in a simple round pipe.

7. RELAP5/MOD1 cannot accurately predict the low flow CHF conditions as evidenced from the ORNL post-CHF and FRIGG loop tests. Other CHF correlations should be investigated.

8. RELAP5/MOD1 tends to overpredict the vapor generation rate at the post-CHF region. This results in almost no vapor superheating until all the liquid droplets are evaporated in the RELAP5/MOD1 calculation. However, this does not represent the reality. Thus, the RELAP5/MOD1 model for vapor generation in the post-CHF regime should be improved.

9. For the steam generator (IEOTSG) tests, the RELAP5/MOD1 (Cycle 14) results are slightly improved over those of Cycle 1. However, the new results still suffer from numerical instability. Therefore, restrictions on the maximum time steps are necessary for the RELAP5/MOD1 calculation. This is valid for both once-through and U-tube steam generator simulations.

10. For RELAP5/MOD1, use of more nodes does not necessarily lead to better agreement with the experimental data of the steam generator (IEOTSG) thermal performance.

11. Although RELAP5/MOD1 produced reasonable results for the OTSG loss-of-feedwater transient, it fails to predict the initial superheated steam condition at the exit of the secondary side. Consequently, the total primary-to-secondary heat transfer at steady state is underpredicted by as much as 10%.

12. For large-break LOCA conditions, RELAP5/MOD1 tends to overpredict the secondary-to-primary heat transfer. The actual nonequilibrium effects are also underpredicted by RELAP5/MOD1, as in the post-CHF tests. Thus, the code would tend to exaggerate the steam-binding effects and would tend to predict slower core reflood.

13. RELAP5/MOD1 tends to overpredict the vapor-to-droplet heat transfer in the dispersed droplet regime. Improvement in this area is needed.

14. RELAP5/MOD1 also produced an anomalous void profile in the secondary side of the FLECHT-SEASET U-tube steam generator which indicated some errors in the code (either FORTRAN or in interfacial shear).

15. The bundle mass-flux during natural circulation has been overpredicted by RELAP5/MOD1 for all three sets of FRIGG loop runs. The overprediction is believed to be due to underestimation of the two-phase wall friction and form losses.

16. Further efforts should be directed toward improving the numerical stability of RELAP5/MOD1.

8.3 Conclusions and Recommendations for TRAC-BD1

1. For situations where liquid is injected in the middle of a test channel, the CCFL phenomenon is greatly influenced by the liquid entrainment inception and rate. In such cases, TRAC-BD1 tends to predict good agreement with the data. Thus, the TRAC-BD1 entrainment inception and rate correlations seem to be reasonable.

2. For situations where liquid flows down from an upper plenum, the interfacial shear seems to be the dominant parameter for the CCFL phenomenon. In such cases, TRAC-BD1 tends to overpredict the liquid downflow rate indicating a lower interfacial shear.

3. The interfacial shear coefficient used in the TRAC-BD1 code overpredicts the liquid downflow rate. Use of the Kutateladze CCFL correlations tend to improve the prediction. However, the Kutateladze constant in the CCFL correlation has to be adjusted to achieve a good prediction. It seems that a combination of the Dukler correlation (for small diameter pipe), and the Bharathan-Wallis correlation (for large diameter pipe) should produce a better interfacial shear correlation for the countercurrent annular flow regime.

4. For parallel-tube CCFL tests, the TRAC-BD1 results were, at best, in some qualitative agreement with the data. It seems that the inter-facial shear package must include correlations valid for the entire countercurrent annular flow regime, i.e., wavy-transition-rough film regimes, to enable TRAC-BD1 to adequately predict the parallel-tube CCFL phenomeonon.

5. The CHF correlation used in the TRAC-BD1 code, i.e., the Biasi crit-ical quality boiling length correlation, seems to be adequate. Vapor superheating calculated in the post-CHF regime also looks rea-sonable. However, further assessment with more post-CHF experiments is needed to make a definitive statement about the TRAC-BD1 post-CHF model accuracy.

As a final note, the code assessment conducted at BNL was directed at evaluating the thermal-hydraulic model adequacy, and recommending areas of further improvement. Thus, only the separate-effects experiments were simu-lated. Conclusions regarding the overall code accuracy for full-scale reactor application can only be made by assimilating all code assessment results ob-tained at BNL, INEL, LANL, and SNL. This last task is beyond the scope of the present effort.

9. REFERENCES

ABUAF, N. et al. (1981), "A Study of Nonequilibrium Flashing of Water in a Converging-Diverging Nozzle," NUREG/CR-1864, BNL-NUREG-51317.

ANDERSEN, J.G.M. and CHU, K.H. (1982), "BWR Refill-Reflood Program Task 4.7 - Constitutive Correlations for Shear and Heat Transfer for the BWR Version of TRAC," NUREG/CR-2134, EPRI NP-1582, GEAP-24940.

BHARATHAN, D. (1979), "Air-Water Countercurrent Annular Flow," EPRI NP-1165.

BHARATHAN, D. (1982), Private Communication.

BIASI, L. et al. (1967), "Studies on Burnout: Part 3," Energ. Nucl. 14, 530-536.

BURNELL, J.G. (1948), "Flow of Boiling Water Through Nozzles, Orifices, and Pipes," Engineering, 164, 572.

CLARK, C.R. et al. (1978), "Flooding in Multi-Path Vertical Counter-Current Air-Water Flow," Dartmouth College Report NRC-0193-5.

CONDIE, K. G. and BENGSTON, S.G. (1978), "Development of the MOD7 Correlation," EG&G Report, Attachment PN-181-78.

DUKLER, A.E. and SMITH, L. (1979), "Two-Phase Interaction in Counter-Current Flow: Studies of Flooding Mechanism," NUREG/CR-0617.

DUKLER, A.E. (1980), "Two-Phase Interactions in Countercurrent Flow," University of Houston, Department of Chemical Engineering Annual Report, November 1978-October 1979.

ERICSON, L. et al. (1979), "Marviken Critical Flow Tests," Joint Reactor Safety Experiments in Marviken Power Stations, MXC-224.

FABIC, S. and ANDERSEN, P.S. (1981), "Plans for Assessment of Best Estimate LWR Systems Codes," NUREG-0676.

FINDLAY, J.A. (1981), "BWR Refill-Reflood Program Task 4.8 - Model Qualification Task Plan," NUREG/CR-1899, EPRI NP-1527, GEAP-24898.

HOWARD, R.C. et al. (1980), "PWR FLECHT-SEASET Steam Generator Separate Effects Task Data Report," NUREG/CR-1366.

HSU, Y.Y. and BECKNER, W.D. (1977), "A Correlation for the Onset of Transient CHF," Cited in L.S. Tong and G. L. Bennett, NRC Water Reactor Safety Research Program, Nucl. Safety, 18, No. 1, January/February 1977.

ILOEJE, O.C. et al. (1973), "An Investigation of the Collapse and Surface Rewet in Film Boiling in Forced Vertical Flow," ASME Paper 73-WA/HT-20.

ISHII, M. (1977), "One-Dimensional Drift-Flux Model and Constitutive Equations for Relative Motion Between Phases in Various Two-Phase Flow Regimes," ANL-77-47.

ISHII, M. and MISHIMA, K. (1981), "Correlation for Liquid Entrainment in Annular Two-Phase Flow of Low Viscous Fluid," ANL/RAS/LWR 81-2.

JEANDEY, C. and BARRIERE, G. (1979), "Part I, Etude Experimentale d'Ecoulements Eau-Air a Grande Vitesse," DTCE/STT/SETRE Note T.T. No. 599.

JONES, O.C., Jr. (1980), "Flashing Inception in Flowing Liquids," Journal of Heat Transfer, 102, 439-444.

LILES, D.R. et al. (1979), "TRAC-P1A: An Advanced Best-Estimate Computer Program for PWR LOCA Analysis," NUREG/CR-0665, LA-7777-MS.

LILES, D.R. et al. (1981), "TRAC-PD2: An Advanced Best-Estimate Computer Program for Pressurized Water Reactor Loss-of-Coolant Accident Analysis," NUREG/CR-2054, LA-8709-MS.

LILES, D.R. et al. (1983), "TRAC-PF1/MOD1: An Advanced Best-Estimate Computer Program for Pressurized Water Reactor Thermal-Hydraulic Analysis," LANL Draft Report, Final Report to be published.

LILES, D.R. et al. (1984), "TRAC-PF1: An Advanced Best-Estimate Computer Program for Pressurized Water Reactor Analysis," NUREG/CR-3567, LA-9944-MS.

LOUDIN, G.W. and OBERJOHN, W.J. (1976), "Transient Performance of a Nuclear Integral Economizer Once-Through Steam Generator," B&W Alliance Research Center Report 4679, B&W Proprietary.

MARVIKEN, (1982), "The Marviken Full Scale Critical Flow Tests, Summary Report," Joint Reactor Safety Experiments in the Marviken Power Station Sweden, NUREG/CR-2671, MXC-301.

MOHR, C.M. (1981), "TRAC-BWR Completion Report: Adaptation of Andersen/Ishii Interfacial Shear Package for TRAC-BD1/MOD1," INEL Interim Report WR-CD-81-052.

MULLINS, C.B. et al. (1982), "ORNL Rod Bundle Heat Transfer Test Data, Vol. 7, Thermal-Hydraulic Test Facility Experimental Data Report for Test Series 3.07.9 - Steady State Film Boiling in Upflow," NUREG/CR-2525, Vol. 7, ORNL/NUREG/TM-407/V7.

NYLUND, O. et al. (1968), "Hydrodynamic and Heat Transfer Measurements on a Full-Scale Simulated 36-Rod Marviken Element with Uniform Heat Flux Distribution," FRIGG-2, R4-447/RTL-1007.

PHILLIPS, R.E. (1981a), "TRAC-BWR Completion Report: Subcooled Boiling Model," INEL Interim Report WR-CD-81-050.

PHILLIPS, R.E. et al. (1981b), "Improvements to the Prediction of Boiling Transition During Boiling Water Reactor Transients," in Thermal-Hydraulics in Nuclear Power Technology, K.H. Sun et al., ed., ASME HTD-Vol. 15, 53-62.

POPOV, N.K. and ROHATGI, U.S. (1983), "Effect of Interfacial Shear and Entrainment Models on Flooding Predictions," in Heat Transfer - Seattle 1983, AIChE Symp. Series 225, Vol. 79, N.M. Farukhi, ed., 190-199.

RANSOM, V.H. et al. (1982)," RELAP5/MOD1 Code Manual," NUREG/CR-1826, EGG-2070.

RANSOM, V.H. et al. (1984), "RELAP5/MOD2 Code Manual," EGG-SAAM-6377.

ROHATGI, U.S., and SAHA, P. (1980), "Constitutive Relations in TRAC-P1A," NUREG/CR-1651, BNL-NUREG-51253.

ROHATGI, U.S., JO, J., and NEYMOTIN, L. (1982), "Constitutive Relations in TRAC-PD2," NUREG/CR-3073, BNL-NUREG-51616.

ROHATGI, U.S., JO, J.H., and SLOVIK, G.C. (1985), "A Comparative Analysis of Constitutive Relations in TRAC-PF1 and RELAP5/MOD1," NUREG/CR-4292, BNL-NUREG- 51898.

SAHA, P. (1980), "Moby-Dick Nitrogen-Water Experiments," in Water Reactor Safety Research Division Quarterly Progress Report, January 1 - March 31, 1980, NUREG/CR-1506, BNL-NUREG-51218.

SAHA, P. (1982a), "Use of Separate Effects Experiments in Verification of System Thermal Hydraulics," ANS Trans, $\underline{41}$, 673-674.

SAHA, P. et al. (1982b), "Independent Assessment of TRAC-PD2 and RELAP5/MOD1 Codes at BNL in FY 1981," NUREG/CR-3148, BNL-NUREG-51645.

SLOVIK, G.C., and SAHA, P. (1985), "Independent Assessment of TRAC-PD2/MOD1 Code with BCL ECC Bypass Tests," NUREG/CR-4252, BNL-NUREG-51886.

SMITH, R.A., and GRIFFITH, P. (1976), "A Simple Model for Estimating Time to CHF in a PWR LOCA," ASME Paper No. 76-HT-9.

SPORE, J.W. et al. (1981), "TRAC-BD1: An Advanced Best Estimate Computer Program for Boiling Water Reactor Loss-of-Coolant Accident Analysis," NUREG/CR-2178, EGG-2109.

TAYLOR, D.D. et al. (1984), "TRAC-BD1/MOD1: An Advanced Best Estimate Computer Program for Boiling Water Reactor Transient Analysis," NUREG/CR-3633, EGG-2294.

WALLIS, G.B. (1970), "Annular Two-Phase Flow, Part 1: A Simple Theory," Journal of Basic Eng. $\underline{92}$, 59-72.

WOODRUFF, S.B. (1982), Letter to P. Saha, February 17th.

ZALOUDEK, F.R. (1963), "The Critical Flow of Hot Water Through Short Tubes,"
  AEC Research and Development Report HW- 77594.

DISTRIBUTION

USNRC

O. E. Bassett
W. D. Beckner
Y. S. Chen
C. Graves, NRR
J. Guttmann, NRR
M. W. Hodges, NRR
C. N. Kelber
R. Lee
R. B. Minogue
W. Morrison
F. Odar
J. N. Reyes
D. F. Ross
B. Sheron, NRR
L. M. Shotkin
H. S. Tovmassian
M. Young
N. Zuber

BNL

H. J. C. Kouts
W. Y. Kato
DNE Associate Chairmen
NSP Division Heads and
   Group Leaders
LWR CAAG Staff
Nuclear Safety Library (2)

External

D. R. Liles, LANL
T. D. Knight, LANL

T. R. Charlton, INEL
G. W. Johnsen, INEL
V. H. Ransom, INEL
G. Wilson, INEL

D. Majumdar, DOE/Idaho

L. D. Buxton, SNL

I. Brittain, Winfrith (U.K.)
J. Fell, Winfrith (U.K.)

1. REPORT NUMBER (Assigned by DDC)
NUREG/CR-4359
BNL-NUREG-51919

4. TITLE AND SUBTITLE (Add Volume No., if appropriate)	2. (Leave blank)
Independent Assessment of TRAC-PF1 (Version 7.0), RELAP5/ MOD1 (Cycle 14), and TRAC-BD1 (Version 12.0) Codes Using Separate-Effects Experiments	3. RECIPIENT'S ACCESSION NO.

7. AUTHOR(S)	5. DATE REPORT COMPLETED	
P. Saha, J.H. Jo, L. Neymotin, U.S. Rohatgi, G.C. Slovik & C. Yuelys-Miksis	MONTH JULY	YEAR 1985

9. PERFORMING ORGANIZATION NAME AND MAILING ADDRESS (Include Zip Code)	DATE REPORT ISSUED	
Department of Nuclear Energy Brookhaven National Laboratory Upton, Long Island, New York 11973	MONTH	YEAR
	6. (Leave blank)	
	8. (Leave blank)	

12. SPONSORING ORGANIZATION NAME AND MAILING ADDRESS (Include Zip Code)	10. PROJECT/TASK/WORK UNIT NO.
Division of Accident Evaluation Office of Nuclear Regulatory Research U.S. Nuclear Regulatory Commission Washington, DC 20555	11. FIN NO. A3215

13. TYPE OF REPORT	PERIOD COVERED (Inclusive dates)
Technical Report	

15. SUPPLEMENTARY NOTES	14. (Leave blank)

16. ABSTRACT (200 words or less)

This report presents the results of independent code assessment conducted at BNL. The TRAC-PF1(Version 7.0) and RELAP5/MOD1 (Cycle 14) codes were assessed using the critical flow tests, level swell test, countercurrent flow limitation (CCFL) tests, post-CHF test, steam generator thermal performance tests, and natural circulation tests. TRAC-BD1 (Version 12.0) was applied only to the CCFL and post-CHF tests.

17. KEY WORDS AND DOCUMENT ANALYSIS	17a. DESCRIPTORS
Code Assessment TRAC-PF1 RELAP5/MOD1 TRAC-BD1 Separate-Effects Tests	

17b. IDENTIFIERS/OPEN ENDED TERMS

18. AVAILABILITY STATEMENT	19. SECURITY CLASS (This report)	21. NO. OF PAGES
	20. SECURITY CLASS (This page)	22. PRICE